Bose–Einstein Condensation and Superfluidity

Shosuke Sasaki[1)] and Hidenobu Hori[2)]

[1)] Shizuoka Institute of Science and Technology
Toyosawa 2200-2, Fukuroi, Shizuoka 437-8555, Japan
[2)] Japan Advanced Institute of Science and Technology (JAIST)
Asahidai Tatsunokuchi, Nomi, Ishikawa, 923-1292, Japan

Preface

Bose–Einstein condensation was discovered in atomic gas systems, where Bose condensate occupies 100% of the total system at zero temperature. Liquid helium systems have been investigated based on the Landau theory, where the superfluid component of liquid helium is background flow. According to the Landau theory, it is doubtful that the superfluid component is a Bose condensate.

In experiments, the probability of helium atoms with zero momentum is a few percent of the total liquid helium at ultra-low temperatures. However, the superfluid component occupies 100% of the liquid helium at zero temperature, as macroscopic observations indicate. These two properties of liquid helium mean that the set of helium atoms with zero momentum is not a good approximation of the ground state. What state represents the superfluid component of liquid helium?

We introduce a quasi-particle representing an eigenstate of the total Hamiltonian. We designate the quasi-particle a “dressed boson”. It is the most straightforward answer to the question posed above: the superfluid component is a Bose condensate of dressed bosons.

Experimental data of thermodynamic quantities differ greatly from the theoretical values of the Landau theory near the λ point. The specific heat has a logarithmic singularity at the λ point in the experimental data; however, the theoretical result of the Landau theory has no singularity.

In the present article, the diagonalized form of the total Hamiltonian is

examined and is clarified to have a nonlinear form for the distribution function of the dressed bosons. The nonlinear form produces logarithmic divergence of the specific heat.

Many theoretical approaches have used a linear form in a total energy of a Bose system as

$$E = \sum_i \varepsilon_i n_i \ ,$$

where n_i is the quasi-particle number in quantum level *i*, and where ε_i is the energy per quasi-particle. This familiar form maintains the order of energy from small to large. That is to say, the energy of level 1 is smaller than that of level 2 always if $\varepsilon_1 < \varepsilon_2$. The property changes drastically for a nonlinear form of a total energy as

$$E = \sum_i n_i \varepsilon_i + \sum_{i,j} f_{ij} n_i n_j + \cdots .$$

The energy of a quasi-particle (dressed boson) is definable as

$$\frac{\partial E}{\partial n_i} = \varepsilon_i + \sum_j f_{ij} n_j + \sum_j f_{ji} n_j + \cdots ,$$

which depends upon the other dressed boson numbers. Consequently, the energy of the dressed boson with quantum level *i* varies depending on the distribution of dressed boson number. This nonlinear dependence yields level inversion; that is to say, which momentum level of the dressed boson has a minimum energy depends upon the choice of the distribution of dressed boson number. The level with momentum zero has minimum energy for some distribution. However, when the distribution of dressed boson number changes into a specific distribution, a level with a non-zero momentum has minimum energy. This level inversion produces Bose condensation of the dressed bosons with non-zero momentum. The stability of the moving superfluid component is established on the basis of this level inversion. Many other surprising effects arise from the nonlinearity.

In almost all cases for many body problems, the total energy is nonlinearly dependent upon the distribution function of quasi-particle number. Accordingly, the developed method explained in this book is widely applicable to investigation of the statistical physics of many body problems.

Appendix II

Appendix III

References

Mathematica program 1 (Determination of nonlinear term)

Mathematica program 2 (Approxmation in second order)

Mathematica program 3 (Calculation of entropy)

Mathematica program 4 (Calculation of specific heat for 0.2-2.15K)

Mathematica program 5 (Calculation of specific heat near the λ point)

I. Introduction

Since Kamerlingh Onnes liquefied helium gas in 1908, surprising properties of liquid helium have been revealed [1]. Particularly, after the λ-transition was discovered, striking behavior of liquid helium has been found in the lower temperature phase (which is called helium II). Helium II comprises two components: a non-viscous component called the superfluid component and a viscous component called the normal-fluid component. These two components flow while interpenetrating each other. Each component has an independent velocity, although these two components are mutually mixed uniformly. The two velocities do not average out, even over time. In addition, the entropy value of each component does not take on the mean value: the superfluid component maintains entropy zero and the normal-fluid component maintains all the entropy of the whole liquid helium II. In addition to these properties, superfluid helium exhibits many characteristic phenomena: the fountain effect, the mechano-caloric effect, heat superconductivity and so on.

Many theoreticians have remained fascinated by these phenomena and have made efforts to clarify their origin [2–3]. Traditional theories related to liquid ^{4}He are classified into London's theory and Landau's theory. Actually, F. London [2] neglected interatomic potentials among helium atoms, and investigated the statistical physics of the system. Subsequently, he arrived at the result that Bose–Einstein condensation occurs at some finite temperature. He regarded this condensate of non-interacting helium atoms as the superfluid component. According to his theory, the velocity of the condensate must be equal to the velocity of the center of mass of liquid helium, which does not agree with the experimental results.

On the other hand, Tisza and Landau [3] independently proposed a two-fluid model. Landau developed this theory, in which he assumed the existence of a background flow inside the liquid helium II, which he named the superfluid component. In addition, he assumed that the residual component (normal fluid component) comprises a set of quasi-particles representing quantized modes of density waves, which he named the phonon and the roton. This theory explained the superfluidity of liquid helium and concurred with the specific heat near temperature zero. Many theoreticians followed Landau's method in their investigations of liquid helium.

Some calculated the single excitation energies of the quantized density wave (elementary excitation) approximately from the total Hamiltonian of liquid helium [4–7]. Bogoliubov [4] assumed macroscopic occupation of helium atoms with momentum zero and replaced the creation and annihilation operators with momentum zero to a c-number (classical number, not quantum number). He obtained an excitation spectrum like that of a phonon. Bogoliubov's transformation violates the number conservation law of helium atoms, although his work is very important to clarify the existence of phonons in an interacting bosen system. Based on Bogoliubov's theory, Miller, Pines and Nozieres [6] tried to take account of the backflow, which was first considered by Feynman and Cohen [6]. Feenberg [6] calculated the expansion series of the excitation energy systematically using the correlation functions. Sunakawa, Yamasaki, and Kebukawa [6] derived the same result on the basis of the density fluctuation and velocity operators. Sasaki and Matsuda [7] obtained the same result through unitary transformation.

The single particle excitation energy has been thus obtained using various perturbational approaches. However, it is necessary to clarify the structure of the total energy for a case with a macroscopic number of excitations because the number of excitations is macroscopically large at a nonzero temperature in a real liquid helium system. Several works have examined the structure of multiple excitations. For example, R. Balian and C. de Dominicis [4] used a self-consistent Bogoliubov transformation, and developed the old theory. However, the theory violates the number conservation law. Therefore, the number of quasi-particles is not equal to the number of helium atoms. Accordingly, the traditional theories of liquid helium present many difficulties.

About 30 years ago, one of the present authors exactly diagonalized the total Hamiltonian of one-dimensional (1D) interacting boson system with a repulsive delta function potential using unitary transformation [10, 11]. The result shows that the total energy of the multi-excitation is not equal to the sum of the energies of single excitation. In other words, the functional form of the total energy has a nonlinear form for the distribution function of quasi-particle number. This nonlinearity can be derived only from the Galilean covariance of the total energy. Therefore, nonlinearity also appears in almost all interacting many-body systems because the Galilean covariance holds. Therefore, it is necessary to investigate the statistical physics with a nonlinear form of the total energy. The investigation is executed in this book. The nonlinearity produces many important

behaviors in thermodynamic functions.

Experimental data at 1.6 K < T <2.17 K in liquid helium differ greatly from the calculated results according to the Landau theory. As an example, the values of specific heat are shown in the following figure.

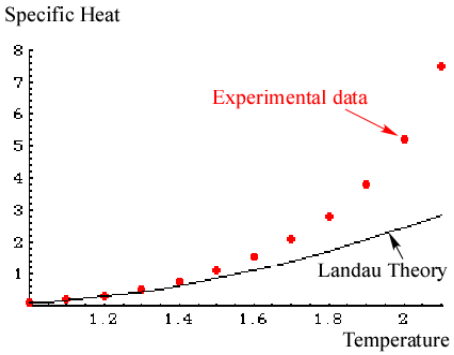

Fig. 1.1 Specific heat of superfluid helium

The dots indicate the experimental data of liquid helium, and the curve shows the calculated value of the Landau theory. Consequently, Landau's results deviate to a great degree from the experimental data at 1.6 K<T<2.17 K. The total energy of the Landau theory depends linearly on the number distribution function of elementary excitations. This property is not good in the actual system of liquid helium. We consider the nonlinear effect and develop the treatment of nonlinear properties. Thereby, we can clarify how the nonlinear structure produces the experimental behavior of liquid helium.

In this book, we assume the following two postulates. We can theoretically derive the qualitative characteristics of superfluid helium merely using the two postulates.

(Postulate l)

A unitary transformation U exists from the non-interacting states to the eigenstates of the total Hamiltonian in a liquid helium system.

It is noteworthy that the explicit form of U is never used herein; only the existence of U. This postulate is true because of the hermitian property of H and because of the property that no bound-state exists: no molecule is composed of plural helium atoms. These properties confirm the existence of a unitary transformation from the complete set of free states to the complete set of the eigenstates of H. In a previous paper [7], we demonstrated the approximated form of U up to the second order in the perturbation series for a 3D system. Moreover, in a 1D many-boson system, we obtained the exact form of U (see reference [10]).

(Postulate 2)
Single excitation energy from the ground state has a phonon-like spectrum in a small momentum region.

The detected dispersion curve of the elementary excitation exhibits phonon-like behavior in a small momentum region. Therefore, Postulate 2 agrees with the experimental results.

It is noteworthy that these two postulates are true in a 1D many-boson system with a repulsive delta function potential. The proofs have been presented in the relevant literature [10, 11], where the unitary transformation exactly diagonalizes the total Hamiltonian of the 1D system. This is summarized in Appendix I.

Using the two postulates described above, we can introduce a new concept, i.e. "dressed boson" whose creation and annihilation operators are defined as follows: Transform the creation and annihilation operators of a helium atom by the inverse unitary transformation of U. Then, new creation and annihilation operators are obtained. These new operators create or annihilate a quasi-particle, which represents the eigenstate of the total Hamiltonian of liquid helium. This quasi-particle is called the "dressed boson", which is the key to clarification of the mysterious mechanism of superfluid helium.

In chapter II, we will examine a diagonalized form of the total Hamiltonian. The functional form is nonlinear with respect to the momentum distribution function of the dressed bosons because the interactions among ^{4}He atoms are Galilean invariant. The nonlinear term is determined concretely using the experimental data of elementary excitation energy in neutron scatterings and using the latent heat per helium atom. This

explicit form of the nonlinear term produces the remarkable properties of liquid helium.

In chapter III, we will derive coupled integral equations that determine the momentum-distribution of the dressed bosons at equilibrium. At temperatures higher than the λ point, these equations have only one solution. On the other hand, for temperatures lower than the λ point, these equations have infinitely many solutions, even in fixing of the values of temperature, total number, and total momentum. The multiple solutions include a Bose condensate of the dressed bosons: a macroscopic number of dressed bosons with only one momentum value. Moreover, the condensed momentum value can be an arbitrary value within some range. The Bose condensate represents the superfluid component, and the residual dressed bosons represent the normal fluid component. Therein, even when the velocity of the normal fluid is fixed to a single value, many solutions exist in which the Bose condensed momenta differ from one another. Consequently, the velocity value of superfluid component can be chosen to be any value independent of the normal fluid velocity. For that reason, the solutions of momentum distribution of the dressed bosons reproduce the two-fluid model, which will be discussed in detail in chapter VIII.

H. Kojima et al. [9] measured the decreasing rate of superfluid velocity. They prepared liquid helium II, whose superfluid component flows with an initial velocity through a toroidal channel, and whose normal-fluid component has velocity zero. Then, the superfluid velocity did not decrease for the case of the initial superfluid velocity smaller than 33 cm/s. That is to say, the superfluid component flows permanently in this case. The superfluid velocity would decrease to 60 cm/s after 10^{10} years in their experimental result when the initial velocity was 67.7 cm/s. Accordingly the two-fluid states are extremely stable. The solutions obtained in the nonlinear theory have local maximum entropies. Therefore, the nonlinear theory well explains the stability of the two fluid states in liquid helium.

It is clarified in this book that the nonlinear theory produces the properties of liquid helium as

1) Existence of the λ-transition.

2) Two interpenetrating fluids coexist at a temperature lower than the λ- transition.

3) Any solution representing a two-fluid state has a local maximum entropy among the

thermal fluctuated states.

4) The fountain effect in superfluid helium. Dressed bosons satisfy the London equation.

5) Superfluidity and zero entropy for the superfluid component.

We can calculate the thermodynamic functions of liquid helium numerically using the concrete form of the nonlinear term determined in chapter II and using the iteration method presented in chapter III. We execute the calculations and obtain the theoretical results in good agreement with the experimental data for entropy and heat capacity. Moreover, examining the nonlinear properties in detail, we evaluate the specific heat near the λ point. The numerical result has logarithmic divergence at the λ point. The reason for the appearance of the logarithmic singularity is also clarified in an analytical method. We theoretically obtain the phase diagram between He II and He I, the critical index of the Bose-condensed number at the λ point, etc. via the nonlinear theory.

Accordingly, the nonlinear theory presented in this book engenders the theoretical explanation for the macroscopic behavior of liquid helium.

II. General Form of Total Energy

2.1 Unitary transformation

The total Hamiltonian *H* of liquid helium is given as

$$H = \sum_{\mathbf{p}} \frac{\mathbf{p}^2}{2m} a_{\mathbf{p}}^* a_{\mathbf{p}} + \frac{1}{2V} \sum_{\mathbf{p},\mathbf{q},\mathbf{k}} g(\mathbf{k}) a_{\mathbf{p}+\mathbf{k}}^* a_{\mathbf{q}-\mathbf{k}}^* a_{\mathbf{p}} a_{\mathbf{q}}\,, \tag{2.1}$$

where *m* is the mass of a helium atom, $a_{\mathbf{p}}^*$ and $a_{\mathbf{p}}$ respectively signify the creation and annihilation operators, $g(\mathbf{k})$ is the inter-atomic potential between helium atoms, *V* is the volume of the system, and $\mathbf{p},\mathbf{q},\mathbf{k}$ are the momenta whose values satisfy the periodic boundary conditions in a cubic box with side length *L* ($V = L^3$):

$$\begin{aligned} &p_x = (2\pi\hbar/L)\times \text{integer},\ p_y = (2\pi\hbar/L)\times \text{integer},\ p_z = (2\pi\hbar/L)\times \text{integer}, \\ &q_x = (2\pi\hbar/L)\times \text{integer}, q_y = (2\pi\hbar/L)\times \text{integer}, \cdots \\ &\hbar = \text{Planck's constant}/(2\pi). \end{aligned} \tag{2.2}$$

The operators $a_{\mathbf{p}}^*$ and $a_{\mathbf{p}}$ are the creation and annihilation operators satisfying the commutation relations

$$\left[a_{\mathbf{p}}, a_{\mathbf{q}}^*\right] = \delta_{\mathbf{p},\mathbf{q}}\,, \left[a_{\mathbf{p}}, a_{\mathbf{q}}\right] = \left[a_{\mathbf{p}}^*, a_{\mathbf{q}}^*\right] = 0\,, \tag{2.3}$$

where $\delta_{\mathbf{p},\mathbf{q}}$ represents Kronecker's delta function.

In this chapter, we examine the general form of the total energy of liquid helium system via the unitary transformation *U* diagonalizing the total Hamiltonian *H*. Actually, the existence of *U* is ensured by the fundamental requirement of quantum

physics, although the explicit form of U is unknown because of difficulty of the many-body problem. All eigenstates of H can be written using the transformation from free states of helium atoms (see Postulate 1 in chapter I), as

$$\left|\text{eigen state}\right\rangle = U a^*_{\mathbf{p}_1} a^*_{\mathbf{p}_2} a^*_{\mathbf{p}_3} \cdots a^*_{\mathbf{p}_N} \left|0\right\rangle, \tag{2.4}$$

where $\left|0\right\rangle$ denotes the vacuum state of the system, and where N is the total number of helium atoms. New creation and annihilation operators are defined as

$$A^*_{\mathbf{p}} = U a^*_{\mathbf{p}} U^{-1}, A_{\mathbf{p}} = U a_{\mathbf{p}} U^{-1}. \tag{2.5}$$

These new operators indicate creation and annihilation operators of a quasi-particle with an interaction cloud. We designate this quasi-particle as a "dressed boson" hereinafter. We rewrite the eigenstate (2.4) using the dressed boson operators, thereby obtaining

$$\left|\text{eigen state}\right\rangle = U a^*_{\mathbf{p}_1} U^{-1} U a^*_{\mathbf{p}_2} U^{-1} U a^*_{\mathbf{p}_3} \cdots a^*_{\mathbf{p}_N} U^{-1} U \left|0\right\rangle = A^*_{\mathbf{p}_1} A^*_{\mathbf{p}_2} A^*_{\mathbf{p}_3} \cdots A^*_{\mathbf{p}_N} U \left|0\right\rangle. \tag{2.6}$$

Because the vacuum state $\left|0\right\rangle$ is the eigenstate of H, we get

$$U\left|0\right\rangle = \left|0\right\rangle \tag{2.7}$$

Substitution of that equation into the right-hand-side of Eq. (2.6) yields

$$\left|\text{eigenstate}\right\rangle = A^*_{\mathbf{p}_1} A^*_{\mathbf{p}_2} A^*_{\mathbf{p}_3} \cdots A^*_{\mathbf{p}_N} \left|0\right\rangle . \tag{2.8}$$

Therefore, the direct products of the dressed boson operators express all the eigenstates of liquid helium. Accordingly, the operator $A^*_{\mathbf{p}}$ creates a quasi-particle representing an eigenstate of *H*. Using the dressed boson operators; we can rewrite the eigenequation of *H* as the following.

$$H\ A^*_{\mathbf{p}_1} A^*_{\mathbf{p}_2} A^*_{\mathbf{p}_3} \cdots A^*_{\mathbf{p}_N} \left|0\right\rangle = E\left(\mathbf{p}_1, \mathbf{p}_2, \cdots, \mathbf{p}_N\right) A^*_{\mathbf{p}_1} A^*_{\mathbf{p}_2} A^*_{\mathbf{p}_3} \cdots A^*_{\mathbf{p}_N} \left|0\right\rangle \tag{2.9}$$

This equation indicates that the total energy of the liquid helium depends only upon the number distribution of the dressed bosons in momentum space. That is to say, the eigenenergy *E* is expressed with the number distribution $\left\{n_{\mathbf{p}}\right\}$ as

$$E = E\left(\left\{n_{\mathbf{p}}\right\}\right), \tag{2.10}$$

where

$$n_{\mathbf{p}} = A^*_{\mathbf{p}} A_{\mathbf{p}} \tag{2.11}$$

is the number of dressed bosons with momomtum **p**.

2.2 Galilean covariant form of total energy

The total Hamiltonian *H* is Galilean covariant. Therefore the diagonal form of *H* is the sum of the kinetic energy *K* of the center of mass and Galilean invariant terms *X*.

$$H = K + X \tag{2.12}$$

$$K = \frac{\mathbf{Q}^2}{2M} \tag{2.13}$$

In Eq. (2.13), M is the total mass and $\mathbf{Q}$ is the total momentum of liquid helium. Because of the total momentum conservation, we obtain the following relations.

$$\mathbf{Q} = \sum_{\mathbf{q}} \mathbf{q} a_{\mathbf{q}}^* a_{\mathbf{q}} = U \sum_{\mathbf{q}} \mathbf{q} a_{\mathbf{q}}^* a_{\mathbf{q}} U^{-1} = \sum_{\mathbf{q}} \mathbf{q} A_{\mathbf{q}}^* A_{\mathbf{q}} = \sum_{\mathbf{q}} \mathbf{q} n_{\mathbf{q}} \tag{2.14}$$

Hamiltonian H conserves the total number of helium atoms; therefore, the unitary transformation U diagonalizes H and N simultaneously.

$$N = \sum_{\mathbf{q}} a_{\mathbf{q}}^* a_{\mathbf{q}} = U \sum_{\mathbf{q}} a_{\mathbf{q}}^* a_{\mathbf{q}} U^{-1} = \sum_{\mathbf{q}} A_{\mathbf{q}}^* A_{\mathbf{q}} = \sum_{\mathbf{q}} n_{\mathbf{q}} \tag{2.15}$$

Accordingly, the total number of helium atoms is equal to the total number of the dressed bosons. Substitution of Eqs.(2.14) and (2.15) into Eq. (2.13) yields

$$K = \frac{\sum_{\mathbf{p}} \mathbf{p} n_{\mathbf{p}} \bullet \sum_{\mathbf{q}} \mathbf{q} n_{\mathbf{q}}}{2M} = \frac{\sum_{\mathbf{p},\mathbf{q}} \left[-\frac{1}{2}(\mathbf{p}-\mathbf{q})^2 + \frac{1}{2}(\mathbf{p}^2 + \mathbf{q}^2) \right] n_{\mathbf{p}} n_{\mathbf{q}}}{2M} = \frac{-\sum_{\mathbf{p},\mathbf{q}} \frac{1}{2}(\mathbf{p}-\mathbf{q})^2 n_{\mathbf{p}} n_{\mathbf{q}}}{2M} + \sum_{\mathbf{p}} \frac{\mathbf{p}^2}{2m} n_{\mathbf{p}} \tag{2.16}$$

where

$$m = M/N \tag{2.17}$$

is the mass of the helium atom. Then, the diagonal form of the total Hamiltonian H is expressed as the following.

$$H = K + X = \sum_{\mathbf{p}} \frac{\mathbf{p}^2}{2m} n_{\mathbf{p}} - \frac{1}{2M} \sum_{\mathbf{p},\mathbf{q}} \frac{1}{2}(\mathbf{p}-\mathbf{q})^2 n_{\mathbf{p}} n_{\mathbf{q}} + X = \sum_{\mathbf{p}} \frac{\mathbf{p}^2}{2m} n_{\mathbf{p}} + (\text{Galilean invariant terms}) \tag{2.18}$$

Galilean invariant terms are described only by relative momenta of dressed bosons. They are expressed using arbitrary functions f_s as

$$(\text{Galileaninvariantterms}) = \frac{1}{N}\sum_{\mathbf{p},\mathbf{q}} f_2(\mathbf{p}-\mathbf{q}) n_{\mathbf{p}} n_{\mathbf{q}} + \frac{1}{N^2}\sum_{\mathbf{p},\mathbf{q},\mathbf{k}} f_3(\mathbf{p}-\mathbf{q},\mathbf{p}-\mathbf{k}) n_{\mathbf{p}} n_{\mathbf{q}} n_{\mathbf{k}} + \cdots \quad (2.19)$$

The function f_s indicates the coefficient of term where *s* dressed bosons mutually correlate. It is also noteworthy that f_1 does not exist because the relative momenta cannot be made of only one momentum. Galilean invariant terms are nonlinearly dependent upon number operators of dressed bosons. According to (2.18) and (2.19), the total energy of liquid helium has the following form.

$$E = \sum_{\mathbf{p}} \frac{\mathbf{p}^2}{2m} n_{\mathbf{p}} + \frac{1}{N}\sum_{\mathbf{p},\mathbf{q}} f_2(\mathbf{p}-\mathbf{q}) n_{\mathbf{p}} n_{\mathbf{q}} + \frac{1}{N^2}\sum_{\mathbf{p},\mathbf{q},\mathbf{k}} f_3(\mathbf{p}-\mathbf{q},\mathbf{p}-\mathbf{k}) n_{\mathbf{p}} n_{\mathbf{q}} n_{\mathbf{k}} + \cdots \quad (2.20)$$

The correlation with many particles decreases when the system becomes dilute. The terms $f_3\ f_4\ f_5 \cdots$ are smaller than f_2 because a three particle collision is a rare case for diluteness of liquid helium compared with an ordinary liquid. We can therefore neglect higher terms. Thereby we obtain

$$E = \sum_{\mathbf{p}} \frac{\mathbf{p}^2}{2m} n_{\mathbf{p}} + \frac{1}{N}\sum_{\mathbf{p},\mathbf{q}} f(\mathbf{p}-\mathbf{q}) n_{\mathbf{p}} n_{\mathbf{q}} \quad (2.21)$$

As the details are examined in Sec. 2.5, the function form $f(\mathbf{k}) - f(0)$ is related directly to $|\mathbf{k}|$ for a small value of $|\mathbf{k}|$. The property is derived from Postulate 2 in chapter I to yield a phonon-like behavior in the excitation of dressed boson. The nonlinear form of (2.21) produces characteristic properties of liquid helium: temperature dependence of thermodynamic functions, two fluid mechanism, and so on. The mechanism will be examined in greater detail in chapters III–XI.

In a 1D system, we have exact quantum solutions for interacting of many bosons. The total energy of the system also has a nonlinear form. The details are discussed in section 2.3. (Readers who are only interested in properties of liquid helium can skip sections 2.3 and 2.4.).

2.3 Exact form of total energy in a one-dimensional system

We have an exact solution for an interacting many-boson system. The system is a 1D many-boson system via a repulsive delta-function potential. The eigenenergies were obtained by Girardeau, Lieb, and Liniger [5]. The diagonalization of the total Hamiltonian via the unitary transformation was solved by Sasaki and Kebukawa [10].

The Hamiltonian is

$$H = \sum_p \frac{p^2}{2m} a_p^* a_p + \frac{g}{2L} \sum_{p,q,k} a_{p+k}^* a_{q-k}^* a_p a_q \ , \tag{2.22}$$

where m is the mass of a boson and L is the length of the 1D space. The diagonal form of the Hamiltonian is

$$H = \sum_p \frac{p^2}{2m} A_p^* A_p + \sum_{p,q} \frac{\pi\hbar|p-q|}{2mL} A_p^* A_p A_q^* A_q + \frac{1}{2m}\left(\frac{\pi\hbar}{L}\right)^2 \frac{N\left(N^2-1\right)}{3} \tag{2.23}$$

for an infinitely large coupling constant g, where

$$A_p = U a_p U^{-1} \text{, and } A_p^* = U a_p^* U^{-1} \text{.} \tag{2.24}$$

The unitary transformation U is described explicitly in Appendix I. In a finite coupling constant value, the diagonal form is expanded by $(1/g)$ as the following.

$$\begin{aligned} H = & \sum_p \frac{p^2}{2m} A_p^* A_p + \frac{1}{2m}\left\{-\frac{2\hbar^2}{Lmg} + \left(\frac{2\hbar^2}{Lmg}\right)^2 \frac{3N}{2}\right\} \sum_{p,q} (p-q)^2 A_p^* A_p A_q^* A_q \\ & + \frac{1}{2m}\left\{1 - \frac{2\hbar^2}{Lmg} 2N + \left(\frac{2\hbar^2}{Lmg}\right)^2 3N^2\right\}\left\{\sum_{p,q} \frac{\pi\hbar|p-q|}{L} A_p^* A_p A_q^* A_q + \left(\frac{\pi\hbar}{L}\right)^2 \frac{N\left(N^2-1\right)}{3}\right\} \\ & + \text{Order}\left(1/g^3\right) \end{aligned} \tag{2.25}$$

This result shows that the nonlinear form (2.21) is reasonable. More details are presented in Appendix I.

2.4 Calculation of single excitation energy in liquid Helium

A liquid helium system in three-dimensional (3D) space cannot be solved exactly. Many investigations have been carried out to find an approximate form of the single excitation energy for the Hamiltonian (2.1) [4–7].

One is the Bogoliubov theory [4]. Therein, almost all bosons are considered to have momentum zero; the operators a_0 and a_0^* are replaced by the c-number $\sqrt{N}$ as

$$a_0 \to \sqrt{N} \text{ and } a_0^* \to \sqrt{N} . \tag{2.26}$$

Then, the total Hamiltonian is approximately equal to the following form.

$$H \approx \frac{N^2}{V}\frac{g(0)}{2} + H_{\mathrm{B}} + \text{higher order terms} \tag{2.27}$$

$$H_B = \sum_{\mathbf{p}} \frac{\mathbf{k}^2}{2m} a_{\mathbf{k}}^* a_{\mathbf{k}} + \frac{N}{2V}\sum_{\mathbf{k}} g(\mathbf{k})\left(a_{\mathbf{k}}^* a_{-\mathbf{k}}^* + a_{\mathbf{k}}^* a_{\mathbf{k}} + a_{-\mathbf{k}}^* a_{-\mathbf{k}} + a_{-\mathbf{k}} a_{\mathbf{k}}\right) \tag{2.28}$$

We call H_B a Bogoliubov Hamiltonian. This Bogoliubov Hamiltonian does not conserve the total boson number because the replacement from the operators a_0 and a_0^* to the c-number $\sqrt{N}$ violates the total number conservation. This simple Hamiltonian can be diagonalized as the following.

$$H_{\mathrm{B}} = \sum_{\mathbf{k}} E_{\mathbf{k}}^{\mathrm{B}} c_{\mathbf{k}}^* c_{\mathbf{k}} - \sum_{\mathbf{k}\neq 0} \frac{\mathbf{k}^2}{8m} \frac{(\lambda_{\mathbf{k}} - 1)^2}{\lambda_{\mathbf{k}}^2} \tag{2.29}$$

$$a_{\mathbf{k}} = \cosh(2f(\mathbf{k}))c_{\mathbf{k}} - \sinh(2f(\mathbf{k}))c_{-\mathbf{k}}^* \tag{2.30a}$$

$$a_{\mathbf{k}}^* = \cosh(2f(\mathbf{k}))c_{\mathbf{k}}^* - \sinh(2f(\mathbf{k}))c_{-\mathbf{k}} \tag{2.30b}$$

$$E_{\mathbf{k}}^{B} = \mathbf{k}^2 / (2m\lambda_{\mathbf{k}}) \tag{2.31}$$

$$\cosh(2f(\mathbf{k})) = (4\lambda_{\mathbf{k}})^{-1/2}(1+\lambda_{\mathbf{k}}), \quad \sinh(2f(\mathbf{k})) = (4\lambda_{\mathbf{k}})^{-1/2}(1-\lambda_{\mathbf{k}}) \tag{2.32}$$

$$\lambda_{\mathbf{k}} = k\left(\mathbf{k}^2 + 4mN\, g(\mathbf{k}) / (\hbar^2 V)\right)^{-1/2} \tag{2.33}$$

The excitation energy in the Bogoliubov theory $E_{\mathbf{k}}^{B}$ is proportional to the momentum k for a small value of k. It is theoretically clarified that the elementary excitation energy has a phonon-like behavior at a small momentum.

Subsequently, many physicists tried to improve the Bogoliubov theory. The backflow effect is considered by Feynman and Cohen, and is investigated based on the Bogoliubov theory by Miller, Pines, and Nozieres [6]. Feenberg calculated the expansion series of the excitation energy systematically on the basis of correlation functions. Nishiyama also investigated a new formulation using the number density operator and the phase operator [6].

Sunakawa, Yamasaki, and Kebukawa [6] rewrote the total Hamiltonian of liquid helium using the density fluctuation operator and its velocity operator. Hereafter, we call that theory the *SYK theory*. They evaluated the single excitation spectrum for a potential with square shape. As Fig. 2.1 shows, their numerical calculation of the excitation energy showed good agreement with the experimental data. Their operators indicate the creation and annihilation operators of density wave mode. Therefore the total number of the modes in SYK theory does not relate with the total number of helium atoms. Consequently, it is difficult in their theory to discuss Bose condensation.

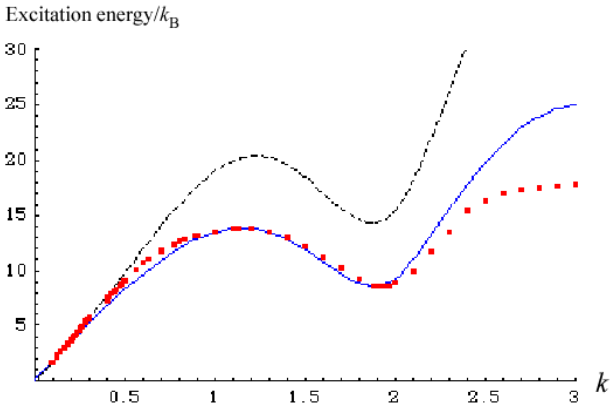

Fig. 2.1 Elementary excitation energy ($E_{\mathbf{k}}/k_B$)

Dots signify the experimental values of the excitation energy in neutron scatterings. The blue curve represents the calculation result of Sunakawa et al. The curve shown with a dashed line portrays the result obtained using the Bogoliubov theory.

Sasaki and Matsuda [7] attempted to improve the SYK theory. Sasaki and Matsuda found the unitary transformation satisfying number conservation in perturbation method up to the second order. The unitary transformation produces the dressed boson operators $\alpha_{\mathbf{p}}^*, \alpha_{\mathbf{p}}$. Then the total number conservation holds as

$$\alpha_0^* \alpha_0 + \sum_{\mathbf{p}\neq 0} \alpha_{\mathbf{p}}^* \alpha_{\mathbf{p}} = \sum_{all\ \mathbf{p}} a_{\mathbf{p}}^* a_{\mathbf{p}} \ , \tag{2.34}$$

which was shown in (4.32) of reference [7]. Accordingly, the Bose condensate of dressed bosons appears at a sufficiently low temperature. The dressed boson excitation energy from momentum zero to **p** is equal to the excitation energy of the density mode in SYK theory.

The single particle excitation energy has been approximately obtained in various perturbational approaches. It is necessary to determine properties of multiple

excitations to study the thermodynamic functions of liquid helium. That property is examined in subsequent sections.

2.5 Determination of Galilean invariant term in energy using experimental data

The ground state of the system is expressed as

$$\left|\text{Ground state}\right\rangle = U\left(a_0^*\right)^N \left|0\right\rangle = \left(A_0^*\right)^N \left|0\right\rangle . \tag{2.35}$$

The eigenequation of H is

$$H\left(A_0^*\right)^N \left|0\right\rangle = E_G \left(A_0^*\right)^N \left|0\right\rangle , \text{ and} \tag{2.36a}$$

$$E_G = f(0)N , \tag{2.36b}$$

which are readily derived from Eq. (2.21). This equation indicates that the value $-f(0)$ is the latent heat per atom at zero Kelvin.

$$f(0) = -\text{ (latent heat per atom at zero Kelvin)} \tag{2.37}$$

The single excitation state is

$$\left|\text{single excitation state}\right\rangle = A_{\mathbf{p}}^* \left(A_0^*\right)^{N-1} \left|0\right\rangle . \tag{2.38}$$

Because the number distribution of the single excitation state is $\left\{n_0 = N-1,\, n_{\mathbf{p}} = 1\right\}$, the total energy can be expressed as the following.

$$E = \frac{\mathbf{p}^2}{2m} + \frac{1}{N}\left(f(0)(N-1)^2 + f(\mathbf{p})(N-1) + f(-\mathbf{p})(N-1) + f(\mathbf{p}-\mathbf{p})\right)$$
$$\approx f(0)N + \frac{\mathbf{p}^2}{2m} + 2\left(f(\mathbf{p}) - f(0)\right) \tag{2.39}$$

In that equation, we used $1/N \approx 0$ and the spherical symmetric property of the function $f(\mathbf{p})$ in (2.21). Comparison of two energies (2.36b) and (2.39) gives the energy increase as $\frac{\mathbf{p}^2}{2m} + 2\left(f(\mathbf{p}) - f(0)\right)$. This increasing energy indicates the single excitation energy ε_p^0.

$$\varepsilon_p^0 = \frac{\mathbf{p}^2}{2m} + 2\left(f(\mathbf{p}) - f(0)\right) \tag{2.40}$$

The energy was detected by neutron scattering experiments in liquid helium [1, 8, 25]. Therefore, the Galilean invariant term is expressed as the following.

$$f(\mathbf{p}) = \tfrac{1}{2}\left(\varepsilon_p^0 - \mathbf{p}^2/(2m)\right) + f(0) \tag{2.41}$$

The function form of $f(\mathbf{p})$ is thus determined from experimental data of the elementary excitation energy ε_p^0 and the latent heat $-f(0)$ per atom at the temperature $T = 0$.

The energy spectrum of elementary excitation is measured using neutron scattering experiments [8, 25]. These experimental values are presented in Table I. We can apply the experimental values of 1.1 K for ε_p^0 (which is the excitation energy at zero Kelvin) because the experimental energy spectrum does not vary for changing of temperature value in the region lower than 1.3 K.

Table I Experimental data of elementary excitation energy

(The unit of $p/(10^{10}\hbar)$ is $\overset{\circ}{A}^{-1}$; the unit of ε_p^0/k_B is K.)

$p/(10^{10}\hbar)$	ε_p^0/k_B	$p/(10^{10}\hbar)$	ε_p^0/k_B	$p/(10^{10}\hbar)$	ε_p^0/k_B	$p/(10^{10}\hbar)$	ε_p^0/k_B
0.0894	1.6131	0.3	5.65	1.1	13.8	1.94	8.63
0.0946	1.7175	0.4	7.4	1.13	13.82	1.94	8.609
0.115	2.1005	0.4036	7.6361	1.2	13.75	1.95	8.65
0.121	2.2514	0.4082	7.7173	1.3	13.5	1.95	8.633
0.139	2.6111	0.4187	7.9146	1.4	12.95	1.96	8.683
0.143	2.6343	0.4232	7.9958	1.5	12.2	1.96	8.672
0.1594	2.9709	0.4355	8.1815	1.6	11.2	1.97	8.695
0.1767	3.2958	0.4498	8.3788	1.7	10.25	2	8.95
0.1818	3.3887	0.4643	8.6457	1.8	9.25	2.1	10
0.1938	3.6324	0.4785	8.8662	1.88	8.694	2.2	11.65
0.199	3.7368	0.4926	9.1099	1.89	8.657	2.3	13.55
0.2	3.7	0.5	9.15	1.9	8.7	2.4	15.5
0.211	3.9689	0.5605	10.1544	1.9	8.654	2.5	16.45
0.2162	4.085	0.6	10.75	1.9	8.634	2.6	17
0.2278	4.2822	0.6243	11.0015	1.91	8.635	2.7	17.3
0.2329	4.3867	0.6965	11.8023	1.91	8.616	2.8	17.5
0.2445	4.6072	0.7	11.75	1.915	8.611	2.9	17.7
0.2495	4.7116	0.7649	12.4173	1.92	8.626	3	17.85
0.2611	4.9205	0.8	12.72	1.92	8.61	3.1	18
0.2776	5.2339	0.8	12.65	1.925	8.606	3.2	18.15
0.2825	5.3267	0.83	12.8815	1.93	8.626	3.3	18.3
0.2938	5.524	0.8925	13.2297	1.93	8.606	3.4	18.35
0.2988	5.6284	0.9	13.15	1.935	8.63	3.5	18.4
0.3	5.57	1	13.55	1.935	8.612	3.6	18.45

We find the analytical form of ε_p^0 which fits the experimental data. The momentum region is divided into five regions: phonon, maxon, roton, high-momentum region 1, and high-momentum region 2. The function forms for each region are chosen as the following.

(Phonon region)

$$\varepsilon_p^0 = c_1\, p \qquad \text{for } 0 \le p \le p_1 \tag{2.42}$$

(Maxon region)

$$\varepsilon_p^0 = k_B\left(g_0 + g_2(p - p_M)^2 + g_3(p - p_M)^3 + g_4(p - p_M)^4 + g_5(p - p_M)^5\right)$$

$$\text{for } p_1 \le p \le p_2 \tag{2.43}$$

(Roton region)

$$\varepsilon_p^0 = \Delta + \frac{(p - p_0)^2}{2m \times r} \qquad \text{for } p_2 \le p \le p_3 \tag{2.44}$$

(High momentum region 1)

$$\varepsilon_p^0 = b_0 + c_1(p - p_3) + b_2(p - p_3)^2 + b_3(p - p_3)^3 \qquad \text{for } p_3 \le p \le p_4$$

(2.45)

(High momentum region 2)

$$\varepsilon_p^0 = d_0 + d_1(p - p_4) + d_2(p - p_4)^2 \qquad \text{for } p_4 \le p \le 3.6 \times 10^{10}\hbar \tag{2.46}$$

We abbreviate the momentum region larger than $3.6 \times 10^{10}\hbar$. These function forms have several properties: (1) The excitation energy in the phonon region has the first sound velocity. (2) The shape near the roton minimum is a parabolic curve. (3) In the high-momentum region 1, the velocity is in agreement with the first sound velocity. Therefore, we adopt the following values for several parameters.

$$c_1 = 238\,[\mathrm{m/s}] \tag{2.47}$$

This value is used in (2.42) and (2.45).

The roton parameters are

$$\Delta = 8.61\, k_B \tag{2.48}$$

$$p_0 = 1.92 \times 10^{10}\, \hbar \tag{2.49}$$

$$r = 0.153 \tag{2.50}$$

Table I shows that the maximum energy in the maxon region is 13.82 k_B at momentum $1.13 \times 10^{10}\ \hbar$. We apply these values as

$$g_0 = 13.82 \tag{2.51}$$

$$p_M = 1.13 \times 10^{10}\ \hbar \tag{2.52}$$

The function form of (2.46) fits the experimental data for the parameter values as

$$d_0 = 16.7526 \times k_B \tag{2.53}$$

$$d_1 = 3.22877 \times k_B / \left(10^{10} \hbar\right) \tag{2.54}$$

$$d_2 = -1.56968 \times k_B / \left(10^{10} \hbar\right)^2 \tag{2.55}$$

Three boundaries between four momentum regions are given as

$$p_1 = 0.5 \times 10^{10}\ \hbar \tag{2.56}$$

$$p_2 = 1.78 \times 10^{10}\ \hbar \tag{2.57}$$

$$p_4 = 2.55 \times 10^{10}\ \hbar \tag{2.58}$$

The remaining boundary is determined as follows: Equation (2.45) shows that the velocity of high-momentum region 1 becomes the first sound velocity c_1 at $p = p_3$. Accordingly, the roton energy is expected to have the same derivative at the boundary $p = p_3$ to hold a smooth connection at the boundary. Accordingly, the value of p_3 is

$$p_3 = 2.1495 \times 10^{10}\ \hbar\,. \tag{2.59}$$

The continuous connection at $p = p_3$ leads to the following value of parameter b_0.

$$b_0 = \Delta + \frac{(p_3 - p_0)^2}{2m \times r} = 10.696 \times k_B\,. \tag{2.60}$$

The parameters g_2, g_3, g_4 and g_5 are determined so that the phonon curve and roton curve connect smoothly to the maxon curve at $p = p_1$ and $p = p_2$: the function value and the derivative are connected to both curves. In addition, the values of b_2 and b_3 are determined by the conditions for smooth connection at $p = p_4$. The numerical results are the following.

$$g_2 = -10.8805 \Big/ \left(10^{10}\hbar\right)^2 \tag{2.61}$$

$$g_3 = -1.81497 \Big/ \left(10^{10}\hbar\right)^3 \tag{2.62}$$

$$g_4 = -0.966809 \Big/ \left(10^{10}\hbar\right)^4 \tag{2.63}$$

$$g_5 = 7.19044 \Big/ \left(10^{10}\hbar\right)^5 \tag{2.64}$$

$$b_2 = 14.4344 \times k_B / \left(10^{10}\hbar\right)^2 \tag{2.65}$$

$$b_3 = -55.0958 \times k_B / \left(10^{10}\hbar\right)^3 \tag{2.66}$$

Therefore, all the parameters have been determined. The analytical forms of (2.42)–(2.46) show good agreement with the experimental data of the elementary excitation energies, as presented in Fig. 2.2.

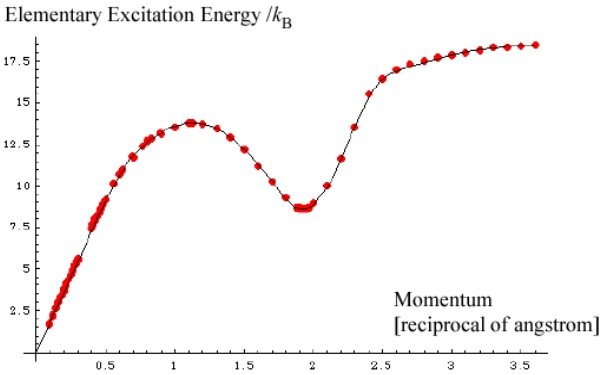

Fig. 2.2 Elementary excitation energy ($\varepsilon_{\mathbf{p}} / k_B$)

The dots express the excitation energies detected in neutron scatterings. The curve also expresses the function defined by (2.42)–(2.46). The unit for the vertical axis scale is K; the horizontal axis expresses $p/\left(10^{10}\hbar\right)$ in the unit of the reciprocal of angstrom.

Using the explicit forms (2.42)–(2.46) and the parameter values (2.47)–(2.66), we determined the function form $f(\mathbf{p})$. In other words, the Galilean invariant term is determined concretely. The value of $f(0)$ is shown on page 393 of reference [24]:

$$f(0) \approx -7.16 \times k_B \ . \tag{2.67}$$

Consequently, the nonlinear term is expressed as

$$f(\mathbf{p}) = \tfrac{1}{2}\left(c_1 p - \mathbf{p}^2/(2m)\right) - 7.16k_B \qquad \text{for } 0 \le p \le p_1 \tag{2.68a}$$

$$f(\mathbf{p}) = \tfrac{1}{2}k_B\left(g_0 + g_2(p-p_M)^2 + g_3(p-p_M)^3 + g_4(p-p_M)^4 + g_5(p-p_M)^5\right) - \tfrac{1}{2}\mathbf{p}^2/(2m) - 7.16k_B$$

$$\text{for } p_1 \le p \le p_2 \tag{2.68b}$$

$$f(\mathbf{p}) = \tfrac{1}{2}\left(\Delta + \frac{(p-p_0)^2}{2m \times r} - \mathbf{p}^2/(2m)\right) - 7.16k_B \qquad \text{for } p_2 \le p \le p_3 \tag{2.68c}$$

$$f(\mathbf{p}) = \tfrac{1}{2}\left(b_0 + c_1(p-p_3) + b_2(p-p_3)^2 + b_3(p-p_3)^3\right) - \tfrac{1}{2}\mathbf{p}^2/(2m) - 7.16k_B \qquad \text{for } p_3 \le p \le p_4 \tag{2.68d}$$

$$f(\mathbf{p}) = \tfrac{1}{2}\left(d_0 + d_1(p-p_4) + d_2(p-p_4)^2 - \mathbf{p}^2/(2m)\right) - 7.16k_B$$

$$\text{for } p_4 \le p \le 3.6 \times 10^{10}\hbar \tag{2.68e}$$

The parameter values are shown in Eqs. (2.47)–(2.66).

The excitation energy of dressed boson depends upon T via the nonlinear dependence (which is discussed in detail in subsequent chapters) when the temperature becomes high. The nonlinear mechanism was investigated by the authors in several previous studies [12], [19], [20], [22], and [27].

III. Temperature Dependence of the Excitation Energy

Nonlinearity in Eq. (2.21) produces the temperature dependence of the excitation energy. We examine the dressed boson energy. The energy of one dressed boson is an increase value of the total energy when one dressed boson is added to the system. Therefore, the dressed boson energy is defined as

$$\omega_{\mathbf{p}} = \frac{\delta E}{\delta n_{\mathbf{p}}} . \tag{3.1}$$

Substitution of (2.21) into (3.1) yields

$$\omega_{\mathbf{p}}(T) = \frac{\mathbf{p}^2}{2m} + \frac{2}{N}\sum_{\mathbf{q}} f(\mathbf{p}-\mathbf{q}) n_{\mathbf{q}} - \frac{1}{N^2}\sum_{\mathbf{s},\mathbf{t}} f(\mathbf{s}-\mathbf{t}) n_{\mathbf{s}} n_{\mathbf{t}} , \tag{3.2}$$

where we have used $f(\mathbf{p}-\mathbf{q}) = f(\mathbf{q}-\mathbf{p})$. The dressed boson energy depends upon the distribution $\{n_{\mathbf{q}}\}$, as is readily apparent in Eq. (3.2). The distribution $\{n_{\mathbf{q}}\}$ varies with the change of temperature: the dressed boson energy is temperature-dependent. This nonlinear effect has been examined in the literature [12].

3.1 Dressed Boson distribution

We examine the number distribution of dressed bosons in this section. The calculation method determining the distribution function is explained separately in two cases of $T < T_\lambda$ and $T > T_\lambda$.

3.1.1 Case of $T < T_\lambda$

The energy $\omega_{\mathbf{p}}$ depends upon the number distribution of the other dressed bosons. This property produces a two-fluid state with different velocities of the superfluid component and the normal fluid component for $T < T_\lambda$. The complex mechanism will be examined in chapter VIII. We study the case for $\mathbf{v}_n = 0$ and $\mathbf{v}_s = 0$ in this chapter, where $\mathbf{v}_n$ and $\mathbf{v}_s$ respectively represent the velocities of normal fluid and superfluid components.

For $\mathbf{v}_n = \mathbf{v}_s = 0$, the number distribution of dressed bosons in a thermal equilibrium is given as the following.

$$n_{\mathbf{p}} = \frac{1}{\exp\left(\left(\omega_{\mathbf{p}}(T) - \mu\right)/\left(k_{\mathrm{B}}T\right)\right) - 1} \tag{3.3}$$

$$\omega_0(T) \approx \mu \qquad (\text{for } T < T_\lambda) \tag{3.4}$$

Therein, μ is the chemical potential and k_B is Boltzmann's constant. This distribution is a well-known form in boson system, except the nonlinear mechanism of Eq. (3.2). The derivation is explained in details in chapter VIII. The chemical potential μ is nearly equal to ω_0 when a temperature T is lower than the λ transition temperature T_λ. Therein, n_0 becomes a macroscopic number (for $T < T_\lambda$). Consequently, Bose–Einstein condensation of the dressed bosons appears.

The dressed boson energy in the Bose condensate is ω_0; therefore the excitation energy from the Bose condensate is the difference between $\omega_{\mathbf{p}}$ and ω_0.

$$\varepsilon_{\mathbf{p}}(T) = \omega_{\mathbf{p}}(T) - \omega_0(T) = \frac{\mathbf{p}^2}{2m} + \frac{2}{N}\sum_{\mathbf{q}}\left(f(\mathbf{p}-\mathbf{q}) - f(-\mathbf{q})\right)n_{\mathbf{q}} \tag{3.5}$$

Hereinafter, we call an excitation from the Bose–Einstein condensate *excitation from BEC*. We denote the excitation energy from BEC as $\varepsilon_{\mathbf{p}}(T)$; then we obtain the simultaneous equations as the following.

$$n_{\mathbf{p}} = \frac{1}{\exp\left(\varepsilon_{\mathbf{p}}(T)/(k_{\mathrm{B}}T)\right)-1} \tag{3.6a}$$

$$\varepsilon_{\mathbf{p}}(T) = \frac{\mathbf{p}^2}{2m} + \frac{2\left(f(\mathbf{p}) - f(0)\right)n_0}{N} + \frac{2}{N}\sum_{\mathbf{q}\neq 0}\left(f(\mathbf{p}-\mathbf{q}) - f(-\mathbf{q})\right)n_{\mathbf{q}} \tag{3.6b}$$

We cannot exactly solve these simultaneous equations because of their nonlinearity. Nevertheless, it is possible to find approximate solutions, as explained in section 3.2.

At $T = 0$, all dressed bosons have momentum of zero ($n_0 = N$). Accordingly, Eq. (3.6b) becomes

$$\begin{aligned}\varepsilon_{\mathbf{p}}(T) &= \frac{\mathbf{p}^2}{2m} + 2\left(f(\mathbf{p}) - f(0)\right) \\ &= \varepsilon_{\mathbf{p}}^0\end{aligned}, \tag{3.7}$$

where we have used (2.41). In this case, the number of dressed bosons becomes

$$n_{\mathbf{p}} = \frac{1}{\exp\left(\varepsilon_{\mathbf{p}}^0/(k_{\mathrm{B}}T)\right)-1} \qquad \text{(near zero Kelvin).} \tag{3.8}$$

Consequently, the momentum distribution of dressed bosons near zero Kelvin is equal to the number distribution of the elementary excitations in the Landau theory. The dressed boson energy with momentum zero at zero Kelvin is

$$\omega_0(0) = \frac{2}{N} f(0)n_0 - \frac{1}{N^2} f(0)n_0 n_0 = f(0). \tag{3.9}$$

This concept does not exist in the Landau theory. This value is the chemical potential of liquid helium at zero Kelvin. The excitation energy $\omega_{\mathbf{p}} - \omega_0$ from the Bose–Einstein condensate depends upon the temperature value when the temperature becomes high. The dependence is calculated in section 3.2.

3.1.2 Case of $T > T_\lambda$

In this case, the value of n_0 is not a macroscopic number. Therefore, the simultaneous equations are the following.

$$n_{\mathbf{p}} = \frac{1}{\exp\left(\left(\omega_{\mathbf{p}}(T) - \mu\right)/\left(k_{\mathrm{B}}T\right)\right) - 1} \tag{3.10a}$$

$$\omega_{\mathbf{p}}(T) = \frac{\mathbf{p}^2}{2m} + \frac{2}{N}\sum_{\mathbf{q}} f(\mathbf{p}-\mathbf{q}) n_{\mathbf{q}} - \frac{1}{N^2}\sum_{\mathbf{s},\mathbf{t}} f(\mathbf{s}-\mathbf{t}) n_{\mathbf{s}} n_{\mathbf{t}} \tag{3.10b}$$

There is no singularity in the simultaneous equations (3.10a,b) because of $\omega_0(T) > \mu$ for $T > T_\lambda$. These simultaneous equations are solvable approximately. The method is discussed below.

3.2 Integral equation for determining dressed boson energy

3.2.1 Integral equation

We substitute (3.6a) into (3.6b) to rewrite the simultaneous equations to an integral equation as in the following expression.

$$\varepsilon_{\mathbf{p}}(T) = \frac{\mathbf{p}^2}{2m} + \frac{2\left(f(\mathbf{p}) - f(0)\right)n_0}{N} + \frac{2}{N}\sum_{\mathbf{q}\neq 0}\left(f(\mathbf{p}-\mathbf{q}) - f(-\mathbf{q})\right)\frac{1}{\exp\left(\varepsilon_{\mathbf{q}}(T)/\left(k_{\mathrm{B}}T\right)\right) - 1} \tag{3.11}$$

There is no singularity in the summation (3.11) because the term at $q = 0$ is removed from the summation. For that reason, we can rewrite the summation into integration as

$$\varepsilon_{\mathbf{p}}(T) = \frac{\mathbf{p}^2}{2m} + \frac{2}{N}\left(f(\mathbf{p}) - f(0)\right)n_0 + \frac{2V}{N(2\pi\hbar)^3}\iiint\left(f(\mathbf{p}-\mathbf{q}) - f(-\mathbf{q})\right)\frac{1}{\exp\left(\varepsilon_{\mathbf{q}}(T)/\left(k_{\mathrm{B}}T\right)\right) - 1}\mathrm{d}^3\mathbf{q} \tag{3.12}$$

where we have used momentum interval $2\pi\hbar/L$ and $V = L^3$. The number n_0 of the condensed dressed bosons is

$$n_0 = N - \frac{V}{(2\pi\hbar)^3}\iiint \frac{1}{\exp\left(\varepsilon_{\mathbf{q}}(T)/(k_{\mathrm{B}}T)\right)-1}\mathrm{d}^3\mathbf{q} \ , \tag{3.13}$$

which is derived from number conservation (2.15). Substitution of (3.13) into (3.12) yields the equation shown below.

$$\begin{aligned}\varepsilon_{\mathbf{p}}(T) = {} & \frac{\mathbf{p}^2}{2m} + \frac{2}{N}\left(f(\mathbf{p}) - f(0)\right)\left(N - \frac{V}{(2\pi\hbar)^3}\iiint \frac{1}{\exp\left(\varepsilon_{\mathbf{q}}(T)/(k_{\mathrm{B}}T)\right)-1}\mathrm{d}^3\mathbf{q}\right) \\ & + \frac{2V}{N(2\pi\hbar)^3}\iiint \left(f(\mathbf{p}-\mathbf{q}) - f(-\mathbf{q})\right)\frac{1}{\exp\left(\varepsilon_{\mathbf{q}}(T)/(k_{\mathrm{B}}T)\right)-1}\mathrm{d}^3\mathbf{q}\end{aligned} \tag{3.14}$$

Substituting the function form (2.41) into (3.14), we obtain the following expression.

$$\begin{aligned}\varepsilon_{\mathbf{p}}(T) = {} & \frac{\mathbf{p}^2}{2m} + \left(\varepsilon_{\mathbf{p}}^0 - \mathbf{p}^2/(2m)\right)\left(1 - \frac{V}{N(2\pi\hbar)^3}\iiint \frac{1}{\exp\left(\varepsilon_{\mathbf{q}}(T)/(k_{\mathrm{B}}T)\right)-1}\mathrm{d}^3\mathbf{q}\right) \\ & + \frac{V}{N(2\pi\hbar)^3}\iiint \left(\varepsilon_{|\mathbf{p}-\mathbf{q}|}^0 - (\mathbf{p}-\mathbf{q})^2/(2m) - \varepsilon_{|-\mathbf{q}|}^0 + \mathbf{q}^2/(2m)\right)\frac{1}{\exp\left(\varepsilon_{\mathbf{q}}(T)/(k_{\mathrm{B}}T)\right)-1}\mathrm{d}^3\mathbf{q}\end{aligned} \tag{3.15}$$

These two integrations in (3.15) are gathered into an integration as shown below.

$$\begin{aligned}\varepsilon_{\mathbf{p}}(T) = {} & \varepsilon_p^0 + \frac{V}{N(2\pi\hbar)^3}\times \\ & \times\iiint \left(\varepsilon_{|\mathbf{p}-\mathbf{q}|}^0 - \varepsilon_{|-\mathbf{q}|}^0 - \varepsilon_p^0 - (\mathbf{p}-\mathbf{q})^2/(2m) + \mathbf{q}^2/(2m) + \mathbf{p}^2/(2m)\right)\frac{1}{\exp\left(\varepsilon_{\mathbf{q}}(T)/(k_{\mathrm{B}}T)\right)-1}\mathrm{d}^3\mathbf{q} \\ = {} & \varepsilon_p^0 + \frac{V}{N(2\pi\hbar)^3}\iiint \left(\varepsilon_{|\mathbf{p}-\mathbf{q}|}^0 - \varepsilon_{|-\mathbf{q}|}^0 - \varepsilon_p^0 + 2\mathbf{p}\bullet\mathbf{q}/(2m)\right)\frac{1}{\exp\left(\varepsilon_{\mathbf{q}}(T)/(k_{\mathrm{B}}T)\right)-1}\mathrm{d}^3\mathbf{q}\end{aligned} \tag{3.16}$$

The term including $2\mathbf{p}\bullet\mathbf{q}/(2m)$ disappears by integration of (3.16) because the dressed boson energy $\varepsilon_{\mathbf{p}}(T)$ is spherically symmetric for the momentum vector. Then we obtain

$$\varepsilon_{\mathbf{p}}(T)=\varepsilon_p^0+\frac{V}{N(2\pi\hbar)^3}\iiint\left(\varepsilon^0_{|\mathbf{p}-\mathbf{q}|}-\varepsilon^0_{|-\mathbf{q}|}-\varepsilon^0_p\right)\frac{1}{\exp\left(\varepsilon_{\mathbf{q}}(T)/(k_{\mathrm{B}}T)\right)-1}\mathrm{d}^3\mathbf{q} \tag{3.17}$$

where $d^3\mathbf{q}=d\varphi\,dt\,q^2dq$ and $t=\cos\theta=\mathbf{p}\bullet\mathbf{q}/(pq)$. Performing integration by angle φ, the result is as shown below.

$$\varepsilon_{\mathbf{p}}(T)=\varepsilon_p^0+\frac{2\pi V}{N(2\pi\hbar)^3}\int_{q=0}^{\infty}\int_{t=-1}^{1}\left(\varepsilon^0_{\sqrt{p^2-2pqt+q^2}}-\varepsilon_q^0-\varepsilon_p^0\right)\mathrm{d}t\,\frac{1}{\exp\left(\varepsilon_{\mathbf{q}}(T)/(k_{\mathrm{B}}T)\right)-1}q^2\mathrm{d}q \tag{3.18}$$

We define the kernel function as

$$K(p,q)=\int_{t=-1}^{1}\left(\frac{\varepsilon^0}{\sqrt{p^2-2pqt+q^2}}-\varepsilon_q^0-\varepsilon_p^0\right)dt\,. \tag{3.19}$$

Making use of the kernel (3.19), integral equation (3.18) takes the following form.

$$\varepsilon_{\mathbf{p}}(T)=\varepsilon_p^0+\frac{2\pi V}{N(2\pi\hbar)^3}\int_{q=0}^{\infty}K(p,q)\frac{1}{\exp\left(\varepsilon_{\mathbf{q}}(T)/(k_{\mathrm{B}}T)\right)-1}q^2\mathrm{d}q \tag{3.20}$$

We can approximately solve this integral equation using an iteration method. The details are explained in subsequent sections.

3.2.2 Approximate solution in the first order

The excitation number from the Bose–Einstein condensate is very small when the temperature is very low, i.e. lower than 1.3 K. Therefore, we can apply ε_p^0 for $\varepsilon_{\mathbf{p}}(T)$ of the right-hand-side of (3.20); then obtain the first approximation of $\varepsilon_{\mathbf{p}}(T)$. We describe the first approximation energy by $\varepsilon_1(p,T)$ and obtain the following expression:

$$\varepsilon_1(p,T) = \varepsilon_p^0 + \frac{2\pi V}{N(2\pi\hbar)^3}\int_{q=0}^{\infty} K(p,q)\frac{1}{\exp\left(\varepsilon_q^0/(k_{\mathrm{B}}T)\right)-1}q^2\mathrm{d}q\,. \tag{3.21}$$

In this case, we obtain the first approximation of the distribution function for dressed bosons as the following.

$$n_1(p,T) = \frac{1}{\exp\left(\varepsilon_1(p,T)/(k_{\mathrm{B}}T)\right)-1} \tag{3.22}$$

We can use the approximation forms of (3.21) and (3.22) for evaluating thermodynamic functions in a low-temperature region. Higher order approximations are examined in the next section.

3.2.3 Approximate solution in higher order

Iteration is useful to solve the integral equation of (3.20). Replacing $\varepsilon_{\mathbf{p}}(T)$ in the right-hand-side of (3.20) with $\varepsilon_1(p,T)$, we obtain the second order solution $\varepsilon_2(p,T)$ as follows.

$$\varepsilon_2(p,T) = \varepsilon_p^0 + \frac{2\pi V}{N(2\pi\hbar)^3}\int_{q=0}^{\infty} K(p,q)\frac{1}{\exp\left(\varepsilon_1(q,T)/(k_{\mathrm{B}}T)\right)-1}q^2\mathrm{d}q \tag{3.23}$$

The second order distribution function of dressed bosons is given as

$$n_2(p,T)=\frac{1}{\exp\left(\varepsilon_2(p,T)/(k_{\mathrm{B}}T)\right)-1} \tag{3.24}$$

The j-th order approximation is obtainable from using the (j-1)-th order approximation, as follows.

$$\varepsilon_j(p,T)=\varepsilon_p^0+\frac{2\pi V}{N(2\pi\hbar)^3}\int_{q=0}^{\infty}K(p,q)\frac{1}{\exp\left(\varepsilon_{j-1}(q,T)/(k_{\mathrm{B}}T)\right)-1}q^2\mathrm{d}q \tag{3.25}$$

$$n_j(p,T)=\frac{1}{\exp\left(\varepsilon_j(p,T)/(k_{\mathrm{B}}T)\right)-1} \tag{3.26}$$

Long calculation time is necessary to evaluate $\varepsilon_j(p,T)$ and $n_j(p,T)$ because the integrations in (3.19) and (3.25) are very complicated. The second order approximations (3.23) and (3.24) are calculated numerically; thereafter the theoretical values of the entropy and specific heat are calculated using the second order approximate values explained in chapters IV and V.

The excitation energy of the dressed boson depends on the temperature via the nonlinear effect. The velocity of the dressed boson becomes small and vanishes at the λ point when the temperature approaches the λ point. That property was discussed first in the relevant literature [27]. Details are examined in Sec. 5.4.

IV. Calculation of Entropy

The entropy of liquid helium is given as the following equation.

$$S = k_B \sum_{\mathbf{p}} \left\{ \log\left(1 + n_{\mathbf{p}}\right) + n_{\mathbf{p}} \log\left(1 + n_{\mathbf{p}}^{-1}\right) \right\} \tag{4.1}$$

In that equation, k_B is the Boltzmann constant, and $n_{\mathbf{p}}$ is the number distribution of dressed bosons. The derivation of (4.1) is explained in detail in sections (8.6) and (8.15) of chapter VIII. Substitution of (3.6a) into (4.1) gives

$$S = k_B \sum_{\mathbf{p}} \left\{ \log\left(1 + n_{\mathbf{p}}\right) + \frac{\varepsilon_{\mathbf{p}}(T)}{k_B T} n_{\mathbf{p}} \right\}. \tag{4.2}$$

The total entropy *S* has a macroscopic magnitude; in fact, it is proportional to the total number *N*. The entropy of superfluid component S_{super} is given by the term with $\mathbf{p} = 0$ on the right-hand-side of Eq. (4.2) as the following.

$$S_{\text{super}} = k_B \left\{ \log\left(1 + n_0\right) + \frac{\varepsilon_0(T)}{k_B T} n_0 \right\} = k_B \log\left(1 + n_0\right) \tag{4.3a}$$

$$S_{\text{super}} / N \xrightarrow[N \to \infty]{} 0 \tag{4.3b}$$

Therefore, the entropy of superfluid component is not a macroscopic value. For that reason, all entropy belongs to the normal fluid component (which comprises dressed bosons with nonzero momentum). The summation in (4.2) can be changed to integration, as the following expression shows.

$$S = S_{\text{normal}} = k_B \frac{V}{(2\pi\hbar)^3} \int_{p=0}^{\infty} \int_{\theta=0}^{\pi} \int_{\varphi=0}^{2\pi} \left\{ \log(1+n_{\mathbf{p}}) + \frac{\varepsilon_{\mathbf{p}}(T)}{k_B T} n_{\mathbf{p}} \right\} \sin\theta \, \mathrm{d}\theta \, \mathrm{d}\varphi \, p^2 \mathrm{d}p$$

(4.4)

The spherical symmetric property gives

$$S = k_B \frac{4\pi V}{(2\pi\hbar)^3} \int_0^{\infty} \left\{ \log(1+n_{\mathbf{p}}) + \frac{\varepsilon_{\mathbf{p}}(T)}{k_B T} n_{\mathbf{p}} \right\} p^2 \mathrm{d}p \,. \tag{4.5}$$

We substitute (3.6a) into (4.5), and obtain

$$\begin{aligned} S &= k_B \frac{4\pi V}{(2\pi\hbar)^3} \int_0^{\infty} \left\{ \log\left(\frac{\exp(\varepsilon_{\mathbf{p}}(T)/(k_B T))}{\exp(\varepsilon_{\mathbf{p}}(T)/(k_B T)) - 1} \right) + \frac{\varepsilon_{\mathbf{p}}(T)}{k_B T} n_{\mathbf{p}} \right\} p^2 \mathrm{d}p \\ &= k_B \frac{4\pi V}{(2\pi\hbar)^3} \int_0^{\infty} \left\{ -\log(1-\exp(-\varepsilon_{\mathbf{p}}(T)/(k_B T))) + \frac{\varepsilon_{\mathbf{p}}(T)}{k_B T} n_{\mathbf{p}} \right\} p^2 \mathrm{d}p \end{aligned} \quad . \tag{4.6}$$

Then, the entropy per unit mass is expressed from (4.5) or (4.6) as the following.

$$\frac{S}{mN} = k_B \frac{4\pi}{(2\pi\hbar)^3 \rho} \int_0^{\infty} \left\{ \log(1+n_{\mathbf{p}}) + \frac{\varepsilon_{\mathbf{p}}(T)}{k_B T} n_{\mathbf{p}} \right\} p^2 \mathrm{d}p \tag{4.7a}$$

$$\frac{S}{mN} = k_B \frac{4\pi}{(2\pi\hbar)^3 \rho} \int_0^{\infty} \left\{ -\log(1-\exp(-\varepsilon_{\mathbf{p}}(T)/(k_B T))) + \frac{\varepsilon_{\mathbf{p}}(T)}{k_B T} n_{\mathbf{p}} \right\} p^2 \mathrm{d}p$$

(4.7b)

Therein, $\rho = mN/V$ is the mass density of liquid helium. We calculate the entropy using the approximate solution described in chapter III.

4.1 Evaluation using iteration method

We execute the calculation of entropy using second order approximations (3.23) and (3.24), which necessitates a very long computing time to obtain the kernel function $K(p,q)$, the first order energy $\varepsilon_1(p,T)$, and the second order energy $\varepsilon_2(p,T)$. When we calculate the integrations in (3.19), (3.21), (3.23), and (4.7a) numerically, the necessary CPU time is extremely long and the result cannot be obtained within any reasonable time. Therefore, we consider another method for obtaining the approximate values using a computer program.

We produce value tables for $K(p,q)$, $\varepsilon_1(p,T)$, and $\varepsilon_2(p,T)$ using a computer. We calculate the kernel $K(p,q)$ in the region of $0 \le p/\hbar \le 3.6\,\mathring{A}^{-1}$ and $0 \le q/\hbar \le 3.6\,\mathring{A}^{-1}$ numerically for the interval of $0.01\,\mathring{A}^{-1}$. Then, we obtain a list of about 10^5 values of them. These values are stored in computer memories. It is worth noting at this point that the contributions from $p/\hbar > 3.6\,\mathring{A}^{-1}$ or $q/\hbar > 3.6\,\mathring{A}^{-1}$ are negligibly small; for that reason, we abbreviate the momentum region. Next, we produce a computer program producing an approximate value of the kernel for arbitrary momenta (p, q) via the list of about 10^5 values. Using this program, we can numerically calculate $\varepsilon_1(p,T)$ using only a short CPU time. We can then produce a list of function values of $\varepsilon_1(p,T)$ for about 10^4 points of (p, T). The list of $\varepsilon_1(p,T)$ enables the calculation of $\varepsilon_2(p,T)$ in (3.23) with a short CPU time. We can also produce a list of function values of $\varepsilon_2(p,T)$ for about 10^4 points of (p, T).

The second order approximation value of the entropy per unit mass is expressed as

$$\frac{S}{mN} = k_{\mathrm{B}} \frac{4\pi}{(2\pi\hbar)^3 \rho} \int_0^{\infty} \left\{ \log\left(1 + n_2(p,T)\right) + \frac{\varepsilon_2(p,T)}{k_{\mathrm{B}}T} n_2(p,T) \right\} p^2 \mathrm{d}p \qquad (4.8)$$

Consequently, we can evaluate the entropy per unit mass described in (4.8) using the list of function values of $\varepsilon_2(p,T)$. The numerical results are portrayed in Fig. 4.1 and 4.2.

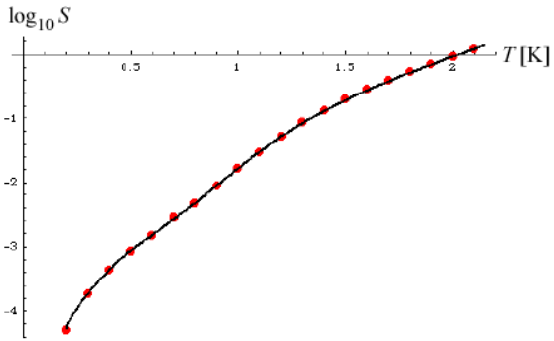

Fig. 4.1 Entropy of liquid helium on a logarithmic scale.

Dots indicate the experimental data. The curve expresses the calculation results obtained using the nonlinear theory.

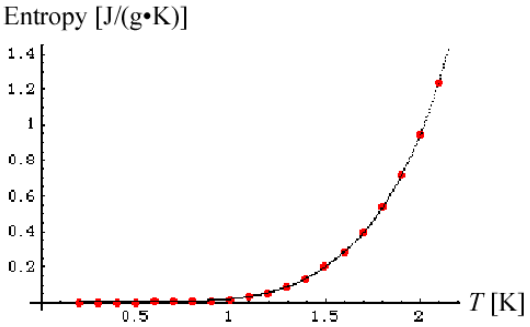

Fig. 4.2 Entropy of liquid helium on a linear scale.

Dots indicate the experimental data. The curve shows calculation results obtained using the nonlinear theory.

The vertical axis of Fig. 4.1 is a logarithmic scale; the vertical axis of Fig. 4.2 is a linear scale. As portrayed in those figures, the calculation values show good agreement with the experimental data for the region of $T \leq 2.1\,K$. This calculation is executed using the Mathematica program (The source list is shown in end of this book).

It is noteworthy that the present calculation incorporates only the experimental data of excitation energy obtained at 1.1 K. In marked contrast, traditional theories have used the data of excitation energy obtained at several different temperatures or have adjusted parameter values for different temperatures to fit the experimental data. Our calculation in this section uses no such an artificial method. Nevertheless, the present results show good agreement with experimental data of the entropy for $0<T<2.1$ K.

4.2 Traditional theories

4.2.1 Landau Theory

Landau calculated thermodynamic functions by applying the excitation energy ε_p^0. The theoretical value of the entropy is expressed as the sum of phonon part S_{ph}

(reference [3] Khalatnikov, page 11) and roton part S_r (reference [3] Khalatnikov, page 12).

The entropy of phonon part per unit mass is

$$\frac{S_{ph}}{mN} = \frac{16\pi^5}{45\rho} k_B \left(\frac{k_B T}{2\pi\hbar c} \right)^3, \tag{4.9}$$

where c is the phonon velocity and ρ is the mass density of liquid helium. The roton part per unit mass is expressed as

$$\frac{S_r}{mN} = k_B \frac{2 {p_0}^2 (\mu k_B T)^{1/2} e^{-\Delta/(k_B T)}}{\rho (2\pi)^{3/2} \hbar^3} \left(\frac{\Delta}{k_B T} + \frac{3}{2} \right), \tag{4.10}$$

where Δ is the roton minimum energy, μ is the effective mass of roton, and p_0 is the momentum of roton minimum. The total entropy per unit mass is as shown below.

$$\frac{S}{mN} = \frac{S_{ph} + S_r}{mN} = \frac{16\pi^5}{45\rho} k_B \left(\frac{k_B T}{2\pi\hbar c} \right)^3 + k_B \frac{2 {p_0}^2 (\mu k_B T)^{1/2} e^{-\Delta/(k_B T)}}{\rho (2\pi)^{3/2} \hbar^3} \left(\frac{\Delta}{k_B T} + \frac{3}{2} \right) \tag{4.11}$$

We use the parameters shown below.

$$c = 238 \text{ [m/s]} \tag{4.12a}$$

$$\rho = 145.5 \text{ [kg/m}^3\text{]} \tag{4.12b}$$

$$\Delta / k_B = 8.606 \text{ [K]} \tag{4.12c}$$

$$\mu = 0.16 \times m = 1.063 \times 10^{-27} \text{ [kg]} \tag{4.12d}$$

$$p_0 / (10^{10} \hbar) = 1.92 [\text{Å}^{-1}] \tag{4.12e}$$

where m is the mass of helium atom. The temperature dependence of Landau's entropy is portrayed in Fig. 4.3 and 4.4.

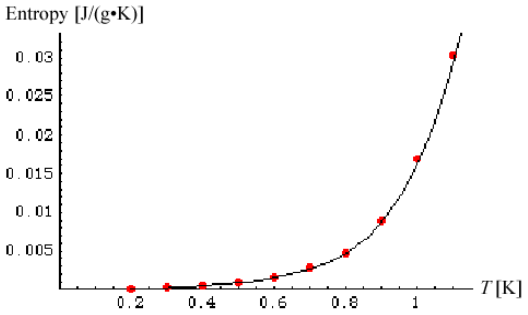

Fig. 4.3 Entropy of Landau Theory for temperatures lower than 1.1 K

Calculated values are expressed by the curve. Dots show the experimental data.

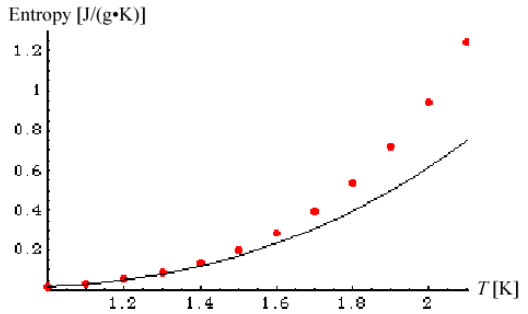

Fig. 4.4 Entropy of Landau Theory for temperatures higher than 1.0 K

Calculated values are expressed by the curve. Dots show the experimental data.

Figure 4.3 shows that Landau's calculation results of entropy have good agreement with the experimental data obtained at less than 1.1 K. Nevertheless, Landau's entropy is approximately 60% of the experimental value at 2.1 K, as portrayed in Fig. 4.4. To improve the Landau theory for the region of $T > 1.1K$, many researchers have

introduced the temperature dependence of excitation energy. We explain their works in later sections of this article.

4.2.2 BCY Theory

To take account of the temperature dependence of excitation energy, P. J. Bendt, R. D. Cowan, and J. L. Yarnell extended Landau's theory [13]. We designate their calculation *BCY calculation*. The momentum range was divided into four intervals: the phonon region, maxon region, roton region, and high-momentum region. Respective forms of the excitation energy for each momentum region are expressed as follows:

The excitation energy in phonon region is given as

$$\varepsilon_p(T) = \mathrm{v}_1(T)p\,, \tag{4.13}$$

where $\mathrm{v}_1(T)$ represents the velocity of the first sound. The excitation energy in maxon region is given by a parabolic curve as

$$\varepsilon_p(T) = k_{\mathrm{B}}\left(a - 11.5\left(p/\left(10^{10}\hbar\right) - 1.113\right)^2\right), \tag{4.14}$$

where parameter a is determined from the conditions of continuous connection among different momentum regions.

In the roton region ($1.58 \le p/\left(10^{10}\hbar\right) \le 2.18$), the excitation energy is calculated using interpolation of the experimental data of neutron scatterings at 1.1 K and 1.8 K. In other words:

$$\varepsilon_p(T) = \text{interpolation formula of the experimental data}. \tag{4.15}$$

The roton minimum energy $\Delta(T)$ is applied to the following interpolation formulas (a–f):(page 1390 in [13]).

Formula (a): $\Delta(T)/k_B = 8.68 - 0.0084\,T^7$ (4.16a)

Formula (b): $\Delta(T)/k_B = 8.69 - 0.0155\,T^6$ (4.16b)

Formula (c): $\Delta(T)/k_B = 8.70 - 0.0289\,T^5$ (4.16c)

Formula (d): $\Delta(T)/k_B = 8.67 - 1.564\,(\rho_n/\rho)$ (4.16d)

Formula (e): $\Delta(T)/k_B = 8.68 - 5.35\times10^{-22}\,N_{\text{excitation}}$ (4.16e)

Formula (f): $\Delta(T)/k_B = 8.66 - 5.93\times10^{-22}\,N_{\text{heavy}}$ (4.16f)

These coefficients were determined to fit the experimental data of excitation energy at 1.1 and 1.8 K. Formulas (c) and (d) yielded better agreement with entropy measurements than the other formulas written in Ref. [13].

The excitation energy in high-momentum region was defined as

$$\varepsilon_p(T) = \mathrm{v}_1(T)p - b\,. \tag{4.17}$$

Parameter b is also determined according to the continuous condition between different regions. The phonon velocity used the value at each temperature. Consequently, the energy dependence is complicated, as described above. Then, they evaluated the theoretical values of entropy and specific heat. The result of entropy calculation is portrayed in Fig. 4.5; it shows good agreement with the experimental data for $T < 1.4\,K$.

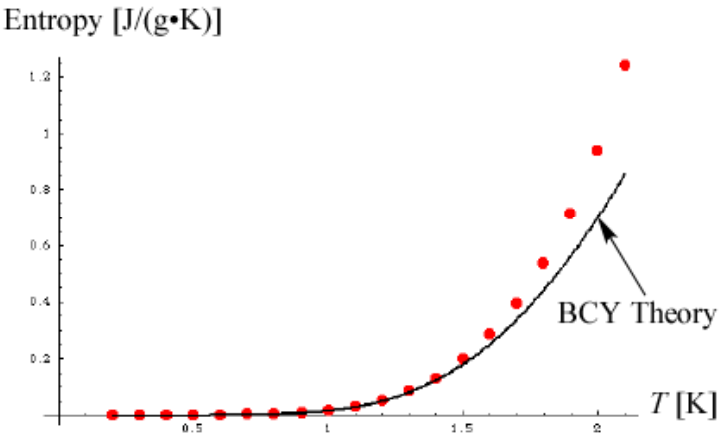

Fig. 4.5 BCY calculation results for the entropy of liquid helium

The curve expresses the results of BCY theory. Dots show experimental values of entropy.

For $1.4\,K < T < 2.2\,K$, their result differs from the experimental data. The entropy value of the BCY calculation is about 70% of the experimental value at 2.1 K. The BCY calculation uses many temperature dependences, as described above.

4.2.3 BD Theory

To explain the experimental results for higher temperature, J. S. Brooks and R. J. Donnelly improved the theoretical calculation of entropy and specific heat of liquid helium. We designate their theory as *BD theory*. Their results were obtained through a lengthy series of investigations [14].

They obtained the numerical values of excitation energies $\varepsilon_p(T)$ by making use of various experimental data. For better understanding of the details of pressure

dependence and temperature dependence, reference [14] is helpful. We present their result for entropy in Fig. 4.6.

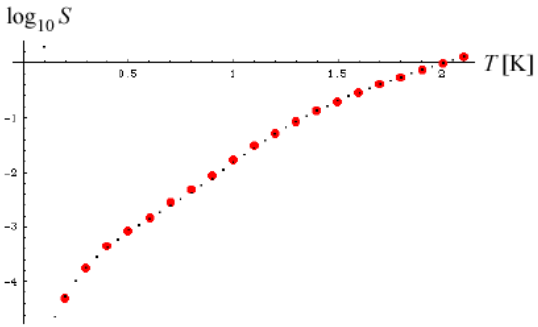

Fig. 4.6 Entropy of the BD theory

Large dots signify the experimental data. Small dots show results obtained using the BD theory. The scale of entropy is measured in units of [J/(g ·K)]

Their results show good agreement with experimental data. It is noteworthy that their results are derived from use of the experimental data obtained at many different temperatures. In contrast, our theoretical results in section 4.1 are derived from experimental data at a temperature 1.1 K only.

The calculated entropy values of the BD theory deviate from the experimental data near the λ transition. Deviations are more readily apparent in the specific heat than in entropy. That fact is discussed in the next chapter.

V. Specific heat

A logarithmic divergence appears in experimental data of specific heat at the temperature T_λ of the λ transition (see Sec. 5.3). However, the calculated functions of the traditional theories have no singularity (see Sec. 5.1). We investigate the singularity on the basis of the nonlinear theory presented in Sec. 5.5.

The derivative of (4.7a) gives the isobaric specific heat per unit mass.

$$C_P = T\left(\frac{\partial(S/mN)}{\partial T}\right)_P = Tk_B\frac{4\pi}{(2\pi\hbar)^3}\left(\frac{\partial(1/\rho)}{\partial T}\right)_P\int_0^\infty\left[\log(1+n_{\mathbf{p}})+\frac{\varepsilon_{\mathbf{p}}}{k_BT}n_{\mathbf{p}}\right]p^2\mathrm{d}p$$
$$+Tk_B\frac{4\pi}{(2\pi\hbar)^3\rho}\int_0^\infty\left(\frac{1}{1+n_{\mathbf{p}}}\left(\frac{\partial n_{\mathbf{p}}}{\partial T}\right)_P+\left(\frac{\partial(\varepsilon_{\mathbf{p}}/(k_BT))}{\partial T}\right)_P n_{\mathbf{p}}+\frac{\varepsilon_{\mathbf{p}}}{k_BT}\left(\frac{\partial n_{\mathbf{p}}}{\partial T}\right)_P\right)p^2\mathrm{d}p \tag{5.1}$$

Here, the derivatives are performed under a constant pressure. Differentiation of (3.6a) by the temperature yields

$$\left(\frac{\partial n_{\mathbf{p}}}{\partial T}\right)_P=\frac{(-1)\exp(\varepsilon_{\mathbf{p}}/(k_BT))}{(\exp(\varepsilon_{\mathbf{p}}/(k_BT))-1)^2}\left(\frac{\partial(\varepsilon_{\mathbf{p}}/(k_BT))}{\partial T}\right)_P, \tag{5.2}$$

which gives the following.

$$\frac{1}{1+n_{\mathbf{p}}}\left(\frac{\partial n_{\mathbf{p}}}{\partial T}\right)_P=\frac{(\exp(\varepsilon_{\mathbf{p}}/(k_BT))-1)}{\exp(\varepsilon_{\mathbf{p}}/(k_BT))}\frac{(-1)\exp(\varepsilon_{\mathbf{p}}/(k_BT))}{(\exp(\varepsilon_{\mathbf{p}}/(k_BT))-1)^2}\left(\frac{\partial(\varepsilon_{\mathbf{p}}/(k_BT))}{\partial T}\right)_P \tag{5.3}$$
$$=(-1)n_{\mathbf{p}}\left(\frac{\partial(\varepsilon_{\mathbf{p}}/(k_BT))}{\partial T}\right)_P$$

Substitution of this equation into the second integral of (5.1) yields the following.

$$C_P = Tk_B\frac{4\pi}{(2\pi\hbar)^3}\left(\frac{\partial(1/\rho)}{\partial T}\right)_P\int_0^\infty\left[\log(1+n_{\mathbf{p}})+\frac{\varepsilon_{\mathbf{p}}}{k_BT}n_{\mathbf{p}}\right]p^2\mathrm{d}p \tag{5.4a}$$
$$+Tk_B\frac{4\pi}{(2\pi\hbar)^3\rho}\int_0^\infty\frac{\varepsilon_{\mathbf{p}}}{k_BT}\left(\frac{\partial n_{\mathbf{p}}}{\partial T}\right)_P p^2\mathrm{d}p$$

On page 101 of reference [19], we expressed the heat capacity of liquid helium with total

mass M as

$$MC_P = Tk_{\mathrm{B}} \frac{4\pi}{(2\pi\hbar)^3}\left(\frac{\partial V}{\partial T}\right)_P \int_0^\infty \left[\log(1+n_{\mathbf{p}}) + \frac{\varepsilon_{\mathbf{p}}}{k_{\mathrm{B}}T} n_{\mathbf{p}}\right] p^2 \mathrm{d}p + Tk_{\mathrm{B}} \frac{4\pi V}{(2\pi\hbar)^3} \int_0^\infty \frac{\varepsilon_{\mathbf{p}}}{k_{\mathrm{B}}T}\left(\frac{\partial n_{\mathbf{p}}}{\partial T}\right)_P p^2 \mathrm{d}p \tag{5.4b}$$

where V is the volume of liquid helium.

Using the derivative of dressed boson number (5.2), Eq. (5.4a) is rewritten as follows.

$$C_P = Tk_{\mathrm{B}} \frac{4\pi}{(2\pi\hbar)^3}\left(\frac{\partial(1/\rho)}{\partial T}\right)_P \int_0^\infty \left[\log(1+n_{\mathbf{p}}) + \frac{\varepsilon_{\mathbf{p}}}{k_{\mathrm{B}}T} n_{\mathbf{p}}\right] p^2 \mathrm{d}p + Tk_{\mathrm{B}} \frac{4\pi}{(2\pi\hbar)^3 \rho} \int_0^\infty \frac{\varepsilon_{\mathbf{p}}}{k_{\mathrm{B}}T} \frac{(-1)\exp\left(\varepsilon_{\mathbf{p}}/(k_{\mathrm{B}}T)\right)}{\left(\exp\left(\varepsilon_{\mathbf{p}}/(k_{\mathrm{B}}T)\right)-1\right)^2}\left(\frac{\partial\left(\varepsilon_{\mathbf{p}}/(k_{\mathrm{B}}T)\right)}{\partial T}\right)_P p^2 \mathrm{d}p \tag{5.5}$$

We execute differentiation $\partial\left(\varepsilon_{\mathbf{p}}/(k_B T)\right)/\partial T$, and obtain the following.

$$C_P = Tk_{\mathrm{B}} \frac{4\pi}{(2\pi\hbar)^3}\left(\frac{\partial(1/\rho)}{\partial T}\right)_P \int_0^\infty \left[\log(1+n_{\mathbf{p}}) + \frac{\varepsilon_{\mathbf{p}}}{k_{\mathrm{B}}T} n_{\mathbf{p}}\right] p^2 \mathrm{d}p + Tk_{\mathrm{B}} \frac{4\pi}{(2\pi\hbar)^3 \rho} \int_0^\infty \frac{\varepsilon_{\mathbf{p}}}{k_{\mathrm{B}}T} \frac{\exp\left(\varepsilon_{\mathbf{p}}/(k_{\mathrm{B}}T)\right)}{\left(\exp\left(\varepsilon_{\mathbf{p}}/(k_{\mathrm{B}}T)\right)-1\right)^2}\left(\frac{\varepsilon_{\mathbf{p}}}{k_{\mathrm{B}}T^2} - \frac{1}{k_{\mathrm{B}}T}\left(\frac{\partial\varepsilon_{\mathbf{p}}}{\partial T}\right)_P\right) p^2 \mathrm{d}p \tag{5.6}$$

Using the number distribution (3.6a), the isobaric specific heat per unit mass is described as

$$C_P = Tk_{\mathrm{B}} \frac{4\pi}{(2\pi\hbar)^3}\left(\frac{\partial(1/\rho)}{\partial T}\right)_P \int_0^\infty \left[\log(1+n_{\mathbf{p}}) + \frac{\varepsilon_{\mathbf{p}}}{k_{\mathrm{B}}T} n_{\mathbf{p}}\right] p^2 \mathrm{d}p + \frac{4\pi}{(2\pi\hbar)^3 \rho} \int_0^\infty (n_{\mathbf{p}})^2 \exp\left(\varepsilon_{\mathbf{p}}/(k_{\mathrm{B}}T)\right)\left(\left(\frac{\varepsilon_{\mathbf{p}}}{k_{\mathrm{B}}T}\right)^2 k_{\mathrm{B}} - \frac{\varepsilon_{\mathbf{p}}}{k_{\mathrm{B}}T}\left(\frac{\partial\varepsilon_{\mathbf{p}}}{\partial T}\right)_P\right) p^2 \mathrm{d}p \tag{5.7}$$

Thereby, the isobaric specific heat of liquid helium per unit mass is expressed using the excitation energy from the Bose–Einstein condensate and the number distribution of the dressed bosons in the nonlinear theory. The numerical calculations are executed in Sec. 5.2 and 5.6.

5.1 Various calculation methods

Many physicists have calculated the specific heat using their own methods. We first explain the traditional calculations of specific heat before explaining the results of the nonlinear theory.

5.1.1 Calculation of Specific Heat using Landau Theory

Landau calculated the specific heat by applying the elementary excitation energy ε_p^0 . His excitation energy is independent of the temperature. Therefore, the right-hand-side of (5.7) can be evaluated. He obtained the approximate analytic forms for phonon part C_{ph} and roton part C_r per unit mass as follows: (see page 11 and 12 in Khalatnikov's book [3]).

$$C_{ph} = \frac{16\pi^5}{15\rho} k_B \left(\frac{k_B T}{2\pi\hbar c} \right)^3 \tag{5.8}$$

$$C_r = k_B \frac{2 p_0{}^2 (\mu k_B T)^{1/2} e^{-\Delta/(k_B T)}}{\rho (2\pi)^{3/2} \hbar^3} \left(\left(\frac{\Delta}{k_B T} \right)^2 + \frac{\Delta}{k_B T} + \frac{3}{4} \right) \tag{5.9}$$

The specific heat per unit mass is given as the sum of two contributions: (5.8) and (5.9).

$$C = C_{ph} + C_r = \frac{16\pi^5}{15\rho} k_B \left(\frac{k_B T}{2\pi\hbar c} \right)^3 + k_B \frac{2 p_0{}^2 (\mu k_B T)^{1/2} e^{-\Delta/(k_B T)}}{\rho (2\pi)^{3/2} \hbar^3} \left(\left(\frac{\Delta}{k_B T} \right)^2 + \frac{\Delta}{k_B T} + \frac{3}{4} \right) \tag{5.10}$$

Therein, the parameter values are already shown in (4.12). Landau's results are drawn in Figs. 5.1 and 5.2. The results show good agreement with the experimental data for $T \le 1.0\,K$, as presented in Fig. 5.1.

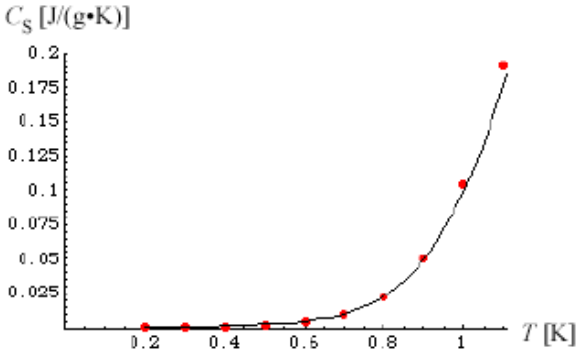

Fig. 5.1 Specific heat of the Landau theory for $T \leq 1.1\,K$

The dots represent the experimental data [15]. The curve expresses Landau's calculation results for the specific heat of liquid helium. The scale of specific heat is [J/(g ·K)].

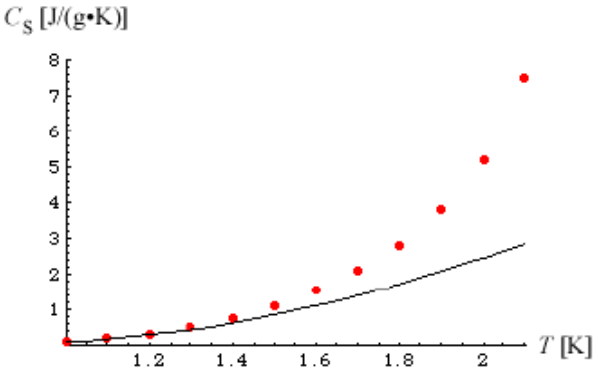

Fig. 5.2 Specific heat of the Landau theory in units of [J/(g ·K)] for $T \geq 1.0\,K$

Dots express experimental data [15]. The curve shows Landau's results.

Landau's results deviate from the experimental values for $T > 1.3\,K$ under the saturated vapor pressure, as portrayed in Fig. 5.2. Many researchers have made efforts to

decrease the disagreement between theoretical values and experimental values for $T > 1.3\,K$. Two approaches among them are explained in the following sections.

5.1.2 Calculation of Specific Heat using BCY Theory

As described in chapter IV, P. J. Bendt, R. D. Cowan, and J. L. Yarnell calculated the specific heat via use of the temperature dependence of excitation energy. Their results are improved to be better fitting with the experimental data than in the Landau theory. The calculated values are depicted in Fig. 5.3.

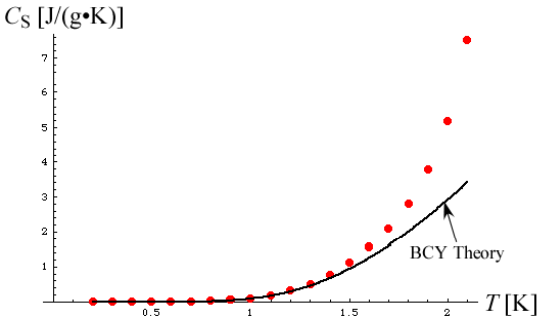

Fig. 5.3 Calculated values of specific heat in BCY theory in units of [J/(g·K)]
The curve shows the theoretical result. The dots express experimental values [15].

However, the result of BCY theory is still smaller than 50% of the experimental data of specific heat at 2.1 K.

5.1.3 Calculation of Specific Heat using BD Theory

In addition, J. S. Brooks and R. J. Donnelly considered the temperature and pressure dependences for single excitation energy of liquid helium. Their calculated values of specific heat are presented in Fig. 5.4, which show good agreement with experimental data for $T < 2.0\,K$.

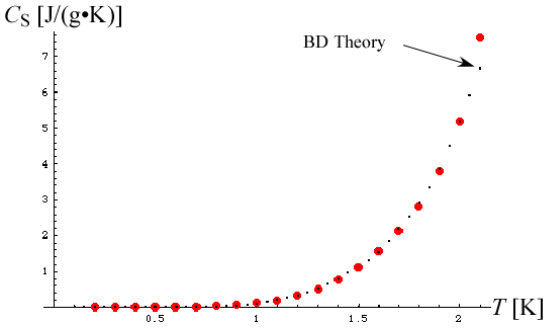

Fig. 5.4 Specific heat calculated using BD theory on the scale of [J/(g · K)]
Large red dots represent experimental values [15]; small black dots show calculated values of the specific heat in BD theory

Their roton parameters are adjusted so that their results fit the experimental values. However, the results deviate by approximately 10% from experimental data at $T = 2.1\,K$. The deviation increases approaching the λ transition. They have used only regular functions without singularity. On the other hand, the experimental behavior shows a logarithmic divergence at $T = T_\lambda \approx 2.172\,K$. Accordingly, BD theory cannot explain the logarithmic divergence.

We discuss the origin of the singularity in sections 5.3–5.6. Then, it is clarified that the nonlinear structure of the total energy causes the logarithmic singularity of the specific heat.

5.2 Evaluation for T<2.15 using the iteration method

The nonlinear theory has clarified that the excitation energy from the Bose–Einstein condensate of the dressed bosons varies with temperature. As discussed in chapter III, the kernel function $K(p,q)$ can be calculated numerically based on Eq. (3.19) using the analytical forms (2.42)–(2.46). Thereafter, we numerically calculated the first order solutions $\varepsilon_1(p,T)$ and $n_1(p,T)$ using Eq. (3.21) and Eq. (3.22), and also the second order solutions $\varepsilon_2(p,T)$ and $n_2(p,T)$ using Eq. (3.23) and Eq. (3.24). The calculation has already been completed in chapter IV to obtain the entropy values. Using

these numerical values of the second order energy $\varepsilon_2(p,T)$ and the second order distribution function $n_2(p,T)$, we can calculate the second order approximation values of specific heat.

$$C_P = Tk_B \frac{4\pi}{(2\pi\hbar)^3}\left(\frac{\partial V}{\partial T}\right)_P \int_0^\infty \left[\log(1+n_2(p,T)) + \frac{\varepsilon_2(p,T)}{k_B T} n_2(p,T)\right] p^2 \mathrm{d}p$$
$$+ \frac{4\pi V}{(2\pi\hbar)^3} \int_0^\infty (n_2(p,T))^2 \exp(\varepsilon_2(p,T)/(k_B T)) \left(\left(\frac{\varepsilon_2(p,T)}{k_B T}\right)^2 k_B - \frac{\varepsilon_2(p,T)}{k_B T}\left(\frac{\partial \varepsilon_2(p,T)}{\partial T}\right)_P \right) p^2 \mathrm{d}p \tag{5.11}$$

The evaluated results are presented in Fig. 5.5.

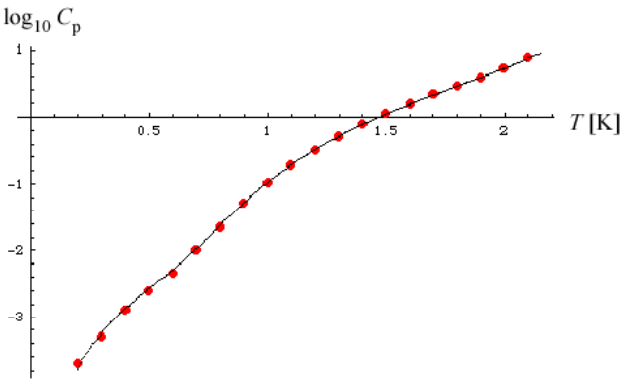

Fig. 5.5 The second order results of specific heat via the nonlinear theory

The curve shows calculated values of $\log_{10}(C_P/[\mathrm{J}/(\mathrm{g}\cdot\mathrm{K})])$ of the nonlinear theory. Red dots indicate the experimental data [15].

As presented in this figure, the theoretical values of the second order show good agreement with experimental data for $T \le 2.1\,K$. It is noteworthy that the present calculation uses the experimental values of excitation energy only for 1.1 K. Of course the iteration method is insufficient in close vicinity of the λ transition temperature. We

discuss the origin of the logarithmic divergence in Secs. 5.5 and 5.6.

5.3 Logarithmic divergence of specific heat at the λ point

The experimental data of specific heat have a logarithmic divergence at the λ point [15]. We portray that behavior in Fig. 5.6, where the scale of specific heat is [J/(mol·K)]. Therefore the values in Fig. 5.6 are approximately four times larger than the values shown previously in Figs. 5.1–5.4.

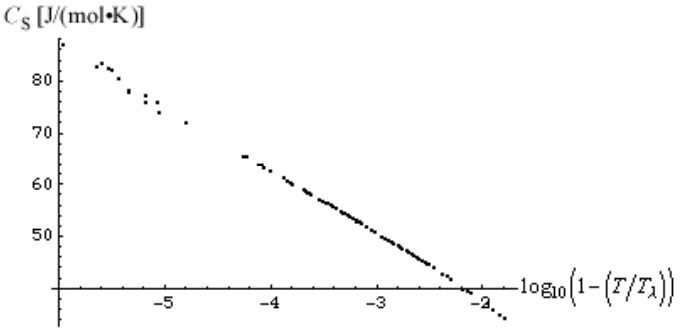

Fig. 5.6 Experimental data of Specific Heat for saturated vapor pressure

The unit of C_S is J/mol·K. The horizontal axis shows $\log_{10}\left(1-\left(T/T_\lambda\right)\right)$.

It is difficult to measure the specific heat in close vicinity of the λ point, i.e. in the region of $1-\left(T/T_\lambda\right)<10^{-5}$. Gravity acts on liquid helium on the earth. Accordingly, the upper part of liquid helium has pressure that is less than in the lower part of liquid helium. This pressure gradient yields deviation of the λ transition temperatures. In other words, the lower part of liquid helium has a λ transition temperature value that is smaller than in the upper part. To eliminate this deviation, microgravity or zero gravity technology is necessary to measure the specific heat, for instance, the environment on the space shuttle.

Those data were obtained in the space shuttle by Lipa et al. [16]. The experimental results are presented in Fig. 5.7. (The authors extend particular appreciation to professor Lipa for these data.). The temperature dependence shows logarithmic divergence at the λ point.

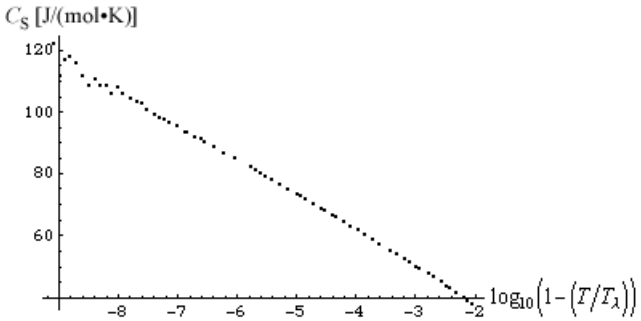

Fig. 5.7 Experimental results of specific heat in space shuttle by Lipa et al. [16]

Specific heat values C_S are shown in units of [J/mol·K] on the vertical axis. The horizontal axis shows $\log_{10}\left(1-\left(T/T_\lambda\right)\right)$.

Landau theory and its improved theories (BCY theory and BD theory) cannot explain the logarithmic singularity of specific heat at the λ point. Moreover, our second order solution in the previous section is insufficient to explain the singularity. Infinitely numerous iterations are necessary to obtain the singularity.

Deriving this singularity, we will examine the energy spectrum near the λ point in the next section. According to the examination of the spectrum, the cause of the singularity is clarified in section 5.5. The specific heat near the λ point is calculated numerically using the nonlinear theory described in section 5.6.

5.4 Dressed boson energy near the λ point

The elementary excitation energy is measurable in inelastic scatterings of neutron or in Brillouin scatterings of laser light. The detected energy value for a small momentum is more precise in Brillouin scattering experiments of laser light than in inelastic neutron scattering experiments. Therefore, we reexamine the data of spectrum in Brillouin scattering in greater detail.

There are many experimental measurements of Brillouin scatterings in liquid helium [17]. We present one datum in Fig. 5.8. The data were measured by Vaughan, Vinen, and Palin as on page 533 of reference [17]. Therein four peaks are detected whose two central peaks represent the second sound peaks (Stokes peak and anti-Stokes peak) and whose remaining two peaks indicate the first sound peaks. The detected width of the second sound peak is almost equal to the instrumental width: the intrinsic width of the second sound is extremely small. The width of the second sound peak was also detected by Winteling, Holmes, and Greytak; its value is less than 1.5 MHz for $T_\lambda - T < 0.1[\mathrm{K}]$, as shown on page 429 of reference [17]. The value 1.5 MHz is the instrumental width; therefore the intrinsic width of second sound is smaller than 1.5 MHz. It is readily apparent in Fig. 5.8 that the second sound width is less than the width of the first sound peak near the λ point.

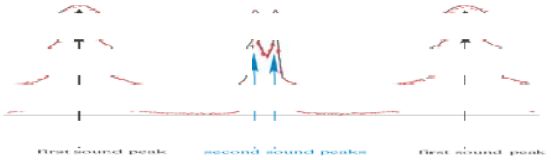

Fig. 5.8 Spectrum of Brillouin scattering in liquid helium [17]

Data measured at $T = T_\lambda - 0.0005[\mathrm{K}]$.

In these measurements [17], the second sound width is smaller than one-sixth of the width of the first sound. Accordingly, the lifetime of the second sound is six times longer than the lifetime of the first sound because the lifetime is directly related to the inverse of the width. That is to say, the second sound mode is more stable than the first sound mode.

In the Landau theory, the theoretical width of the second sound peak becomes infinitely large at the λ point. The discrepancy between Landau's result and the experimental result suggests that the second sound peak detected in Brillouin scattering represents an elementary excitation, i.e. excitation of the dressed boson from Bose–Einstein condensate. The nonlinear theory of this article also supports that supposition. We explain it below.

The excitation energy of dressed boson from Bose–Einstein condensate $\varepsilon_{\mathbf{p}}$ is equal to $\varepsilon_{\mathbf{p}}^{0}$ at $T=0$. The excitation energy from BEC has a value that differs from $\varepsilon_{\mathbf{p}}^{0}$ when the temperature becomes high. We first examine the functional form of the excitation energy from BEC for a very small value of *p*. The summation in (3.2) can be rewritten to an integration, except *q*=0 because of smallness of momentum interval $(2\pi\hbar/L)$:

$$\omega_{\mathbf{p}}=\frac{\mathbf{p}^2}{2m}+\frac{n_0}{N}2f(\mathbf{p})+\frac{2V}{N(2\pi\hbar)^3}\int_{q=0}^{\infty}\iint f(\mathbf{p}-\mathbf{q})n_{\mathbf{q}}\,\mathrm{d}\cos\theta\mathrm{d}\varphi\,q^2\mathrm{d}q-X\,, \tag{5.12}$$

where n_0 represents the number of dressed bosons in the Bose–Einstein condensate, and *X* is independent of momentum *p* as

$$X=\frac{1}{N^2}\sum_{\mathbf{s},\mathbf{t}}f(\mathbf{s}-\mathbf{t})n_{\mathbf{s}}n_{\mathbf{t}}\,. \tag{5.13}$$

We use the approximation form of $f(\mathbf{p}-\mathbf{q})$ in a small momentum as

$$f(\mathbf{p}-\mathbf{q}) = \tfrac{1}{2}\varepsilon^0_{\mathbf{p}-\mathbf{q}} + \mathrm{Order}\left((\mathbf{p}-\mathbf{q})^2\right) + f(0) = \tfrac{1}{2}c|\mathbf{p}-\mathbf{q}| + \mathrm{Order}\left((\mathbf{p}-\mathbf{q})^2\right) + f(0)$$,

where *c* is the phonon velocity at zero Kelvin. The integral region in (5.12) is divided into a small momentum region $q < q_A$ and a large momentum region $q > q_A$, where q_A is an adequately small momentum. Consequently, we obtain

$$\begin{aligned}\omega_{\mathbf{p}} = \frac{\mathbf{p}^2}{2m} + \frac{n_0}{N}c|\mathbf{p}| + \frac{V}{N(2\pi\hbar)^3}\int_{q=0}^{q=q_A}\iint c|\mathbf{p}-\mathbf{q}|n_{\mathbf{q}}\,\mathrm{d}\cos\theta\mathrm{d}\varphi q^2\mathrm{d}q \\ + \frac{2V}{N(2\pi\hbar)^3}\int_{q=q_A}^{\infty}\iint f(\mathbf{p}-\mathbf{q})n_{\mathbf{q}}\,\mathrm{d}\cos\theta\mathrm{d}\varphi q^2\mathrm{d}q + Y\end{aligned}, \qquad (5.14)$$

where *Y* is the constant part independent of *p*. The first integral in (5.14) is

$$\begin{aligned}&\frac{V}{N(2\pi\hbar)^3}\int_{q=0}^{q=q_A}\iint c|\mathbf{p}-\mathbf{q}|n_{\mathbf{q}}\,\mathrm{d}\cos\theta\mathrm{d}\varphi q^2\mathrm{d}q = \frac{2\pi V}{N(2\pi\hbar)^3}\int_{q=0}^{q=q_A}\int_{t=-1}^{t=1} c\sqrt{p^2-2pqt+q^2}\,dt\; n_{\mathbf{q}}q^2\mathrm{d}q \\ &= \frac{2\pi V}{N(2\pi\hbar)^3}\int_{q=0}^{q=q_A} c\frac{|p+q|^3-|p-q|^3}{3pq}n_{\mathbf{q}}q^2\mathrm{d}q\end{aligned}\,. \qquad (5.15)$$

Therein, we examine only the case of $p < q_A$ because of the smallness of *p*. We can also use the approximate function form for a small momentum *q* as

$$n_{\mathbf{q}} \approx \frac{k_B T}{uq}, \qquad (5.16)$$

where the value of *u* represents the velocity of the excitation in a small momentum. This value is determined later. Accordingly, the integral in (5.15) is equal to

$$\begin{aligned}&\frac{2\pi V}{N(2\pi\hbar)^3}\int_{q=0}^{q=q_A} c\frac{|p+q|^3-|p-q|^3}{3pq}n_{\mathbf{q}}q^2\mathrm{d}q = \frac{2\pi V k_{\mathrm{B}}T}{N(2\pi\hbar)^3}\left[\int_{q=0}^{q=p} c\frac{6p^2q+2q^3}{3pu}\mathrm{d}q + \int_{q=p}^{q=q_A} c\frac{2p^3+6pq^2}{3pu}\mathrm{d}q\right] \\ &= \mathrm{Order}\left(p^2\right) + \mathrm{Order}\left(p^3\right) + (\text{constant value})\end{aligned}$$

The second integral in (5.14) is expressed as the following.

$$\frac{2V}{N(2\pi\hbar)^3}\int_{q=q_A}^{\infty}\iint f(\mathbf{p}-\mathbf{q})n_{\mathbf{q}}\,\mathrm{d}\cos\theta\mathrm{d}\varphi q^2\mathrm{d}q=\frac{2V}{N(2\pi\hbar)^3}\int_{q=q_A}^{\infty}\iint\left[f(-\mathbf{q})+\alpha\,\mathbf{p}\bullet\mathbf{q}+\beta\,\mathbf{p}^2+\cdots\right]n_{\mathbf{q}}\,\mathrm{d}\cos\theta\mathrm{d}\varphi q^2\mathrm{d}q$$
$$=\mathrm{Order}\left(p^2\right)+(\text{constant value})$$

These calculation results imply the following expansion.

$$\omega_{\mathbf{p}}=\frac{n_0}{N}c|\mathbf{p}|+\mathrm{Order}\left(p^2\right)+(\text{constant value})$$

Consequently, the velocity of the dressed boson for a small momentum is directly related to n_0 as

$$\omega_{\mathbf{p}}-\omega_0=\frac{n_0}{N}cp+\mathrm{Order}\left(p^2\right). \tag{5.17}$$

Therefore, the velocity of the excitation from BEC is expected to decrease when the temperature approaches the λ point. This property shows agreement with the property of the second sound; it was first examined in reference [27]. Accordingly, it is reasonable that we consider the excitation of the dressed boson from BEC to be the second sound mode for a small momentum near the λ point. The reasons are summarized below:

1. The excitation mode of the dressed boson from BEC is expected to disappear in $T>T_\lambda$ because of disappearance of Bose condensate. The second sound mode also disappears in $T>T_\lambda$.

2. The velocity of the dressed boson from BEC in a small momentum is expected to decrease when the temperature approaches the λ point. Moreover, the velocity for a very small momentum approaches zero at the λ point because of Eq. (5.17) and $n_0 \xrightarrow[T\to T_\lambda]{} 0$. The velocity of the second sound mode has the same property.

3. The width of the second sound peak in Brillouin scattering is extremely small near the λ point; therefore, the mode represents the elementary excitation.

Consequently, we consider the second sound to be the dressed boson excitation from BEC. Then, the dressed boson energy near the λ point can be determined using the experimental data. The experimental results given in reference [18] show that the second sound velocity u near the λ point depends on the temperature as

$$u = c_2\left(1 - T/T_\lambda\right)^{1/3} + D\left(1 - T/T_\lambda\right)^{1/2}. \tag{5.18}$$

According to our viewpoint for the second sound, the excitation energy $\varepsilon_{\mathbf{p}}$ from BEC has the same velocity as Eq. (5.18). For a large momentum p, $\varepsilon_{\mathbf{p}}$ is proportional to p^2 because the kinetic energy occupies a main part of the total energy. Consequently, the function form of excitation energy from BEC might be equal to

$$\varepsilon_{\mathbf{p}} = c_2 p\left(1 - \left(T/T_\lambda\right) + ap^3\right)^{1/3} + Dp\left(1 - \left(T/T_\lambda\right) + bp^2\right)^{1/2}, \tag{5.19}$$

where c_2 and D are determined from experimental data of the second sound velocity, and where a and b are parameters. This energy form certainly has the second sound velocity as

$$\lim_{p\to 0}\left(\frac{\partial \varepsilon_{\mathbf{p}}}{\partial p}\right) = c_2\left(1 - \left(T/T_\lambda\right)\right)^{1/3} + D\left(1 - \left(T/T_\lambda\right)\right)^{1/2},$$

at p=0. We therefore determined the functional form of $\varepsilon_{\mathbf{p}}$ for a small momentum near the λ point. This form is used in the phonon region. The discussion in the next section clarifies that the theoretical form of specific heat has a logarithmic divergence at the λ point.

5.5 Origin of the logarithmic divergence in specific heat

The theoretical form of specific heat is derived from Eq. (5.7). We examine the last integration of Eq. (5.7), which is

$$\frac{4\pi}{(2\pi\hbar)^3\rho}\int_0^\infty (n_{\mathbf{p}})^2 \exp(\varepsilon_{\mathbf{p}}/(k_{\mathrm{B}}T))\left(\left(\frac{\varepsilon_{\mathbf{p}}}{k_{\mathrm{B}}T}\right)^2 k_{\mathrm{B}} - \frac{\varepsilon_{\mathbf{p}}}{k_{\mathrm{B}}T}\left(\frac{\partial\varepsilon_{\mathbf{p}}}{\partial T}\right)_P\right) p^2 \mathrm{d}p \cdot$$

The logarithmic singularity of specific heat is produced from the integral including the last derivative as

$$X = \frac{-4\pi}{(2\pi\hbar)^3\rho}\int_0^\infty (n_{\mathbf{p}})^2 \left[\exp(\varepsilon_{\mathbf{p}}/(k_{\mathrm{B}}T))\right]\frac{\varepsilon_{\mathbf{p}}}{k_{\mathrm{B}}T}\left(\frac{\partial\varepsilon_{\mathbf{p}}}{\partial T}\right)_P p^2 \mathrm{d}p \cdot \qquad (5.20)$$

This integral region is divided into a small momentum region and a large momentum region, as presented in the following.

$$\begin{aligned} X = {} & \frac{-4\pi}{(2\pi\hbar)^3\rho}\int_0^{q_1} (n_{\mathbf{p}})^2 \left[\exp(\varepsilon_{\mathbf{p}}/(k_{\mathrm{B}}T))\right]\frac{\varepsilon_{\mathbf{p}}}{k_{\mathrm{B}}T}\left(\frac{\partial\varepsilon_{\mathbf{p}}}{\partial T}\right)_P p^2 \mathrm{d}p \\ & + \frac{-4\pi}{(2\pi\hbar)^3\rho}\int_{q_1}^\infty (n_{\mathbf{p}})^2 \left[\exp(\varepsilon_{\mathbf{p}}/(k_{\mathrm{B}}T))\right]\frac{\varepsilon_{\mathbf{p}}}{k_{\mathrm{B}}T}\left(\frac{\partial\varepsilon_{\mathbf{p}}}{\partial T}\right)_P p^2 \mathrm{d}p \end{aligned} \qquad (5.21)$$

We can use the energy form of (5.19) for the first integral in (5.21) because q_1 is small. We can also use the following approximations for a small value of p near the λ point.

$$(n_{\mathbf{p}})^2 \left[\exp(\varepsilon_{\mathbf{p}}/(k_{\mathrm{B}}T))\right]\frac{\varepsilon_{\mathbf{p}}}{k_{\mathrm{B}}T} \approx \left(\frac{\varepsilon_{\mathbf{p}}}{k_{\mathrm{B}}T}\right)^{-1} \qquad (5.22a)$$

$$\varepsilon_{\mathbf{p}} = c_2 p\left(1-\left(T/T_\lambda\right)+ap^3\right)^{1/3} + Dp\left(1-\left(T/T_\lambda\right)+bp^2\right)^{1/2} \quad (5.22b)$$
$$\approx c_2 p\left(1-\left(T/T_\lambda\right)+ap^3\right)^{1/3}$$

$$\left(\frac{\partial\varepsilon_{\mathbf{p}}}{\partial T}\right)_P \approx c_2 p\frac{-1}{3T_\lambda}\left(1-\left(T/T_\lambda\right)+ap^3\right)^{-2/3} \quad (5.22c)$$

Accordingly, the integrand of (5.21) is nearly equal to the following.

$$\left(n_{\mathbf{p}}\right)^2\left[\exp\left(\varepsilon_{\mathbf{p}}/\left(k_{\mathrm{B}}T\right)\right)\right]\frac{\varepsilon_{\mathbf{p}}}{k_{\mathrm{B}}T}\left(\frac{\partial\varepsilon_{\mathbf{p}}}{\partial T}\right)_P \approx \left(\frac{k_{\mathrm{B}}T}{\varepsilon_{\mathbf{p}}}\right)c_2 p\frac{-1}{3T_\lambda}\left(1-\left(T/T_\lambda\right)+ap^3\right)^{-2/3} \quad (5.23)$$
$$\approx \frac{-k_{\mathrm{B}}}{3}\left(1-\left(T/T_\lambda\right)+ap^3\right)^{-1}$$

These approximations yield the following expression.

$$X = \frac{-4\pi}{\left(2\pi\hbar\right)^3\rho}\int_0^{q_1}\frac{-k_{\mathrm{B}}}{3}\left(1-\left(T/T_\lambda\right)+ap^3\right)^{-1}p^2\mathrm{d}p$$
$$+\frac{-4\pi}{\left(2\pi\hbar\right)^3\rho}\int_{q_1}^{\infty}\left(n_{\mathbf{p}}\right)^2\left[\exp\left(\varepsilon_{\mathbf{p}}/\left(k_{\mathrm{B}}T\right)\right)\right]\frac{\varepsilon_{\mathbf{p}}}{k_{\mathrm{B}}T}\left(\frac{\partial\varepsilon_{\mathbf{p}}}{\partial T}\right)_P p^2\mathrm{d}p$$

$$X = \frac{4\pi}{\left(2\pi\hbar\right)^3\rho}\frac{k_{\mathrm{B}}}{9a}\left[\log\left(1-\left(T/T_\lambda\right)+ap^3\right)\right]_{p=0}^{q_1} \quad (5.24)$$
$$+\frac{-4\pi}{\left(2\pi\hbar\right)^3\rho}\int_{q_1}^{\infty}\left(n_{\mathbf{p}}\right)^2\left[\exp\left(\varepsilon_{\mathbf{p}}/\left(k_{\mathrm{B}}T\right)\right)\right]\frac{\varepsilon_{\mathbf{p}}}{k_{\mathrm{B}}T}\left(\frac{\partial\varepsilon_{\mathbf{p}}}{\partial T}\right)_P p^2\mathrm{d}p$$

We write only a singular term at the λ transition temperature as

$$X = -\frac{4\pi}{\left(2\pi\hbar\right)^3\rho}\frac{k_{\mathrm{B}}}{9a}\log\left(1-\left(T/T_\lambda\right)\right)+\text{regularpart} \quad . \quad (5.25)$$

This theoretical result shows that the logarithmic divergence of the specific heat is derived from the nonlinear property of the total energy, as presented in Eq. (2.21). On the

other hand, the logarithmic singularity does not exist in the theoretical results of the Landau theory, BCY theory, or BD theory because their phonon velocity at the λ point is not zero.

5.6 Evaluation of specific heat in nonlinear theory near the λ point

We next calculate the temperature dependence of the specific heat near the λ point on the basis of the nonlinear theory. The theoretical value of the isobaric specific heat per unit mass is given as shown in Eq. (5.7) where the integration range is separable into four momentum regions: phonon, maxon, roton, and higher momentum. We use four functional forms of the excitation energy from BEC, two of which are the same functional forms for the roton region and for high-momentum region as those in the BD theory. (We obtain almost same result even if we use the second order energy form (3.23) for roton region and for high-momentum region.) For the phonon region, we use Eq. (5.19). Moreover, the function parameters in the maxon region are determined such that the excitation energy and its tangent are connected continuously to both neighbor curves.

The integrations in Eq. (5.7) are evaluated using a computer in the temperature range $0 < \left(1 - \left(T/T_\lambda\right)\right) < 0.04$, the results of which are presented in Fig. 5.9 (see reference [19]). The mathematica program of this calculation is attached in end of this book. The upper curve expresses our calculated values of specific heat. Dots in Fig. 5.9 portray the experimental data [15] of specific heat for a saturated vapor pressure. Our calculation is performed under pressure P=0.05 bar. The difference between saturated vapor pressure and P=0.05 bar is negligibly small. The middle curve and the lower curve in Fig. 5.9 depict the results of the BD theory and the BCY theory respectively.

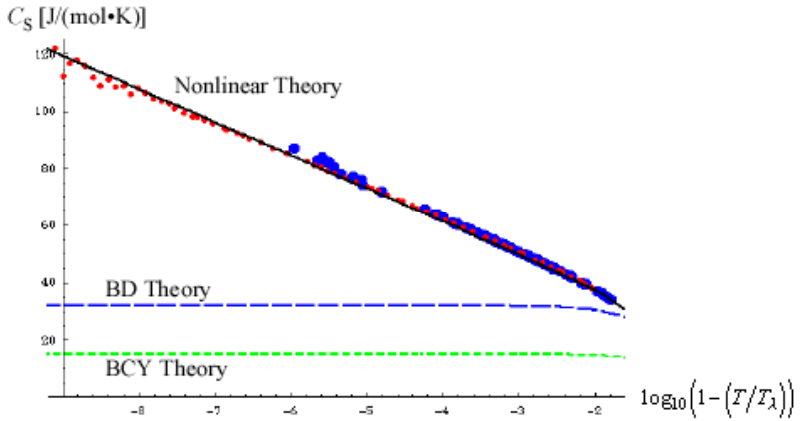

Fig. 5.9 Calculation result of the nonlinear theory for the specific heat

The upper curve portrays the calculation result of the nonlinear theory. The middle curve and the lower curve represent the results of the BD theory and the BCY theory respectively. Small red dots indicate the data of Lipa et al [16]. Large blue dots represent the data of references [15]. The specific heat values C_S are shown in units of [J/(mol·K)]. The horizontal axis shows $\log_{10}\left(1-\left(T/T_\lambda\right)\right)$.

As that figure depicts, the result of the nonlinear theory agree well with the experimental data for $0<\left(1-\left(T/T_\lambda\right)\right)<0.04$: the nonlinear theory produces logarithmic divergence of specific heat at the λ point. On the other hand, the curve of BD theory depicts no divergent behavior. Consequently, the present theory is inferred to explain the temperature dependence of specific heat in superfluid helium well for the whole temperature region. The second order solution in Sec. 5.2 is applicable to $0<T<2.1[\mathrm{K}]$; and the present method in this section is applicable to $2.1[\mathrm{K}]<T<T_\lambda$.

The transition temperature for Bose-Einstein condensation of dressed bosons is simultaneously calculated and the result is 2.172 K using the same parameter values as in the calculation of specific heat mentioned above. It can be seen in the mathematica program attached in this book.

VI. Bose–Einstein condensate of dressed bosons

The properties of a Bose–Einstein condensate are studied for nonlinear theory.

6.1 Number of condensed dressed bosons near the λ point

Using the method explained in sections 5.5 and 5.6, we examine the Bose-condensed number of dressed bosons near the λ point. The dressed boson number in the Bose–Einstein condensate and the dressed boson number in the excited states are denoted respectively as N_{super} and N_{normal}. The number N_{normal} is defined as

$$N_{\mathrm{normal}} = \frac{V}{(2\pi\hbar)^3}\int_{0(\mathbf{p}\neq 0)}^{\infty} n_{\mathbf{p}}\, 4\pi p^2 \mathrm{d}p \tag{6.1}$$

where

$$n_{\mathbf{p}} = \left(\exp\left[\left(\omega_{\mathbf{p}} - \mu\right)/\left(k_{\mathrm{B}}T\right)\right] - 1\right), \text{ and} \tag{6.2}$$

$$\mu = \omega_0 \qquad (\text{for } T < T_\lambda). \tag{6.3}$$

The number N_{super} is defined as

$$N_{super} = n_0 . \tag{6.4}$$

The total number conservation of dressed bosons gives the following relation as

$$N_{super} + N_{normal} = N \tag{6.5}$$

That is to say, the total number of dressed bosons is equal to the total number of helium atoms N in liquid helium. The excited dressed boson number approaches N at the λ point, and N_{super} approaches zero, as shown in the following.

$$N_{normal} \xrightarrow[T \to T_\lambda]{} N \tag{6.6a}$$

$$N_{super} \xrightarrow[T \to T_\lambda]{} 0 \tag{6.6b}$$

We can evaluate the integration (6.1) using the same method as that used in sections 5.5 and 5.6. Near the λ point, we adopt the excitation energy from BEC in the phonon region as

$$\omega_{\mathbf{p}} - \mu = \omega_{\mathbf{p}} - \omega_0 = \varepsilon_{\mathbf{p}} =$$
$$= c_2 p\left(1-\left(T/T_\lambda\right)+ap^3\right)^{1/3} + Dp\left(1-\left(T/T_\lambda\right)+bp^2\right)^{1/2}$$
$$(\text{for } 0 < p < q_1). \qquad (6.7)$$

Coefficients c_2 and D are determined as explained in Sec. 5.4. All functional forms are adopted to be equal to those of chapter 5. The integration (6.1) is also separable into four regions. Consequently, the integration can be calculated numerically using a computer. The temperature dependence of N_{normal}/N is portrayed in Fig. 6.1.

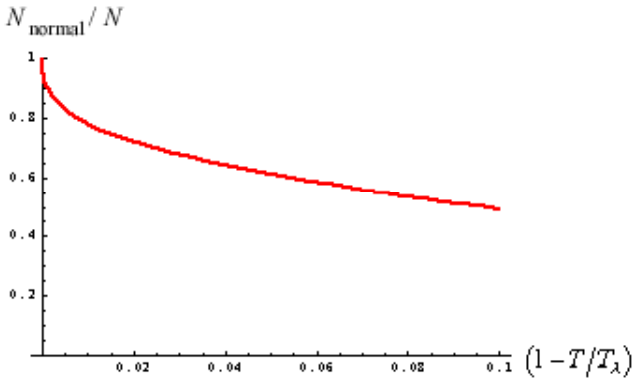

Fig. 6.1. The red curve shows the calculated values of N_{normal}/N.

It is shown here that the value of N_{normal}/N is certainly equal to 1.0 at the λ point, namely at $\left(1-T/T_\lambda\right)=0$.

In the integration in (6.1), the contribution from the phonon region is 87.0%, the contribution from the roton region is 8.8%, the contribution from the maxon region is 2.7%, and the contribution from the high-momentum region is 1.5% at the λ point. Accordingly, the total fraction of dressed bosons with nonzero momenta becomes 100%

of liquid helium at the λ point. That is to say, the Bose condensate of dressed bosons with momentum zero disappears at the λ point.

It is illustrative to examine the number of excitations in the Landau theory. The total excitation number of the Landau theory is approximately 14% of the total number of helium atoms at the λ point. Accordingly, it remains unclear in terms of the Landau theory whether the λ transition results from Bose–Einstein condensation.

The number of dressed bosons inside the Bose–Einstein condensate, $N_{super} = n_0$, has a temperature dependence near the λ point as depicted in Fig. 6.2 (see reference [20]).

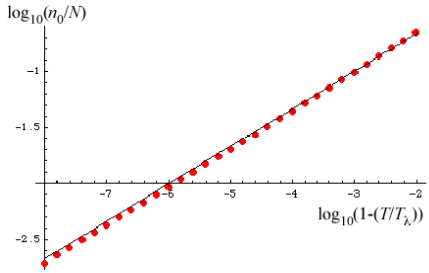

Fig. 6.2 Dots represent the calculated values of $\log_{10}\left(N_{\text{super}}/N\right)$

The function form of $(1-T/T_\lambda)^{1/3}$ is plotted as a black line, which well fits the calculated value of n_0/N. Therefore, the critical exponent of n_0/N is equal to 1/3. This mechanism is reexamined via an analytic method presented in the next section.

6.2 Critical index of condensed dressed boson number near the λ point

We use the functional form of energy as in chapter V: Eq. (5.22b) is applied to the dressed boson energy as

$$\omega_p - \omega_0 \approx pc_2\left(t + ap^3\right)^{1/3}, \tag{6.8}$$

where

$$t = 1 - T/T_\lambda , \tag{6.9}$$

for a small momentum region ($0 < p < p_s$) and for a vicinity of the λ point. We divide the integral (6.1) into two regions, $0 < p < p_s$ and $p_s < p$, as

$$\frac{N_{\text{normal}}}{N} = \frac{4\pi m}{(2\pi\hbar)^3 \rho}\left(\int_{0(p\neq 0)}^{p_s} n_p p^2 \mathrm{d}p + \int_{p_s}^{\infty} n_p p^2 \mathrm{d}p\right), \tag{6.10}$$

where

$$m/\rho = V/N . \tag{6.11}$$

Therein, m is the mass of a helium atom and ρ is the mass density of liquid helium. The dressed boson number in the first region is nearly equal to the following.

$$n_p = \frac{1}{\exp\left(\left(\omega_p - \omega_0\right)/\left(k_{\mathrm{B}}T\right)\right) - 1} \approx \frac{k_{\mathrm{B}}T}{pc_2\left(t + ap^3\right)^{1/3}} \tag{6.12}$$

Substitution of this equation into (6.10) yields

$$\frac{N_{\text{normal}}}{N} \approx \frac{4\pi m}{(2\pi\hbar)^3 \rho}\left(\int_{0(p\neq 0)}^{p_s} \frac{k_B T}{pc_2\left(t + ap^3\right)^{1/3}} p^2 \mathrm{d}p + \int_{p_s}^{\infty} n_p p^2 \mathrm{d}p\right) . \tag{6.13}$$

The first integral shows a singular behavior at the λ point, but the second integral has no singularity. Therefore, the second integral can be expanded into a Maclaurin series of t as

$$\int_{p_s}^{\infty} n_p p^2 \mathrm{d}p = G_0 + G_1 t + \mathrm{Order}\left(t^2\right) . \tag{6.14}$$

The first integral is expressed using the hyper geometric function as

$$\int_0^{p_s} \frac{1}{p\left(t + ap^3\right)^{1/3}} p^2 \mathrm{d}p = \frac{{p_s}^2 \ \mathrm{Hypergeometric2F1}\left[\frac{2}{3}, \frac{1}{3}, \frac{5}{3}, -\left(a\,{p_s}^3\right)/t\right]}{2t^{1/3}} . \tag{6.15}$$

This value is expanded to the following series:

$$\int_0^{p_s} \frac{1}{p\left(t+ap^3\right)^{1/3}} p^2 \mathrm{d}p = \frac{p_s}{a^{1/3}} + \frac{\Gamma\left(-\frac{1}{3}\right)\Gamma\left(\frac{5}{3}\right)}{2\Gamma\left(\frac{1}{3}\right)} \frac{t^{1/3}}{a^{2/3}} + \frac{1}{6} \frac{t}{a^{4/3} {p_s}^2} + \mathrm{Order}\left(t^2\right), \quad (6.16)$$

where $\Gamma(x)$ is the Gamma function. The second term on the right-hand-side of (6.16) has a singular value for its derivative by t at $t=0$. This expansion is explained in detail in Appendix II. Substitution of (6.14) and (6.16) into (6.13) yields the following expansion.

$$\frac{N_{\mathrm{normal}}}{N} = \frac{4\pi m}{(2\pi\hbar)^3 \rho_\lambda} \left(\frac{k_{\mathrm{B}} T_\lambda}{c_2} \left(\frac{p_s}{a^{1/3}} + \frac{\Gamma\left(-\frac{1}{3}\right)\Gamma\left(\frac{5}{3}\right)}{2\Gamma\left(\frac{1}{3}\right)} \frac{t^{1/3}}{a^{2/3}} \right) + G_0 + \mathrm{Order}(t) \right) \quad (6.17)$$

The fraction N_{normal}/N becomes 1 at the λ point because the Bose–Einstein condensate disappears at T_λ. This property is expressed by the equation shown below.

$$1 = \frac{4\pi m}{(2\pi\hbar)^3 \rho_\lambda} \left(\frac{k_{\mathrm{B}} T_\lambda}{c_2} \left(\frac{p_s}{a^{1/3}} \right) + G_0 \right) \quad (6.18)$$

The fraction of condensed dressed boson number for the total number is

$$\frac{n_0}{N} = \left(1 - \frac{N_{\mathrm{normal}}}{N}\right) = -\frac{4\pi m k_{\mathrm{B}} T_\lambda}{(2\pi\hbar)^3 \rho_\lambda c_2} \frac{\Gamma\left(-\frac{1}{3}\right)\Gamma\left(\frac{5}{3}\right)}{2\Gamma\left(\frac{1}{3}\right)} \frac{t^{1/3}}{a^{2/3}} + \mathrm{Order}(t) . \quad (6.19)$$

The function depends upon the temperature as $t^{1/3}$, which means that the critical index of n_0/N is 1/3. The result shows good agreement with the numerical calculation, as depicted in Fig. 6.2.

This temperature dependence $n_0/N \propto (1-T/T_\lambda)^{1/3}$ shows that the dressed boson velocity is directly related to $(1-T/T_\lambda)^{1/3}$ based on Eq. (5.17). Consequently, this analytical result reproduces that the second sound velocity is directly related to $(1-T/T_\lambda)^{1/3}$ near the λ point.

6.3 No friction against macroscopic body

The Landau theory has clarified that the background flow cannot be excited using a collision against a macroscopic body. We also examine a collision of the dressed bosons against a macroscopic body. The dressed bosons inside the Bose condensate cannot be

excited but the dressed bosons outside the Bose condensate can transfer to the other momentum state by a collision against a macroscopic body. This mechanism is examined as follows: The macroscopic body has a velocity $\mathbf{v}$, an initial energy E_i and an initial momentum P_i as

$$E_i = \frac{1}{2} M\mathbf{v}^2 \tag{6.20}$$

$$\mathbf{P}_i = M\mathbf{v}\ , \tag{6.21}$$

where M and $\mathbf{V}$ respectively signify the mass and the velocity of the macroscopic body. We consider the case in which this macroscopic body loses momentum $\mathbf{q}$ by the collision. The final energy E_f and the final momentum P_f of the macroscopic body are given as

$$\mathbf{P}_f = \mathbf{P}_i - \mathbf{q}\ \text{, and} \tag{6.22}$$

$$E_f = \frac{(M\mathbf{v}-\mathbf{q})^2}{2M} = E_i - \mathbf{v}\bullet\mathbf{q} + \frac{\mathbf{q}^2}{2M} \approx E_i - \mathbf{v}\bullet\mathbf{q}\ , \tag{6.23}$$

where the final equality in (6.23) is derived from neglecting the value $q^2/(2M)$ because q is a microscopic value and M is a macroscopic value. When the initial momentum of the dressed boson is described by $\mathbf{p}_A$ and the final momentum of the dressed boson is described by $\mathbf{p}_B$, the energy-momentum conservation is expressed as the following.

$$\mathbf{P}_f + \mathbf{p}_B = \mathbf{P}_i + \mathbf{p}_A \tag{6.24}$$

$$E_f + \omega_{\mathbf{p}_B} = E_i + \omega_{\mathbf{p}_A} \tag{6.25}$$

Then, we obtain the following equation from (6.22–25).

$$\mathbf{p}_B = \mathbf{p}_A + \mathbf{q} \tag{6.26}$$

$$\omega_{\mathbf{p}_B} = \omega_{\mathbf{p}_A} + \mathbf{v}\bullet\mathbf{q} \tag{6.27}$$

The transition of a dressed boson from momentum $\mathbf{p}_A$ to $\mathbf{p}_B$ is drawn in Fig. 6.3.

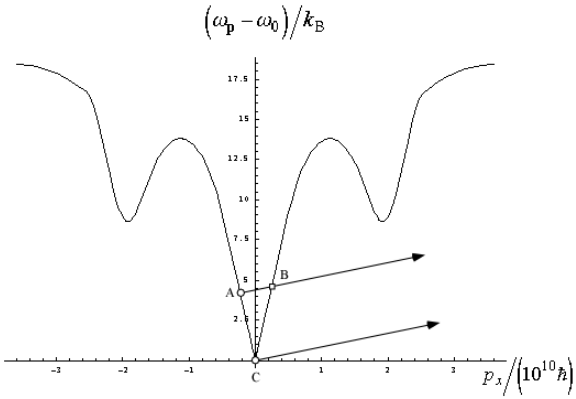

Fig. 6.3 Transition of the dressed bosons by a collision against a macroscopic body

This figure shows the case of $p_y = p_z = 0$. The horizontal axis indicates $p_x/(10^{10}\hbar)$. The dressed boson at point C cannot transfer to any state. The dressed boson at point A can transfer to point B.

In Fig. 6.3, the gradient value of the arrows is $(v\cos\theta)$ where θ is the angle between $\mathbf{v}$ and $\mathbf{q}$. The dressed boson with $\mathbf{p}_A \neq 0$ can transfer to momentum $\mathbf{p}_B$ (at point B) via a collision against a macroscopic body. However, there is no transition of the dressed bosons with zero momentum ($\mathbf{p}_C = 0$) for a velocity value smaller than the critical value $\mathrm{V_c}$. The critical velocity is the gradient of a tangential line from point C to the roton curve. This criterion is the same as that of Landau's mechanism. However, it is noteworthy that no quasi-particle exists at $\mathbf{p} = 0$ in the Landau theory because the density wave has no quantized mode at zero momentum. Landau assumed the background flow. The background flow is not excited via a collision against a macroscopic body; therefore, the background flow has been considered to be the superfluid component of liquid helium.

On the other hand, all dressed bosons are in the eigenstates of the total Hamiltonian. Only the dressed bosons in the Bose condensate have no friction against a macroscopic body, as shown clearly in Fig. 6.3. Therefore, the dressed bosons in the Bose

condensate are the superfluid component, and the dressed bosons with nonzero momentum are the normal fluid component (Later in chapter VIII, we examine the case in which Bose condensation occurs at nonzero momentum: the case of running superfluid.). Consequently the superfluid component comprises the dressed bosons in a Bose condensate.

The ratio of the dressed boson number with zero momentum to the total number of helium atoms, n_0/N , signifies the number fraction of superfluid component to the total liquid helium:

$$\eta_s = n_0/N \ . \tag{6.28}$$

The number fraction of normal fluid component is

$$\eta_n = \sum_{\mathbf{p}\neq 0} n_{\mathbf{p}}/N \ . \tag{6.29}$$

The temperature dependences of the number fractions were calculated in Sec. 6.1 and 6.2. It is noteworthy here that the quantities η_s and η_n are not mass fractions, but number fractions. The following equation is derived from the total number conservation.

$$\eta_s + \eta_n = \frac{1}{N}\left(n_0 + \sum_{\mathbf{p}\neq 0} n_{\mathbf{p}} \right) = \frac{N}{N} = 1 \tag{6.30}$$

In that equation, we used (2.15). These number fractions have typical values at $T = 0$ and $T = T_\lambda$.

$$\eta_n = 0, \ \eta_s = 1 \qquad (\text{at } T = 0) \tag{6.31}$$

$$\eta_n = 1, \ \eta_s = 0 \qquad (\text{at } T = T_\lambda) \tag{6.32}$$

The Bose condensate of the dressed bosons occupies 100% of the total number at zero Kelvin. The dressed bosons inside the Bose condensate cannot receive a friction force from a macroscopic body. Consequently, the dressed bosons with zero momentum are the superfluid component. Accordingly, Eq. (6.31) means that the superfluid component occupies 100% and the normal component disappears at zero Kelvin.

On the other hand, at the λ point, the fraction of Bose condensate of dressed bosons, η_s , disappears and the value of η_n becomes 1: the normal fluid component of dressed bosons occupies 100% of liquid helium at $T = T_\lambda$.

Number n_0 is not equal to the number of helium atoms with zero momentum.

As presented in chapter II, the dressed boson operator A_0^* is defined by the unitary transformation U from the operator a_0^* of helium atom as

$$A_0^* = U a_0^* U^{-1} \ . \tag{6.33}$$

The operator is approximately expressed as

$$A_0^* = \alpha a_0^* + \sum_{r,s} g(r,s) a_r^* a_s^* a_{r+s} + \cdots \ , \tag{6.34a}$$

where

$$\alpha \neq 1 \ . \tag{6.34b}$$

Therefore, the dressed boson number in the Bose condensate is

$$n_0 = A_0^* A_0 = \left(\alpha a_0^* + \sum_{r,s} g(r,s) a_r^* a_s^* a_{r+s} + \cdots \right) \left(\alpha a_0 + \sum_{t,u} g(t,u) a_{t+u}^* a_t a_u + \cdots \right) \neq a_0^* a_0 \ . \tag{6.35}$$

As described above, the dressed boson number with zero momentum is not equal to the number of helium atoms with zero momentum. The experimental data show that the number of helium atoms with zero momentum is a few percent of the total number of helium atoms at an ultra-low temperature.

Next we point out features of a one-dimensional (1D) boson system. The difference between $A_0^* A_0$ and $a_0^* a_0$ is remarkable in a 1D boson system with delta-functional potential. The expected values of $A_0^* A_0$ and $a_0^* a_0$ are, in the case of infinitely large coupling constant for the ground state:

$$\langle G | A_0^* A_0 | G \rangle / N \xrightarrow[N \to \infty]{} 1 \text{ and} \tag{6.36}$$

$$\langle G | a_0^* a_0 | G \rangle / N \xrightarrow[N \to \infty]{} 0 , \tag{6.37}$$

where $|G\rangle$ is the ground state.

VII. λ transition and phase diagram

7.1 Transition temperature of Bose–Einstein condensation

The phase diagram of liquid helium can be determined based on the nonlinear theory by calculating the temperature at which η_n becomes 1. That is to say, we evaluate the temperature value at which the dressed boson condensation disappears. The difference value $\omega_0 - \mu$ is zero for $T < T_\lambda$ (ω_0 is the lowest energy of a dressed boson and μ is the chemical potential) because the Bose condensate exists (see Eq. (3.4), and see (8.28) for more details). At $T > T_\lambda$, $\omega_0 - \mu$ becomes a positive value because the Bose–Einstein condensate disappears. This property is presented schematically in Fig. 7.1.

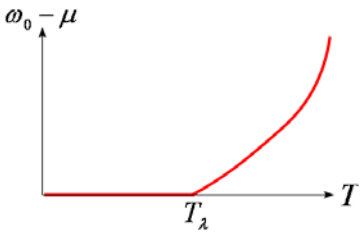

Fig. 7.1 Schematic figure for behavior of $\omega_0 - \mu$

The temperature dependence of N_{normal}/N and n_0/N is portrayed schematically in Fig. 7.2, where the value of N_{normal}/N is equal to 1 for $T > T_\lambda$.

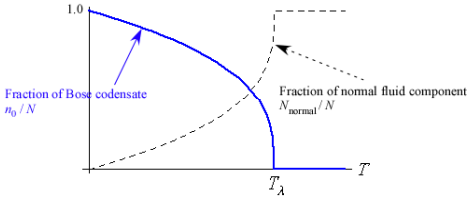

Fig. 7.2. The fraction of Bose condensate and the fraction of normal fluid component
The blue curve represents n_0/N of Bose condensate; the dashed curve represents N_{normal}/N

London calculated the transition temperature, the result of which is approximately 3.2 K for saturated vapor pressure [21]. It is noteworthy that the Bose condensate in London's theory is not superfluid because London's bosons with zero momentum are excited via a collision against a macroscopic body. On the other hand, the condensed dressed boson described in the present theory cannot be excited by collision against a macroscopic body because of its nonlinear form of energy, as clarified in Sec. 6.3.

The lowest energy is zero in London's theory. Therefore, London's chemical potential is equal to zero for $T < T_\lambda$. This result does not agree with the experimental data. In the nonlinear theory, $\omega_0(T)$ depends upon the temperature. Therefore, the chemical potential $\mu = \omega_0(T)$ depends also upon T for $T < T_\lambda$. This property shows good agreement with the experimental result.

The fraction N_{normal}/N in the nonlinear theory has been calculated numerically in Sec. 6.1 for $T < T_\lambda$. The fraction value depends upon the temperature. We find a value of transition temperature where the fraction N_{normal}/N becomes 1. For pressure P=0.05 bar, we obtain the value T_λ as

$$T_\lambda = 2.172\mathrm{K} \text{ for } P = 0.05\,\mathrm{bar}. \tag{7.1}$$

After changing the pressure value, we evaluate the transition temperature of Bose–Einstein condensation of the dressed bosons. Thereby, we obtain the phase diagram of He I and II (helium I represents a normal liquid for $T > T_\lambda$. Helium II represents a superfluid state for $T < T_\lambda$). The numerical result is portrayed in Fig. 7.3 (see reference [22]).

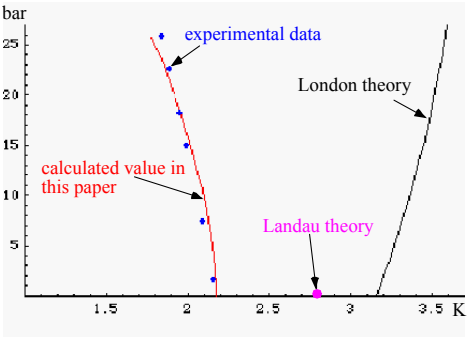

Fig. 7.3 Phase diagrams of the three theories

The red curve shows results obtained using the nonlinear theory; the black curve represents results obtained using the London theory. For the Landau theory, the transition temperature is calculated in reference [21]

London's result shows that the transition temperature becomes large for the increment of pressure value. The experimental value of the λ transition temperature decreases for the increment of pressure value. The calculation results of the nonlinear theory show good agreement with experimental data. The decrement of T_λ for the increment of pressure results from a nonlinear form of the total energy and by decrement of the roton minimum energy for the increment of pressure.

In the Landau theory, the λ transition is not caused by Bose–Einstein condensation. The excitation number $N_{\text{normal}}^{\text{Landau Theory}}$ depends upon the temperature. The temperature dependence of $N_{\text{normal}}^{\text{Landau Theory}}/N$ is depicted schematically in Fig. 7.4.

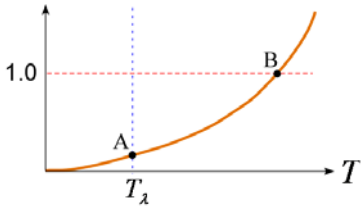

Fig. 7.4 Temperature dependence of $N_{\text{normal}}^{\text{Landau Theory}}/N$

The value of $N_{\text{normal}}^{\text{Landau Theory}}/N$ at the λ point is approximately 0.14.

As might be apparent in Fig. 7.4, $N_{\text{normal}}^{\text{Landau Theory}} / N$ is only 14% at the λ point. In addition, $N_{\text{normal}}^{\text{Landau Theory}} / N$ is larger than 1 for $T > T_B$ where T_B is the temperature at the point B. It might be difficult to consider the case of $N_{\text{normal}}^{\text{Landau Theory}} / N > 1$, although the number $N_{\text{normal}}^{\text{Landau Theory}}$ is not directly related to the total number of helium atoms. In the Landau theory, the transition temperature is determined by the calculation of mass density, which is explained in section 7.2.

7.2 λ transition temperature in Landau Theory

Landau calculated the mass density of normal fluid, which is described by ρ_n (see reference [3]). The functional form is presented on page 15 of Khalatnikov's book [3].

$$\rho_n = \frac{4}{3}\frac{E_{ph}}{c^2} + \frac{p_0^{\,2}}{3kT} n_r \tag{7.2}$$

Rough dependence of ρ_n upon the temperature is portrayed in Fig. 7.5.

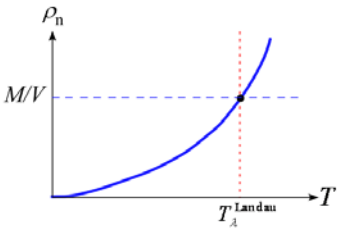

Fig. 7.5 Temperature dependence of ρ_n in the Landau theory

M/V is the mass density of liquid helium

The transition temperature in the Landau theory is determined as the

temperature at which the calculated value of ρ_n is equal to *M/V* (ρ_n , *M*, and *V* respectively denote the mass density of normal fluid component, the total mass, and the volume of liquid helium). The value is shown as approximately 2.8 K on page 195 of the book by Landau and Lifshitz [21].

$$T_\lambda^{\text{Landau}} = 2.8[\text{K}] \tag{7.3}$$

By that logic, the calculated value of ρ_n is greater than the total mass density *M/N* of liquid helium for $T > T_\lambda^{Landau}$. It is difficult to conceive of a normal fluid having a mass that is greater than the total mass of liquid helium. Therefore, the Landau theory is inapplicable to a liquid helium system for $T > T_\lambda$.

VIII. Two-fluid mechanism caused by nonlinear energy form

In Landau's work, elementary excitations are considered to be density waves in liquid helium. Accordingly, Landau's elementary excitations with momentum zero never exist. Landau's normal fluid component is constructed by the excitation modes, but his superfluid component is a background flow. The substantial existence of the background flow is unknown.

On the other hand, in the present theory, dressed bosons with momentum zero exist as described above. The total number of dressed bosons is conserved and is equal to the total number of helium atoms. This number conservation causes the Bose–Einstein condensation of dressed bosons. Moreover, the condensation occurs at any momentum value inside some region. This property is derived from the nonlinear form of the total energy of liquid helium. We first examine the distribution function of the dressed bosons.

8.1 Determination of the distribution function of the dressed bosons

By the present theory, the total number N, the total energy E, and the total momentum P_{tot} of the dressed bosons are conserved. We consider a micro-canonical ensemble of the dressed bosons where N, E, and P_{tot} are fixed to each value. Next we find the momentum distribution of the dressed bosons at equilibrium.

First, we count the quantum levels. The momentum interval from p_x to $p_x + \Delta p_x$ contains $\Delta p_x L/(2\pi\hbar)$ levels where L is the side length of the cubic container filled with liquid helium. Therefore, the number of quantum levels, X, inside the momentum region $\Delta p_x \Delta p_y \Delta p_z$ becomes

$$X = \Delta p_x \Delta p_y \Delta p_z \left(L/(2\pi\hbar)\right)^3 = \Delta p_x \Delta p_y \Delta p_z V/(2\pi\hbar)^3 , \tag{8.1}$$

where $V = L^3$ is the volume of the container. Next, we designate the number of the dressed bosons inside the momentum region $\Delta p_x \Delta p_y \Delta p_z$ by Y as

$$Y = \sum_{p_x \le s_x \le p_x + \Delta p_x} \sum_{p_y \le s_y \le p_y + \Delta p_y} \sum_{p_z \le s_z \le p_z + \Delta p_z} n_{\mathbf{s}} , \tag{8.2}$$

where the running variables (s_x, s_y, s_z) have values within the momentum range $p_x \le s_x \le p_x + \Delta p_x$, $p_y \le s_y \le p_y + \Delta p_y$, and $p_z \le s_z \le p_z + \Delta p_z$. Accordingly, the mean number of dressed bosons per quantum level is

$$\overline{n_{\mathbf{p}}} = Y/X = \frac{(2\pi\hbar)^3}{\Delta p_x \Delta p_y \Delta p_z V} \sum_{p_x \le s_x \le p_x + \Delta p_x} \sum_{p_y \le s_y \le p_y + \Delta p_y} \sum_{p_z \le s_z \le p_z + \Delta p_z} n_{\mathbf{s}}, \tag{8.3}$$

where the upper line in $\overline{n_{\mathbf{p}}}$ denotes the mean value. Here, the momentum region $\Delta p_x \Delta p_y \Delta p_z$ is sufficiently small, but contains an enormous number of levels. These two conditions are satisfied simultaneously because the value of *V* is a macroscopically large value.

The *Y* dressed bosons are distributed among the *X* levels. To quantify the modes of the distributions, first we determine the number of all possible ways of distribution expressed by $\Delta\Omega$, which is equal to

$$\Delta\Omega = (X + Y - 1)!/\{(X - 1)!Y!\}, \tag{8.4}$$

where we have used the bosonic property that any number of dressed bosons can occupy a single quantum level. Taking the logarithm of both sides of Eq. (8.4), we obtain

$$\begin{aligned} \log(\Delta\Omega) &\approx (X + Y)\log(X + Y) - X \log X - Y \log Y \\ &= X \log(1 + Y/X) + Y \log(1 + X/Y) \\ &= X\left[\log(1 + Y/X) + (Y/X)\log(1 + X/Y)\right] \\ &= \frac{\Delta p_x \Delta p_y \Delta p_z V}{(2\pi\hbar)^3}\left[\log\left(1 + \overline{n_p}\right) + \left(\overline{n_p}\right)\log\left(1 + \left(\overline{n_p}\right)^{-1}\right)\right] \end{aligned}, \tag{8.5}$$

where we have used Eqs. (8.1)–(8.4) and Stirling's formula. The total number of the distribution modes Ω is the multi-product of $\Delta\Omega$ as

$$\Omega = \prod \Delta\Omega,$$

which gives

$$\log\Omega = \sum \log\Delta\Omega \cdot$$

Summing up Eq. (8.5) over the whole momentum space, we obtain the total number of the distribution ways as

$$\log\Omega \approx \sum_{\text{all states}} \left[\log\left(1+\overline{n_p}\right) + \left(\overline{n_p}\right) \log\left(1+\left(\overline{n_p}\right)^{-1}\right) \right] . \tag{8.6}$$

The total number of dressed bosons N, the total energy E, and the total momentum $\mathbf{P}_{tot}$ are given as

$$N = \sum_{\mathbf{p}} \overline{n_{\mathbf{p}}} , \tag{8.7}$$

$$\mathbf{P}_{tot} = \sum_{\mathbf{p}} \mathbf{p} \overline{n_{\mathbf{p}}} , \tag{8.8}$$

$$E = \sum_{\mathbf{p}} \frac{\mathbf{p}^2}{2m} \bar{n}_{\mathbf{p}} + \frac{1}{N} \sum_{\mathbf{p},\mathbf{q}} f_2(\mathbf{p}-\mathbf{q}) \bar{n}_{\mathbf{p}} \bar{n}_{\mathbf{q}} + \frac{1}{N^2} \sum_{\mathbf{p},\mathbf{q},\mathbf{k}} f_3(\mathbf{p}-\mathbf{q},\mathbf{p}-\mathbf{k}) \bar{n}_{\mathbf{p}} \bar{n}_{\mathbf{q}} \bar{n}_{\mathbf{k}} + \cdots \tag{8.9}$$

where we have used Eq. (2.20) for the total energy. Although we can exchange (8.9) to a simpler form (2.21), we study the most general case in section 8.1.

We find the distribution function in which the number of states, Ω, becomes a maximum value under fixing the values of N, E and $\mathbf{P}_{tot}$. The maximization derives the following relation by making use of Lagrange multipliers.

$$\frac{\delta(\log\Omega)}{\delta \overline{n_{\mathbf{p}}}} = \beta \left\{ \frac{\delta E}{\delta \overline{n_{\mathbf{p}}}} - \mu \frac{\delta N}{\delta \overline{n_{\mathbf{p}}}} - \mathbf{u} \bullet \frac{\delta \mathbf{P}_{\text{tot}}}{\delta \overline{n_{\mathbf{p}}}} \right\} \tag{8.10}$$

Therein the functional derivatives are the following.

$$\frac{\delta(\log\Omega)}{\delta \overline{n_{\mathbf{p}}}} = \log\left(1+\left(\overline{n_{\mathbf{p}}}\right)^{-1}\right) \tag{8.11}$$

$$\frac{\delta E}{\delta \overline{n_{\mathbf{p}}}} = \omega_{\mathbf{p}} \tag{8.12a}$$

$$\omega_{\mathbf{p}} = \frac{\mathbf{p}^2}{2m} + \frac{1}{N}\sum_{\mathbf{q}} f_2(\mathbf{p}-\mathbf{q})\bar{n}_{\mathbf{q}} + \frac{1}{N}\sum_{\mathbf{q}} f_2(\mathbf{q}-\mathbf{p})\bar{n}_{\mathbf{q}} - \frac{1}{N^2}\sum_{\mathbf{s},\mathbf{t}} f_2(\mathbf{s}-\mathbf{t})\bar{n}_{\mathbf{s}}\bar{n}_{\mathbf{t}}$$
$$+\frac{1}{N^2}\sum_{\mathbf{q},\mathbf{k}} f_3(\mathbf{p}-\mathbf{q},\mathbf{p}-\mathbf{k})\bar{n}_{\mathbf{q}}\bar{n}_{\mathbf{k}} + \frac{1}{N^2}\sum_{\mathbf{q},\mathbf{k}} f_3(\mathbf{q}-\mathbf{p},\mathbf{q}-\mathbf{k})\bar{n}_{\mathbf{q}}\bar{n}_{\mathbf{k}} \tag{8.12b}$$
$$+\frac{1}{N^2}\sum_{\mathbf{q},\mathbf{k}} f_3(\mathbf{k}-\mathbf{q},\mathbf{k}-\mathbf{p})\bar{n}_{\mathbf{q}}\bar{n}_{\mathbf{k}} - \frac{2}{N^3}\sum_{\mathbf{s},\mathbf{q},\mathbf{k}} f_3(\mathbf{s}-\mathbf{q},\mathbf{s}-\mathbf{k})\bar{n}_{\mathbf{s}}\bar{n}_{\mathbf{q}}\bar{n}_{\mathbf{k}} + \cdots$$

$$\frac{\delta N}{\delta \bar{n}_{\mathbf{p}}} = 1 \tag{8.13a}$$

$$\frac{\delta \mathbf{P}_{tot}}{\delta \bar{n}_{\mathbf{p}}} = \mathbf{p} \tag{8.13b}$$

It is noteworthy in Eq. (8.12b) that we neglect the total number dependence of functions $f_2, f_3, f_4, \cdots$. Substitution of (8.11), (8.12a) and (8.13a,b) into (8.10) gives

$$\log\left(1 + \left(\bar{n}_{\mathbf{p}}\right)^{-1}\right) = \beta\left(\omega_{\mathbf{p}} - \mu - \mathbf{u}\bullet\mathbf{p}\right), \tag{8.14a}$$

which yields

$$\bar{n}_{\mathbf{p}} = \frac{1}{\exp\left(\beta\left(\omega_{\mathbf{p}} - \mu - \mathbf{u}\bullet\mathbf{p}\right)\right) - 1}, \tag{8.14b}$$

where $\beta, -\beta\mu, -\beta\mathbf{u}$ are the Lagrange multipliers. The well-known relation between the entropy S and the number of states Ω is

$$S = k_{\mathrm{B}} \log\Omega, \tag{8.15}$$

where k_B is Boltzmann's constant. Accordingly, the distribution function $\{\bar{n}_{\mathbf{p}}\}$ has a local maximum entropy when it satisfies (8.12b) and (8.14b).

We examine the physical meanings of the Lagrange multipliers $\beta, -\beta\mu, -\beta\mathbf{u}$. The following relation is derived using Eq. (8.10) when the distribution function $\{\bar{n}_{\mathbf{p}}\}$ of the liquid helium changes slightly by $\{\delta\bar{n}_{\mathbf{p}}\}$:

$$\sum_{\mathbf{p}} \frac{\delta(\log\Omega)}{\delta\bar{n}_{\mathbf{p}}}\delta\bar{n}_{\mathbf{p}} = \sum_{\mathbf{p}} \beta\left\{\frac{\delta E}{\delta\bar{n}_{\mathbf{p}}} - \mu\frac{\delta N}{\delta\bar{n}_{\mathbf{p}}} - \mathbf{u}\bullet\frac{\delta\mathbf{P}_{tot}}{\delta\bar{n}_{\mathbf{p}}}\right\}\delta\bar{n}_{\mathbf{p}},$$

which yields

$$\delta S = k_{\mathrm{B}}\beta\{\delta E - \mu\delta N - \mathbf{u}\bullet\delta\mathbf{P}_{tot}\}.$$

Therefore, for $\mathbf{u}=0$, we obtain

$$\delta E = \frac{1}{k_{\mathrm{B}}\beta}\delta S + \mu\delta N\,, \tag{8.16a}$$

where we have fixed the volume of liquid helium, namely $\delta V = 0$. As is well known, the thermodynamic relation gives

$$dE = -PdV + TdS + \mu\, dN\ . \tag{8.16b}$$

Comparison of (8.16a) and (8.16b) yields the following.

$$\beta = \frac{1}{k_{\mathrm{B}}T}, \qquad \mu = \text{chemicalpotential} \tag{8.17}$$

Therefore, knowing the physical meaning of the Lagrange multipliers, the distribution function of the dressed boson $\{\overline{n_{\mathbf{p}}}\}$ is determined using the following simultaneous equations.

$$\overline{n_{\mathbf{p}}} = \frac{1}{\exp\left(\left(\omega_{\mathbf{p}} - \mu - \mathbf{u}\bullet\mathbf{p}\right)/\left(k_{\mathrm{B}}T\right)\right)-1} \tag{8.18a}$$

$$\begin{aligned}\omega_{\mathbf{p}} = {} & \frac{\mathbf{p}^2}{2m} + \frac{1}{N}\sum_{\mathbf{q}} f_2(\mathbf{p}-\mathbf{q})\overline{n}_{\mathbf{q}} + \frac{1}{N}\sum_{\mathbf{q}} f_2(\mathbf{q}-\mathbf{p})\overline{n}_{\mathbf{q}} - \frac{1}{N^2}\sum_{\mathbf{s},\mathbf{t}} f_2(\mathbf{s}-\mathbf{t})\overline{n}_{\mathbf{s}}\overline{n}_{\mathbf{t}} \\ & + \frac{1}{N^2}\sum_{\mathbf{q},\mathbf{k}} f_3(\mathbf{p}-\mathbf{q},\mathbf{p}-\mathbf{k})\overline{n}_{\mathbf{q}}\overline{n}_{\mathbf{k}} + \frac{1}{N^2}\sum_{\mathbf{q},\mathbf{k}} f_3(\mathbf{q}-\mathbf{p},\mathbf{q}-\mathbf{k})\overline{n}_{\mathbf{q}}\overline{n}_{\mathbf{k}} \\ & + \frac{1}{N^2}\sum_{\mathbf{q},\mathbf{k}} f_3(\mathbf{k}-\mathbf{q},\mathbf{k}-\mathbf{p})\overline{n}_{\mathbf{q}}\overline{n}_{\mathbf{k}} - \frac{2}{N^3}\sum_{\mathbf{s},\mathbf{q},\mathbf{k}} f_3(\mathbf{s}-\mathbf{q},\mathbf{s}-\mathbf{k})\overline{n}_{\mathbf{s}}\overline{n}_{\mathbf{q}}\overline{n}_{\mathbf{k}} + \cdots\end{aligned} \tag{8.18b}$$

The coupled integral equation (8.18 a, b) has a single solution for $T > T_\lambda$. However, infinitely many solutions satisfy the coupled integral equation (8.18 a, b) for $T < T_\lambda$ because there are infinitely many values for the condensed momentum. To better elucidate this mechanism, we examine the following simple example in which there are only two quantum levels with a nonlinear form of energy. Which level has lower energy depends upon the distribution of bosons in the two levels.

8.2 Explanation of level inversion

We study this simple system which includes only two levels. The total energy of the system is given as

$$E = E_1 n_1 + E_2 n_2 + f_{12} n_1 n_2 , \tag{8.19}$$

in which n_1 and n_2 are boson numbers belonging to level 1 and 2, respectively, and the following inequalities hold:

$$E_1 < E_2 \text{ and } f_{12} > 0 . \tag{8.20}$$

The energy (8.19) would become a linear form with respect to the boson numbers if the coefficient f_{12} were equal to zero. Then, the energy of level 1 would always be lower than that of level 2 because of the inequality $E_1 < E_2$.

On the other hand, when $f_{12} > 0$, the total energy has a nonlinear form. In this case, which of level 1 or 2 has a lower energy depends upon the number distribution $\{n_1, n_2\}$. This fact is understood by studying the boson energy. The value of ω_i is defined as the energy increase, when we add one bose particle to level *i* (*i*=1 or 2):

$$\omega_1 = \partial E / \partial n_1 = E_1 + f_{12} n_2 , \ \omega_2 = \partial E / \partial n_2 = E_2 + f_{12} n_1 . \tag{8.21}$$

As the number n_2 becomes larger, the energy ω_1 becomes large because of $f_{12} > 0$, reaches the value of ω_2, and finally becomes larger than ω_2. Consequently, the energy magnitudes of the two levels are reversed by increasing the occupation number at the higher level, as presented Fig. 8.1.

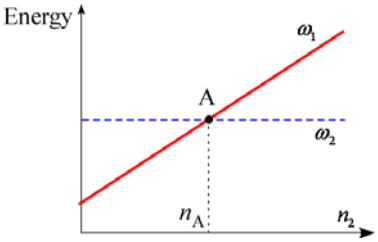

Fig. 8.1 Number dependence of dressed boson energies for two levels
ω_2 is smaller than ω_1 when $n_2 > n_A$

This example shows the level inversion mechanism which results from nonlinear form of the energy. A similar inversion between energy magnitudes of levels also occurs in the present theory because the total energy (2.20) has a nonlinear form.

8.3 Various values of momentum at which dressed bosons condense

Galilean invariant terms of the total energy have nonlinear forms. Therefore Eqs. (8.18a) and (8.18b) are never separated from each other. These nonlinear terms produce multiple solutions that satisfy the coupled integral equation (8.18a, b) for $T < T_\lambda$.

To elucidate this mechanism more precisely, we consider a case at an ultra-low temperature. We restrict ourselves to the following number distribution $\{\overline{n_{\mathbf{p}}}\}$, where almost all dressed bosons have momentum **Q**:

$$\overline{n}_{\mathbf{Q}} \approx 1 \text{, namely, } N - \overline{n}_{\mathbf{Q}} << \overline{n}_{\mathbf{Q}} . \tag{8.22}$$

The condensed momentum **Q** can have any value within some momentum range. We explain this mechanism in the energy form of (2.21). In this case, the dressed boson

energy $\omega_{\mathbf{p}}$ is expressed as in Eq. (3.2).

$$\omega_{\mathbf{p}}(T)=\frac{\mathbf{p}^2}{2m}+\frac{2}{N}\sum_{\mathbf{q}} f(\mathbf{p}-\mathbf{q})\bar{n}_{\mathbf{q}}-\frac{1}{N^2}\sum_{\mathbf{s},\mathbf{t}} f(\mathbf{s}-\mathbf{t})\bar{n}_{\mathbf{s}}\bar{n}_{\mathbf{t}} \tag{8.23}$$

The summations in Eq. (8.23) are approximately equal to the following form because $\bar{n}_{\mathbf{Q}}$ is large.

$$\omega_{\mathbf{p}}\approx\frac{\mathbf{p}^2}{2m}+\frac{2}{N}f(\mathbf{p}-\mathbf{Q})\bar{n}_{\mathbf{Q}}-\frac{1}{N^2}f(\mathbf{Q}-\mathbf{Q})\bar{n}_{\mathbf{Q}}\bar{n}_{\mathbf{Q}}+(\text{smallterms}) \tag{8.24}$$

Therein, the Galilean invariant term *f* is expressed as Eq. (2.41).

$$f(\mathbf{p})=\tfrac{1}{2}\left(\varepsilon_p^0-\mathbf{p}^2/(2m)\right)+f(0) \tag{8.25}$$

Then, Eq. (8.24) becomes the following.

$$\omega_{\mathbf{p}}\approx\frac{\mathbf{p}^2}{2m}+\frac{\bar{n}_{\mathbf{Q}}}{N}\left(\varepsilon_{\mathbf{p}-\mathbf{Q}}^0-(\mathbf{p}-\mathbf{Q})^2/(2m)\right)+\frac{2\bar{n}_{\mathbf{Q}}}{N}f(0)-\left(\frac{\bar{n}_{\mathbf{Q}}}{N}\right)^2 f(0)+(\text{smallterms}) \tag{8.26}$$

We present the momentum dependence of $\omega_{\mathbf{p}}$ schematically in Fig. 8.2.

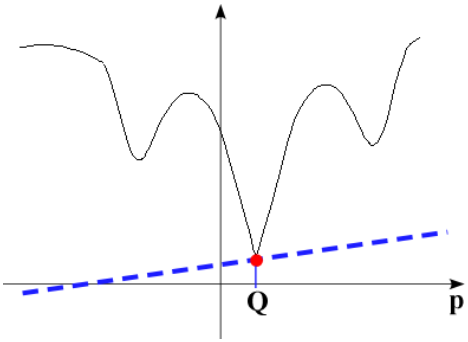

Fig. 8.2 Momentum dependence of dressed boson energy $\omega_{\mathbf{p}}$.

The dashed line represents $\mu + \mathbf{u} \bullet \mathbf{p}$

As might be readily apparent from this figure, $\left(\omega_{\mathbf{p}} - \mu - \mathbf{u} \bullet \mathbf{p}\right)$ has a minimum value at $\mathbf{p} = \mathbf{Q}$; the value is approximately zero.

$$\left(\omega_{\mathbf{Q}} - \mu - \mathbf{u} \bullet \mathbf{Q}\right) \approx 0 \tag{8.27}$$

We examine this value more precisely. Equation (8.18a) is written at $\mathbf{p} = \mathbf{Q}$ as follows.

$$\overline{n_{\mathbf{Q}}} = \frac{1}{\exp\left(\left(\omega_{\mathbf{Q}} - \mu - \mathbf{u} \bullet \mathbf{Q}\right) / \left(k_{\mathrm{B}} T\right)\right) - 1}$$

$$\approx \frac{k_{\mathrm{B}} T}{\omega_{\mathbf{Q}} - \mu - \mathbf{u} \bullet \mathbf{Q}}$$

Therefore, the chemical potential μ relates to the dressed boson energy as follows.

$$\mu = \omega_{\mathbf{Q}} - \mathbf{u} \bullet \mathbf{Q} - \frac{k_B T}{\overline{n_{\mathbf{Q}}}} \tag{8.28}$$

In that equation, the magnitude of $\frac{k_B T}{\overline{n_{\mathbf{Q}}}}$ is an order of 10^{-23}. Accordingly, the chemical potential μ deviates from $\omega_{\mathbf{Q}} - \mathbf{u} \bullet \mathbf{Q}$ by an extremely small value $-\frac{k_B T}{\overline{n_{\mathbf{Q}}}}$.

We consider another value of the condensed momentum which is expressed by $\mathbf{Q}'$. In this case, we obtain another energy form as the following expression.

$$\omega'_{\mathbf{p}} \approx \frac{\mathbf{p}^2}{2m} + \frac{\bar{n}_{\mathbf{Q}'}}{N}\left(\varepsilon^0_{\mathbf{p}-\mathbf{Q}'} - \left(\mathbf{p}-\mathbf{Q}'\right)^2/(2m)\right) + \frac{2\bar{n}_{\mathbf{Q}'}}{N} f(0) - \left(\frac{\bar{n}_{\mathbf{Q}'}}{N}\right)^2 f(0) + (\text{smallterms}) \tag{8.29}$$

The form of (8.29) differs from that of (8.26) because of $\mathbf{Q}' \neq \mathbf{Q}$. Accordingly, we can consider infinitely many solutions corresponding to infinitely many values of the condensed momentum.

It has been clarified that infinite multiple solutions exist in the coupled integral equation (8.18a, b) under fixing of the values of T *and* $\mathbf{u}$. That is to say, the condensed momentum value of $\mathbf{Q}$ can be taken to be an arbitrary value within some momentum region (This restriction within the region is necessary to satisfy positiveness of $\omega_{\mathbf{p}} - \omega_{\mathbf{Q}} - \mathbf{u} \bullet (\mathbf{p}-\mathbf{Q})$). Therefore, we can choose any value for two vectors $\mathbf{u}$ and $\mathbf{Q}$.

This mechanism produces a two-fluid state with two arbitrary velocities of the superfluid component and the normal fluid component. As presented Fig. 8.2, the dressed bosons with momentum $\mathbf{Q}$ have minimum energy because of the level inversion mechanism via Bose condensation at $\mathbf{Q}$.

In London's theory, the Bose condensate must have the same value as the velocity of the center of mass because no level inversion appears. Consequently, the nonlinear mechanism is important for explaining the properties of superfluid helium.

The following is also worth noting. A running superfluid component can be produced experimentally using the following process. A vessel filled with He I (normal liquid) is rotated at a constant angular velocity. Accordingly, the liquid helium has a constant angular velocity. Then, after the liquid helium is cooled by vaporization of the liquid helium, the temperature becomes lower than the λ temperature ($T < T_\lambda$). The superfluid component appears, and has non-zero velocity. Thereafter, the vessel is stopped. Then the normal fluid component also stops because of the viscosity of the normal fluid component. Therefore, we can produce the state in which the superfluid velocity differs from the normal fluid velocity.

8.4 Iteration method

In this section, we find the approximate solutions corresponding to the two-fluid state of He II using iteration.

Eq. (8.27) yields the following equation.

$$\omega_{\mathbf{p}} - \mu - \mathbf{u} \bullet \mathbf{p} = \omega_{\mathbf{p}} - \omega_{\mathbf{Q}} - \mathbf{u} \bullet (\mathbf{p} - \mathbf{Q}) \tag{8.30}$$

Using Eq. (8.23), we obtain

$$\omega_{\mathbf{p}}(T) - \omega_{\mathbf{Q}}(T) = \frac{\mathbf{p}^2 - \mathbf{Q}^2}{2m} + \frac{2}{N}\sum_{\mathbf{q}} \left(f(\mathbf{p} - \mathbf{q}) - f(\mathbf{Q} - \mathbf{q}) \right) \bar{n}_{\mathbf{q}} \,. \tag{8.31}$$

Consequently, we can rewrite the coupled integral equation (8.18a, b) to the following equations.

$$\bar{n}_{\mathbf{p}} = \frac{1}{exp\left(\left(\omega_{\mathbf{p}} - \omega_{\mathbf{Q}} - \mathbf{u} \bullet (\mathbf{p} - \mathbf{Q}) \right) / (k_B T) \right) - 1} \qquad (\text{for } \mathbf{p} \neq \mathbf{Q}) \tag{8.32a}$$

$$\begin{aligned} &\omega_{\mathbf{p}}(T) - \omega_{\mathbf{Q}}(T) - \mathbf{u} \bullet (\mathbf{p} - \mathbf{Q}) \\ &= \frac{\mathbf{p}^2 - \mathbf{Q}^2}{2m} - \mathbf{u} \bullet (\mathbf{p} - \mathbf{Q}) + \frac{2}{N}\sum_{\mathbf{q}} \left(f(\mathbf{p} - \mathbf{q}) - f(\mathbf{Q} - \mathbf{q}) \right) \bar{n}_{\mathbf{q}} \end{aligned} \tag{8.32b}$$

We can solve the coupled integral equation via iteration similarly to that explained in sections 3.2.2 and 3.2.3. We choose the zero-th order energy (i.e. the starting form of the energy in the iteration) as

$$\omega_{\mathbf{p}}^0 = \frac{\mathbf{p}^2}{2m} + \left(\varepsilon_{\mathbf{p}-\mathbf{Q}}^0 - (\mathbf{p} - \mathbf{Q})^2 / (2m) \right) + f(0) \,, \tag{8.33}$$

which is derived from Eq. (8.26) for $\frac{\bar{n}_{\mathbf{Q}}}{N} = 1$. It is noteworthy that the form depends upon the momentum value **Q** in the Bose condensate.

The zero-th order distribution function is given by altering the energy form $\omega_{\mathbf{p}}(T)$ to that of $\omega_{\mathbf{p}}^0$ in Eq. (8.32a).

$$n_{\mathbf{p}}^{0} = \frac{1}{\exp\left(\left(\omega_{\mathbf{p}}^{0} - \omega_{\mathbf{Q}}^{0} - \mathbf{u}\bullet(\mathbf{p}-\mathbf{Q})\right)/(k_{\mathrm{B}}T)\right)-1} \qquad (\text{for } \mathbf{p}\neq\mathbf{Q}) \qquad (8.34)$$

This distribution function depends upon two vectors: **Q** and **u**. We introduce the first order functions as follows.

$$\begin{aligned}&\omega_{1}(\mathbf{p},T)-\omega_{1}(\mathbf{Q},T)-\mathbf{u}\bullet(\mathbf{p}-\mathbf{Q})\\&=\frac{\mathbf{p}^{2}-\mathbf{Q}^{2}}{2m}-\mathbf{u}\bullet(\mathbf{p}-\mathbf{Q})+\frac{2}{N}\sum_{\mathbf{q}\neq\mathbf{Q}}\left(f(\mathbf{p}-\mathbf{q})-f(\mathbf{Q}-\mathbf{q})\right)n_{\mathbf{q}}^{0}\\&\quad+\left(f(\mathbf{p}-\mathbf{Q})-f(0)\right)\frac{2n_{\mathbf{Q}}^{0}}{N}\end{aligned} \qquad (8.35)$$

Therein, the zero-th approximation number of the dressed bosons in the Bose condensate is given as

$$n_{\mathbf{Q}}^{0} = N - \sum_{\mathbf{q}\neq\mathbf{Q}} n_{\mathbf{q}}^{0}\,, \qquad (8.36)$$

which is nearly equal to N at an ultra-cold temperature. Then, the first order form of the distribution function is given as the following expression.

$$n_{1}(\mathbf{p},T) = \frac{1}{\exp\left(\left(\omega_{1}(\mathbf{p},T)-\omega_{1}(\mathbf{Q},T)-\mathbf{u}\bullet(\mathbf{p}-\mathbf{Q})\right)/(k_{\mathrm{B}}T)\right)-1} \qquad (\text{for } \mathbf{p}\neq\mathbf{Q}) \qquad (8.37)$$

We express the $(\ell+1)$-th order forms of the functions using the ℓ–th order forms.

$$\begin{aligned}&\omega_{\ell+1}(\mathbf{p},T)-\omega_{\ell+1}(\mathbf{Q},T)-\mathbf{u}\bullet(\mathbf{p}-\mathbf{Q})\\&=\frac{\mathbf{p}^{2}-\mathbf{Q}^{2}}{2m}-\mathbf{u}\bullet(\mathbf{p}-\mathbf{Q})+\frac{2}{N}\sum_{\mathbf{q}\neq\mathbf{Q}}\left(f(\mathbf{p}-\mathbf{q})-f(\mathbf{Q}-\mathbf{q})\right)n_{\ell}(\mathbf{q},T)\\&\quad+\left(f(\mathbf{p}-\mathbf{Q})-f(0)\right)\frac{2n_{\ell}(\mathbf{Q},T)}{N}\end{aligned} \qquad (8.38)$$

Therein, the ℓ–th approximation number of the condensed dressed bosons is given as

$$n_{\ell}(\mathbf{Q},T) = N - \sum_{\mathbf{q}\neq\mathbf{Q}} n_{\ell}(\mathbf{q},T)\,. \qquad (8.39)$$

Then, the $(\ell+1)$–th order form of the distribution function is expressed as

$$n_{\ell+1}(\mathbf{p},T)=\frac{1}{\exp\left(\left(\omega_{\ell+1}(\mathbf{p},T)-\omega_{\ell+1}(\mathbf{Q},T)-\mathbf{u}\bullet(\mathbf{p}-\mathbf{Q})\right)/(k_{\mathrm{B}}T)\right)-1}\ . \qquad (8.40)$$

These relations (8.38), (8.39), and (8.40) depend on the values of T, N, V, $\mathbf{u}$, and $\mathbf{Q}$. Incidentally, in the bulk limit, these functions depend upon N/V. We can thereby express the higher order forms in our iteration method. We assume convergence of the series in the limit of $\ell \to \infty$; then we obtain the following functions.

$$\omega_{\mathbf{p}}(T, N/V, \mathbf{u}, \mathbf{Q})=\lim_{\ell\to\infty}\omega_{\ell}(\mathbf{p},T) \qquad \text{for } T<T_{\lambda} \qquad (8.41)$$

$$n_{\mathbf{p}}(T, N/V, \mathbf{u}, \mathbf{Q})=\lim_{\ell\to\infty} n_{\ell}(\mathbf{p},T) \qquad \text{for } T<T_{\lambda} \qquad (8.42)$$

These functions are the solutions of the coupled equation (8.18a, b). Using the iteration method, we can adopt an arbitrary value of $\mathbf{Q}$ in fixing the values of T, N, V, and $\mathbf{u}$. Consequently, we obtain infinitely multiple solutions for the coupled integral equation (8.18a, b) at $T<T_{\lambda}$.

On the other hand, no Bose condensate exists at $T>T_{\lambda}$ in the coupled equation (8.18a, b): no condensed momentum $\mathbf{Q}$ exists. Therefore, the coupled equations (8.18a, b) have only one set of solutions.

$$\omega_{\mathbf{p}}(T, N/V, \mathbf{u})=\lim_{\ell\to\infty}\omega_{\ell}(\mathbf{p},T) \qquad \text{for } T>T_{\lambda} \qquad (8.43)$$

$$n_{\mathbf{p}}(T, N/V, \mathbf{u})=\lim_{\ell\to\infty} n_{\ell}(\mathbf{p},T) \qquad \text{for } T>T_{\lambda} \qquad (8.44)$$

We have discussed determination of the number distribution of dressed bosons in both cases of $T<T_{\lambda}$ and $T>T_{\lambda}$. Accordingly, the present theory is applicable to a liquid helium system for any temperature region: He I and He II. On the other hand, the Landau theory cannot treat a liquid helium system at $T>T_{\lambda}$. The next chapter will address nonlinear properties of the solutions.

IX. Properties of the solutions

The solutions of the coupled equations (8.18a) and (8.18b) have important properties, which are summarized in 9.1–9.5.

9.1 Existence of the λ transition

As described in previous chapters, each solution contains the Bose condensate at an ultra-cold temperature, but the condensate disappears at a high temperature. Therefore, the λ transition is derived naturally from the nonlinear theory.

9.2 Superfluidity

The Bose condensate of the dressed bosons gives no friction against a rigid body because the condensed dressed bosons cannot transfer to the other momentum in a collision against a macroscopic rigid body. This mechanism is derived from the nonlinear energy form, as discussed in Sec. 6.3. Therefore, the superfluid component in liquid helium comprises the condensed dressed bosons. The lack of a friction against a rigid body is apparent in Fig. 8.2 for the condensed dreesed bosons with momentum $\mathbf{Q}$.

9.3 Coexistence of two interpenetrating fluids
(Why are the two fluid-states so stable?)

It is a surprising fact that the superfluid component flows permanently in spite of penetration of the normal fluid component. This phenomenon was described by Kojima et al. [9] using a vessel similar to that portrayed in Fig. 9.1.

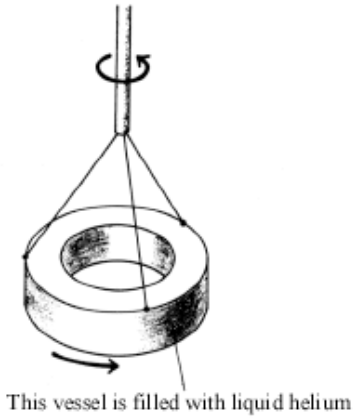

Fig. 9.1 Measurement of persistent current velocity for the superfluid component

The vessel has a narrow annular cavity (inner radius = 5.01 cm, outer radius = 5.48 cm, depth = 0.50 cm) that is packed with Al_2O_3 powder (grain size $170 \sim 325\,\mathring{A}$). First the vessel is filled with He I and is rotated at a constant angular velocity. Then, the liquid helium is cooled by vaporization of the liquid helium; the temperature becomes lower than the λ transition temperature ($T < T_\lambda$). Thereafter, the vessel is stopped. Using fourth-sound techniques, H. Kojima et al. [9] measured the decreasing rate of superfluid velocity. In their paper, the highest decay rate observed is 0.63% per decade. The current decay is 11% during a time interval equal to the age of the earth if this decay rate continues indefinitely. Therefore, the persistent currents of superfluid are indeed persistent. Accordingly, two-fluid states of superfluid helium are extremely stable.

This phenomenon is clearly explained using the nonlinear theory because infinitely many solutions appear at $T < T_\lambda$. The distribution function of the dressed bosons depends upon the two vectors **u** and **Q** as in Eq. (8.42) or (8.18a,b). This property implies that there are infinitely numerous equilibrium states with two velocities of superfluid component and normal fluid component that mutually differ. The distribution function of dressed bosons satisfies the coupled integral equations. The coupled

equations represent the condition maximizing the entropy. Therefore, the solutions have local maximum entropy. This nonlinear mechanism ensures the excellent stability of two-fluid states with two different velocities.

9.4 Zero entropy of the superfluid component

In our theory, the superfluid component comprises a macroscopically large number of the dressed bosons with only one momentum value. This non-spreading of the momentum-distribution yields that the superfluid component has entropy zero. As examined in chapter IV, the Bose condensate of the dressed bosons has entropy of

$$S_{\text{super}} = k_B \log(1+n_0) \quad .$$

However, this value is extremely small in comparison to the total entropy S.

$$S_{\text{super}} / S \xrightarrow[N\to\infty]{} 0 \tag{9.1}$$

All entropy of superfluid helium belongs to the normal fluid component, which comprises the dressed bosons outside the Bose condensate, as shown in Eq. (4.4).

$$S_{\text{normal}} / S \xrightarrow[N\to\infty]{} 1 \tag{9.2}$$

That is to say, the entropy of Bose-condensed dressed bosons is zero.

The momentum-distribution of helium atoms was measured in neutron scattering experiments. The results showed that helium atoms with zero momentum comprise a few percent of all helium atoms. Some researchers have asserted that this percentage is the ratio of Bose condensate to the total helium atoms. However, the helium atoms with zero momentum are not in the eigenstate of the total Hamiltonian because the atoms interact mutually. Therefore, this percentage does not represent the ratio of the real Bose condensate to the total liquid helium. In the nonlinear theory, the dressed bosons with momentum zero constitute 100% of the total dressed bosons at the temperature zero.

This situation is also clearly apparent in a 1D boson system. As shown in Eqs.(A1.17) and (A1.18) in Appendix I, the original free bosons with momentum zero do not constitute any fraction of the total bosons in the ground state. Nevertheless, the dressed bosons with momentum zero constitute 100% of the ground state.

9.5 Galilean covariance of the distribution functions

All solutions of the coupled equations (8.18a, 8.18b) are Galilean covariant. We prove this covariance for the two cases of $T < T_\lambda$ and $T > T_\lambda$.

(First case : $T < T_\lambda$)

In the previous chapter, we used iteration method to obtain the solutions. We consider one solution with vectors **u** and **Q**.

$$\omega_{\mathbf{p}} = \omega_{\mathbf{p}}(T, N/V, \mathbf{u}, \mathbf{Q}) = \lim_{\ell \to \infty} \omega_\ell(\mathbf{p}, T) \tag{9.3a}$$

$$n_{\mathbf{p}} = n_{\mathbf{p}}(T, N/V, \mathbf{u}, \mathbf{Q}) = \lim_{\ell \to \infty} n_\ell(\mathbf{p}, T) \tag{9.3b}$$

We also write the second solution for the other vectors $\mathbf{u}'$ and $\mathbf{Q}'$.

$$\omega'_{\mathbf{p}} = \omega_{\mathbf{p}}(T, N/V, \mathbf{u}', \mathbf{Q}') \tag{9.3c}$$

$$n'_{\mathbf{p}} = n_{\mathbf{p}}(T, N/V, \mathbf{u}', \mathbf{Q}') \tag{9.3d}$$

Therein, the vectors $\mathbf{u}'$ and $\mathbf{Q}'$ are related to the following.

$$\mathbf{u}' = \mathbf{u} + \mathbf{v} \tag{9.4}$$

$$\mathbf{Q}' = \mathbf{Q} + m\mathbf{v} \tag{9.5}$$

The coupled equations (8.32 a, b) are

$$n_{\mathbf{p}} = \frac{1}{\exp\left(\left(\omega_{\mathbf{p}} - \omega_{\mathbf{Q}} - \mathbf{u} \bullet (\mathbf{p} - \mathbf{Q})\right) / (k_{\mathrm{B}} T)\right) - 1}, \tag{9.6a}$$

$$\omega_{\mathbf{p}} - \omega_{\mathbf{Q}} - \mathbf{u} \bullet (\mathbf{p} - \mathbf{Q}) = \frac{\mathbf{p}^2 - \mathbf{Q}^2}{2m} - \mathbf{u} \bullet (\mathbf{p} - \mathbf{Q}) + \frac{2}{N} \sum_{\mathbf{q}} \left(f(\mathbf{p} - \mathbf{q}) - f(\mathbf{Q} - \mathbf{q}) \right) n_{\mathbf{q}}, \tag{9.6b}$$

$$n'_{\mathbf{p}} = \frac{1}{\exp\left(\left(\omega'_{\mathbf{p}} - \omega'_{\mathbf{Q}'} - \mathbf{u}' \bullet (\mathbf{p} - \mathbf{Q}')\right) / (k_{\mathrm{B}} T)\right) - 1} \quad \text{, and} \tag{9.6c}$$

$$\begin{aligned} &\omega'_{\mathbf{p}} - \omega'_{\mathbf{Q}'} - \mathbf{u}' \bullet (\mathbf{p} - \mathbf{Q}') \\ &= \frac{\mathbf{p}^2 - \mathbf{Q}'^2}{2m} - \mathbf{u}' \bullet (\mathbf{p} - \mathbf{Q}') + \frac{2}{N} \sum_{\mathbf{q}} \left(f(\mathbf{p} - \mathbf{q}) - f(\mathbf{Q}' - \mathbf{q}) \right) n'_{\mathbf{q}} \end{aligned} \quad . \tag{9.6d}$$

We use the momenta $\mathbf{p} + m\mathbf{v}$ and $\mathbf{q} + m\mathbf{v}$ in (9.6c, 9.6d) and then obtain the following expressions.

$$n'_{\mathbf{p}+m\mathbf{v}} = \frac{1}{\exp\left(\left(\omega'_{\mathbf{p}+m\mathbf{v}} - \omega'_{\mathbf{Q}'} - \mathbf{u}' \bullet (\mathbf{p} + m\mathbf{v} - \mathbf{Q}')\right) / (k_{\mathrm{B}} T)\right) - 1} \tag{9.7}$$

$$\begin{aligned} &\omega'_{\mathbf{p}+m\mathbf{v}} - \omega'_{\mathbf{Q}'} - \mathbf{u}' \bullet (\mathbf{p} + m\mathbf{v} - \mathbf{Q}') \\ &= \frac{(\mathbf{p} + m\mathbf{v})^2 - \mathbf{Q}'^2}{2m} - \mathbf{u}' \bullet (\mathbf{p} + m\mathbf{v} - \mathbf{Q}') \\ &\quad + \frac{2}{N} \sum_{\mathbf{q}+m\mathbf{v}} \left(f(\mathbf{p} + m\mathbf{v} - (\mathbf{q} + m\mathbf{v})) - f(\mathbf{Q}' - (\mathbf{q} + m\mathbf{v})) \right) n'_{\mathbf{q}+m\mathbf{v}} \end{aligned} \tag{9.8}$$

When we substitute the relations (9.4) and (9.5) into Eq. (9.8), we obtain these expressions.

$$\begin{aligned} &\omega'_{\mathbf{p}+m\mathbf{v}} - \omega'_{\mathbf{Q}'} - \mathbf{u}' \bullet (\mathbf{p} + m\mathbf{v} - \mathbf{Q}') \\ &= \frac{\mathbf{p}^2 - \mathbf{Q}^2 + 2m\mathbf{v} \bullet (\mathbf{p} - \mathbf{Q})}{2m} - \mathbf{u}' \bullet (\mathbf{p} - \mathbf{Q}) \\ &\quad + \frac{2}{N} \sum_{\mathbf{q}+m\mathbf{v}} \left(f(\mathbf{p} - \mathbf{q}) - f(\mathbf{Q} - \mathbf{q}) \right) n'_{\mathbf{q}+m\mathbf{v}} \\ &= \frac{\mathbf{p}^2 - \mathbf{Q}^2}{2m} - \mathbf{u} \bullet (\mathbf{p} - \mathbf{Q}) \\ &\quad + \frac{2}{N} \sum_{\mathbf{q}+m\mathbf{v}} \left(f(\mathbf{p} - \mathbf{q}) - f(\mathbf{Q} - \mathbf{q}) \right) n'_{\mathbf{q}+m\mathbf{v}} \end{aligned}$$

This equation is identical to (9.6b) using the assumption of $n'_{\mathbf{q}+m\mathbf{v}} = n_{\mathbf{q}}$.

$$\begin{aligned} &\omega'_{\mathbf{p}+m\mathbf{v}} - \omega'_{\mathbf{Q}'} - \mathbf{u}' \bullet (\mathbf{p} + m\mathbf{v} - \mathbf{Q}') \\ &\quad = \omega_{\mathbf{p}} - \omega_{\mathbf{Q}} - \mathbf{u} \bullet (\mathbf{p} - \mathbf{Q}) \end{aligned} \tag{9.9}$$

Substitution of (9.9) into (9.7) produces the following relation.

$$n'_{\mathbf{p}+m\mathbf{v}} = n_{\mathbf{p}} \tag{9.10}$$

This relation (9.10) is exactly the same as the assumed equation. Therefore the assumption is certainly correct. These relations (9.9) and (9.10) confirm the Galilean covariance between the solutions of the coupled equations (8.18a, 8.18b).

(Second case: $T > T_\lambda$)

Next we examine Galilean covariance in the second case. We respectively use the solutions (8.43) and (8.44) for $\omega_{\mathbf{p}}$ and $n_{\mathbf{p}}$.

$$\omega_{\mathbf{p}} = \omega_{\mathbf{p}}\left(T, N/V, \mathbf{u}\right) = \lim_{\ell\to\infty} \omega_\ell\left(\mathbf{p}, T\right) \tag{9.11a}$$

$$n_{\mathbf{p}} = n_{\mathbf{p}}\left(T, N/V, \mathbf{u}\right) = \lim_{\ell\to\infty} n_\ell\left(\mathbf{p}, T\right) \tag{9.11b}$$

In the case of $\mathbf{u}' = \mathbf{u} + \mathbf{v}$, we obtain another solution.

$$\omega'_{\mathbf{p}} = \omega_{\mathbf{p}}\left(T, N/V, \mathbf{u}'\right) \tag{9.11c}$$

$$n'_{\mathbf{p}} = n_{\mathbf{p}}\left(T, N/V, \mathbf{u}'\right) \tag{9.11d}$$

Using the energy form of (3.2), the coupled integral equations are satisfied as shown.

$$n_{\mathbf{p}} = \frac{1}{\exp\left(\left(\omega_{\mathbf{p}} - \mu - \mathbf{u}\bullet\mathbf{p}\right)/\left(k_{\mathrm{B}}T\right)\right) - 1} \tag{9.12a}$$

$$\omega_{\mathbf{p}} = \frac{\mathbf{p}^2}{2m} + \frac{2}{N}\sum_{\mathbf{q}} f\left(\mathbf{p}-\mathbf{q}\right) n_{\mathbf{q}} - \frac{1}{N^2}\sum_{\mathbf{s},\mathbf{t}} f\left(\mathbf{s}-\mathbf{t}\right) n_{\mathbf{s}} n_{\mathbf{t}} \tag{9.12b}$$

$$n'_{\mathbf{p}} = \frac{1}{\exp\left(\left(\omega'_{\mathbf{p}} - \mu' - \mathbf{u}' \bullet \mathbf{p}\right)/(k_{\mathrm{B}}T)\right) - 1} \tag{9.12c}$$

$$\omega'_{\mathbf{p}} = \frac{\mathbf{p}^2}{2m} + \frac{2}{N}\sum_{\mathbf{q}} f(\mathbf{p}-\mathbf{q}) n'_{\mathbf{q}} - \frac{1}{N^2}\sum_{\mathbf{s},\mathbf{t}} f(\mathbf{s}-\mathbf{t}) n'_{\mathbf{s}} n'_{\mathbf{t}} \tag{9.12d}$$

Equation (9.12d) is rewritten as the following.

$$\begin{aligned}\omega'_{\mathbf{p}+m\mathbf{v}} &= \frac{(\mathbf{p}+m\mathbf{v})^2}{2m} + \frac{2}{N}\sum_{\mathbf{q}} f(\mathbf{p}+m\mathbf{v}-\mathbf{q}) n'_{\mathbf{q}} - \frac{1}{N^2}\sum_{\mathbf{s},\mathbf{t}} f(\mathbf{s}-\mathbf{t}) n'_{\mathbf{s}} n'_{\mathbf{t}} \\ &= \frac{\mathbf{p}^2}{2m} + \mathbf{v}\bullet\mathbf{p} + \frac{1}{2}m\mathbf{v}^2 + \frac{2}{N}\sum_{\mathbf{q}+m\mathbf{v}} f(\mathbf{p}-\mathbf{q}) n'_{\mathbf{q}+m\mathbf{v}} - \frac{1}{N^2}\sum_{\mathbf{s},\mathbf{t}} f(\mathbf{s}-\mathbf{t}) n'_{\mathbf{s}+m\mathbf{v}} n'_{\mathbf{t}+m\mathbf{v}}\end{aligned}$$

They give the following expressions.

$$\begin{aligned}&\omega'_{\mathbf{p}+m\mathbf{v}} - \mu' - \mathbf{u}'\bullet(\mathbf{p}+m\mathbf{v}) \\ &\quad= \frac{\mathbf{p}^2}{2m} + \mathbf{v}\bullet\mathbf{p} + \frac{1}{2}m\mathbf{v}^2 - \mu' - \mathbf{u}'\bullet(\mathbf{p}+m\mathbf{v}) \\ &\qquad + \frac{2}{N}\sum_{\mathbf{q}+m\mathbf{v}} f(\mathbf{p}-\mathbf{q}) n'_{\mathbf{q}+m\mathbf{v}} - \frac{1}{N^2}\sum_{\mathbf{s},\mathbf{t}} f(\mathbf{s}-\mathbf{t}) n'_{\mathbf{s}+m\mathbf{v}} n'_{\mathbf{t}+m\mathbf{v}} \\ &\quad= \frac{\mathbf{p}^2}{2m} - \mu' - \mathbf{u}\bullet\mathbf{p} - \frac{1}{2}m\mathbf{v}^2 - m\mathbf{u}\bullet\mathbf{v} \\ &\qquad + \frac{2}{N}\sum_{\mathbf{q}+m\mathbf{v}} f(\mathbf{p}-\mathbf{q}) n'_{\mathbf{q}+m\mathbf{v}} - \frac{1}{N^2}\sum_{\mathbf{s},\mathbf{t}} f(\mathbf{s}-\mathbf{t}) n'_{\mathbf{s}+m\mathbf{v}} n'_{\mathbf{t}+m\mathbf{v}}\end{aligned}$$

It is noteworthy that the value of chemical potential μ' in Eq. (9.12c) differs from that of μ in (9.12a). The value of μ' is defined as

$$\mu' = \mu - \frac{1}{2}m\mathbf{v}^2 - m\mathbf{u}\bullet\mathbf{v} \ . \tag{9.13}$$

We can derive the following relation if we assume the relation $n'_{\mathbf{q}+m\mathbf{v}} = n_{\mathbf{q}}$.

$$\begin{aligned}&\omega'_{\mathbf{p}+m\mathbf{v}} - \mu' - \mathbf{u}'\bullet(\mathbf{p}+m\mathbf{v}) \\ &\qquad = \omega_{\mathbf{p}} - \mu - \mathbf{u}\bullet\mathbf{p}\end{aligned} \tag{9.14}$$

Substitution of (9.14) into (9.12c) reproduces the assumed relation as

$$n'_{\mathbf{p}+m\mathbf{v}} = n_{\mathbf{p}} \ . \tag{9.15}$$

Accordingly, (9.14) and (9.15) are satisfied by the solutions of the coupled integral equation (8.18a, 8.18b). As a result, Galilean covariance is verified for the coupled integral equations derived in the nonlinear theory.

X. Contribution of dressed bosons in several phenomena

The Landau theory is based on the excitation modes of phonons and rotons, the total number of which is not conserved. For that reason, there is no chemical potential for Landau's elementary excitation modes. However, the dressed bosons in the nonlinear theory have chemical potential, the value of which is expressed by Eq. (8.28).

$$\mu = \omega_{\mathbf{Q}} - \mathbf{u}\bullet\mathbf{Q} - \frac{k_B T}{n_{\mathbf{Q}}} \approx \omega_{\mathbf{Q}} - \mathbf{u}\bullet\mathbf{Q} \qquad (\text{for } T < T_\lambda) \qquad (10.1)$$

When both the superfluid component and normal fluid component have zero velocity, Eq. (10.1) becomes

$$\mu \approx \omega_0 \qquad (\text{for } T < T_\lambda)\,, \qquad (10.2)$$

which has already been obtained in Eq. (3.4). The relation between the chemical potential μ and the energy of the dressed bosons in the Bose condensate produces the characteristic phenomena in superfluid helium. We discuss London's relation in Sec. 10.1 and Wyatt's quantum evaporation in Sec.10.2.

10.1 London's relation in the fountain effect

We consider a U-tube whose center part is packed with fine powder, as illustrated in Fig. 10.1. Therein the powder size is a few hundred angstroms.

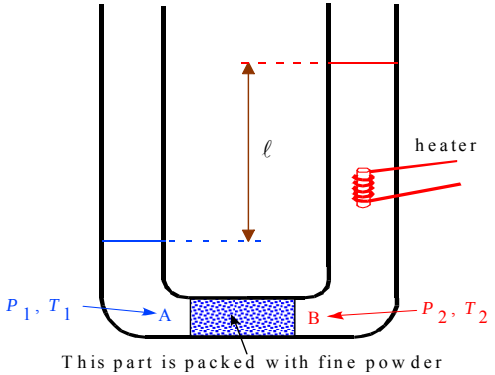

Fig. 10.1 Schematic figure depicting the fountain effect

Both sides of the U-tube are filled with He II. We designate the left side as "part 1" and call the right side part "part 2". The normal fluid component cannot pass

through the central channel of the U-tube because of the fine powder. Only the superfluid component can pass through the central channel because of its non-viscosity. The two liquid heliums inside part 1 and part 2 have different temperatures and different pressures from each other when we apply an electric current to the heater in Fig. 10.1. The two liquid heliums reach quasi-equilibrium. We respectively designate the temperatures and pressures at positions A and B as T_1 and T_2, and P_1 and P_2. Positions A and B have the same height as that shown in Fig. 10.1. The heights of two liquid surfaces for part 1 and part 2 differ. Therefore, the pressures P_1 and P_2 are related as

$$P_2 = P_1 + \rho g \ell , \tag{10.3}$$

where g is the acceleration of gravity and ℓ is the height difference of liquid surfaces presented in Fig. 10.1. Therein we have neglected a small variation of the mass density ρ caused by pressure dependence. At that time, the temperatures T_1 and T_2, and the pressures P_1 and P_2 are mutually related. We will derive the relation between these four values on the basis of the microscopic viewpoint of the nonlinear theory.

In the experiment presented in Fig. 10.1, both values of **u** and **Q** are zero.

$$\mathrm{u} = 0 \text{ and } \mathrm{Q} = 0 \tag{10.4}$$

Therefore, the chemical potentials μ_1 *and* μ_2 at positions A and B are given by Eqs. (10.2) and (8.41).

$$\mu_1 = \omega_0\left(T_1, N_1/V_1, 0, 0\right) \tag{10.5a}$$

$$\mu_2 = \omega_0\left(T_2, N_2/V_2, 0, 0\right) \tag{10.5b}$$

The Bose-condensed dressed bosons can pass through the central channel of the U-tube; then the connected system reaches a quasi-equilibrium state. At the quasi-equilibrium, the energy of a dressed boson inside the Bose condensate in part 1 is expected to be equal to that in part 2. (If the energy of condensed dressed bosons at A is greater than that at B, then the condensed dressed bosons transfer from A to B, and vice versa.) We can express this equality of the dressed boson energies in the Bose condensates.

$$\omega_0\left(T_1, N_1/V_1, 0, 0\right) = \omega_0\left(T_2, N_2/V_2, 0, 0\right) \tag{10.6}$$

This relation and Eqs. (10.5a,b) give the following equation.

$$\mu_1 = \mu_2 \tag{10.7}$$

In that equation, the chemical potentials depend on the temperature and pressure.

$$\mu_1 = \mu(T_1, P_1) \tag{10.8a}$$

$$\mu_2 = \mu(T_2, P_2) \tag{10.8b}$$

The thermodynamic relations are well known to yield the following.

$$\begin{aligned} d\mu &= \left(\frac{\partial \mu}{\partial T}\right)_P dT + \left(\frac{\partial \mu}{\partial P}\right)_T dP \\ &= -(S/N)dT + (V/N)dP \end{aligned} \tag{10.9}$$

Therein, (S/N) and (V/N) are the entropy and volume per particle (i.e. per dressed boson). This equation derives the following relation.

$$\begin{aligned} \mu(T_2, P_2) &= \mu(T_1 + \Delta T, P_1 + \Delta P) \\ &= \mu(T_1, P_1) - (S/N)\Delta T + (V/N)\Delta P \end{aligned} \tag{10.10}$$

where the temperature differnce and pressure difference between part 1 and part 2 are expressed as

$$\Delta T = T_2 - T_1, \text{ and } \Delta P = P_2 - P_1. \tag{10.11}$$

Therein we have assumed the differences ΔT and ΔP to be small. Substitution of (10.7) into (10.10) yields

$$-(S/N)\Delta T + (V/N)\Delta P = 0. \tag{10.12}$$

Denoting the number density and the entropy per dressed boson as η and s, respectively, we obtain the following equalities.

$$\eta = N/V \tag{10.13a}$$

$$s = S/N \tag{10.13b}$$

$$\frac{\Delta P}{\Delta T} = s\eta \tag{10.13c}$$

This relation was obtained by H. London [23] from phenomenological

considerations. We derived this relation from the Bose condensation of dressed bosons on the basis of the nonlinear theory. Regarding the experiment illustrated in Fig. 10.1, the pressure difference ΔP is given by Eq. (10.3). Substitution of (10.3) into (10.13c) yields

$$\rho g \ell = s \eta \left(T_2 - T_1 \right) . \tag{10.14}$$

The relation between the mass density and the number density is

$$\rho = m \eta \ . \tag{10.15}$$

It is substituted into Eq. (10.14); then the following equation is derived as

$$m g \ell = s \left(T_2 - T_1 \right) . \tag{10.16}$$

In F. London's theory (neglecting the inter-atomic potentials), the chemical potential is always zero. In that view, his chemical potential does not depend upon the temperature and the pressure. In Landau's theory, the number of excitations is not conserved. For that reason, the theory does not engender H. London's relation (10.13c). On the other hand, in the new viewpoint presented herein, relation (10.13c) is derived naturally from the nonlinear property of the dressed boson energy.

Actually, H. London's relation engenders the famous "fountain effect" phenomenon illustrated in Fig. 10.2. The powder absorbs the radiation from the left-hand side and is warmed. Therefore, the warmed superfluid helium has higher pressure, and a fountain of liquid helium gushes, as presented in Fig. 10.2.

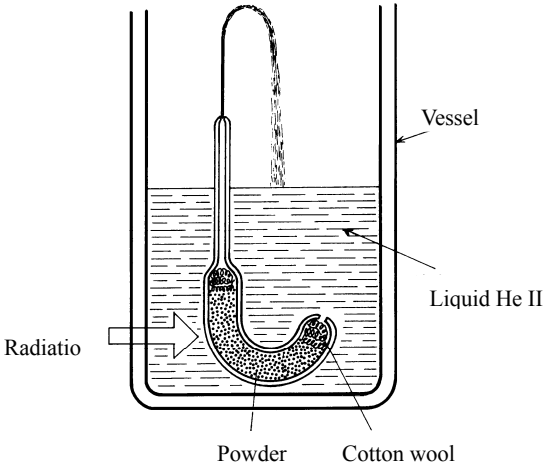

Fig. 10.2 Fountain effect in superfluid helium

10.2 Refraction and reflection of the dressed boson beam at a gas–liquid boundary

Wyatt et al. discovered the phenomenon of quantum evaporation. In the phenomenon, a phonon or a roton in superfluid helium ejects a ^{4}He atom into the helium gas through a single quantum-process (see Ref. [24]). We can explain that phenomenon in terms of the nonlinear theory. The dressed boson throws off its interaction cloud at the gas-liquid boundary when one dressed boson in the superfluid helium approaches the liquid surface. Then, the dressed boson becomes a ^{4}He atom and rushes out of the liquid helium into the vapor. It is our explanation for quantum evaporation.

We first examine a reversal process of the quantum evaporation. Figure 10.3 shows the surface between superfluid and gas of helium at Z=0. A helium atom with energy E rushes into liquid helium at Z=0 X=0. Its momentum value is $\mathbf{p}_A$. The atom interacts with other helium atoms and is dressed with the interaction cloud when the helium atom enters the superfluid helium.

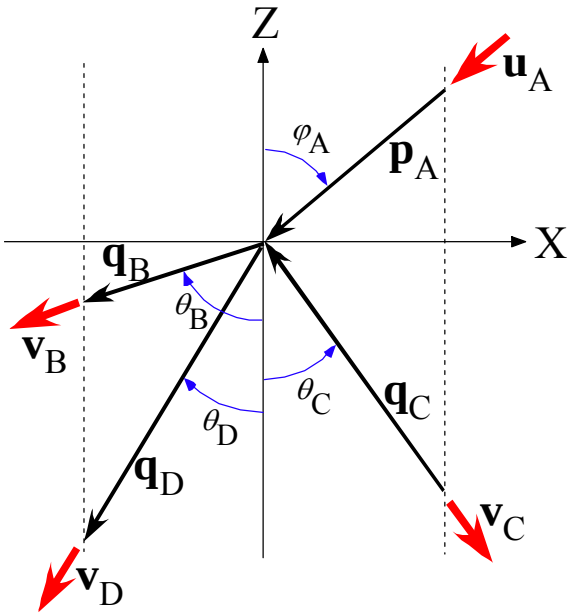

Fig. 10.3 Triple refraction at the boundary between a superfluid and gas

The helium atom has an energy value E between E_1 and E_2 defined in Eq. (10.19).

The energy is expected to be conserved at the liquid–gas boundary. That is to say, the energy of the atom inside the gas is equal to an energy of eigenstate inside superfluid helium, i.e. the energy of the dressed boson.

At an ultra-low temperature, the dressed boson energy is expressed as

$$\omega_{\mathbf{p}}^0 = \varepsilon_{\mathbf{p}}^0 + f(0) \,, \tag{10.17}$$

which is derived from Eqs. (3.5), (3.7), and (3.9) (it is also derived from (8.33)). The value of $f(0)$ is presented in reference [24] as

$$f(0) \approx -7.16 \times k_B \,. \tag{10.18}$$

We show the energy of dressed boson and the energy of helium atom in a gas in Fig. 10.4. The helium atom in gas has only kinetic energy because of the negligibly slight interaction.

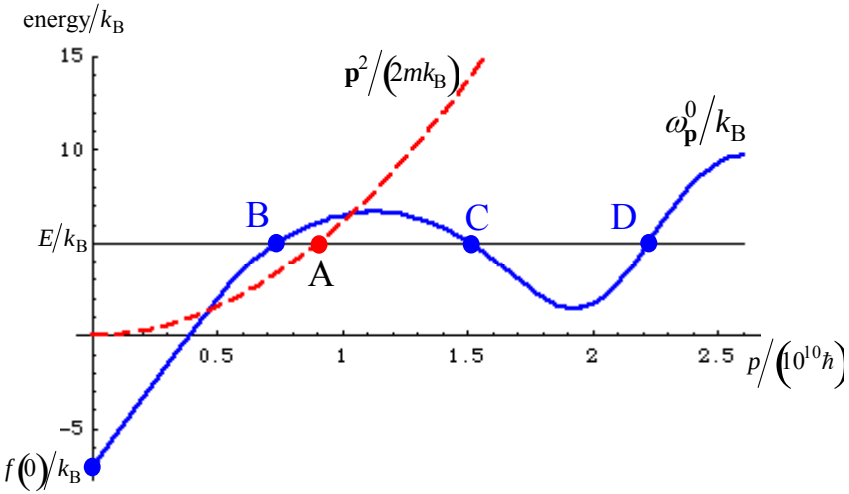

Fig. 10.4 Energy of dressed boson in liquid helium and energy of helium atom in a dilute gas

We consider one example with an energy value E in the region $E_1<E<E_2$ where

$$E_1 = \text{roton energy} + f(0), \quad E_2 = \text{maxon energy} + f(0) \quad .(10.19)$$

In this case, dressed bosons of three kinds have energy value E, as presented in Fig. 10.4.

$$E = \frac{\mathbf{p}_A^{\,2}}{2m} = \omega_{\mathbf{q}_B} = \omega_{\mathbf{q}_C} = \omega_{\mathbf{q}_D} \qquad (10.20)$$

Therefore, the helium atom A in Fig. 10.4 changes to the dressed boson B or C or D at the liquid-gas boundary. The group velocity is expressed as

$$\text{groop velocity} = \frac{\partial \omega_p}{\partial p} \quad . \qquad (10.21)$$

This value is positive for B and D, but is negative for C in Fig. 10.4. Accordingly, the velocity direction of dressed boson at B and D is the same direction as its momentum; however, the velocity direction at C is the opposite direction of its momentum, as portrayed in Fig. 10.3. The momentum magnitudes of the dressed bosons B, C, and D are

obtained as q_A, q_B, and q_C respectively from Fig. 10.4. The surface between the liquid and gas gives the helium atom a force that is vertical to the surface. Therefore, the momentum of the direction Z is not conserved, but the parallel momentum to the surface is conserved. This conservation yields the following relation.

$$p_A \sin\varphi_A = q_B \sin\theta_B = q_C \sin\theta_C = q_D \sin\theta_D \tag{10.22}$$

We calculate the angles for an example as follows: The example is the case of $E=5k_B$ and $\varphi_A = 15^\circ$. Using energy conservation (10.20), we can obtain the momentum magnitudes as follows:

$$p_A/\hbar \approx 0.9\text{A}^{-1},\ q_B/\hbar \approx 0.7\text{A}^{-1},\ q_C/\hbar \approx 1.5\text{A}^{-1},\ q_D/\hbar \approx 2.2\text{A}^{-1} \tag{10.23}$$

where A^{-1} indicates the reciprocal of angstrom. Then, (10.22) gives

$$\sin\theta_B = p_A \sin\varphi_A / q_B,\ \sin\theta_C = p_A \sin\varphi_A / q_C,\ \sin\theta_D = p_A \sin\varphi_A / q_D . \tag{10.24}$$

Substitution of $\varphi_A = 15^\circ$ gives the values of angles as follows.

$$\theta_B \approx 19^\circ,\ \theta_C \approx 9^\circ, \theta_D \approx 6^\circ \tag{10.25}$$

Quantum evaporation is the reverse process of that discussed above, as discovered by Wyatt et al. [24]. In a boundary between liquid and gas, triple refraction occurs when a beam of helium atoms has an appropriate energy and direction. Similarly, there is a triple reflection of a dressed boson beam at a boundary between the superfluid helium and a solid wall. In the triple refraction and triple reflection, the branching ratios are calculable from the interaction at the boundary. The branching ratio with a large momentum transfer is predicted to be smaller than that with a small momentum transfer. More comprehensive investigation is explained in Ref. [29], where the ratios of the transmission rates are calculated and the triple reflection is also discussed.

XI. Thermodynamic functions

In this chapter, we express various thermodynamic functions in terms of the distribution function of dressed bosons in the case of **u**=**Q**=0.

Entropy S is obtainable using Eq. (4.1).

$$S = k_B \sum_{\mathbf{p}} \left\{ \log\left(1 + n_{\mathbf{p}}\right) + n_{\mathbf{p}} \log\left(1 + n_{\mathbf{p}}^{-1}\right) \right\} \tag{11.1}$$

The total energy is expressed as Eq. (2.21) as (a more general case has the energy form (2.20))

$$E = \sum_{\mathbf{p}} \frac{\mathbf{p}^2}{2m} n_{\mathbf{p}} + \frac{1}{N} \sum_{\mathbf{p},\mathbf{q}} f(\mathbf{p}-\mathbf{q}) n_{\mathbf{p}} n_{\mathbf{q}} \ . \tag{11.2}$$

We calculate the free energy F of the present system.

$$\begin{aligned} F &= E - TS \\ &= \sum_{\mathbf{p}} \frac{\mathbf{p}^2}{2m} n_{\mathbf{p}} + \frac{1}{N} \sum_{\mathbf{p},\mathbf{q}} f(\mathbf{p}-\mathbf{q}) n_{\mathbf{p}} n_{\mathbf{q}} \\ &\quad - k_B T \sum_{\mathbf{p}} \left\{ \log\left(1 + n_{\mathbf{p}}\right) + n_{\mathbf{p}} \log\left(1 + n_{\mathbf{p}}^{-1}\right) \right\} \end{aligned} \tag{11.3}$$

Therein the factor $\log\left(1 + n_{\mathbf{p}}^{-1}\right)$ is expressed as

$$\log\left(1 + n_{\mathbf{p}}^{-1}\right) = \left(\omega_{\mathbf{p}} - \mu\right) / \left(k_B T\right) , \tag{11.4}$$

which is derived from (3.3) or (8.18a) in the case of **u**=**Q**=0. Substitution of this equation into (11.3) yields the following expression.

$$
\begin{aligned}
F &= \sum_{\mathbf{p}} \frac{\mathbf{p}^2}{2m} n_{\mathbf{p}} + \frac{1}{N} \sum_{\mathbf{p},\mathbf{q}} f(\mathbf{p}-\mathbf{q}) n_{\mathbf{p}} n_{\mathbf{q}} \\
&\quad - k_B T \sum_{\mathbf{p}} \left\{ \log\left(1+n_{\mathbf{p}}\right) + n_{\mathbf{p}} \left(\omega_{\mathbf{p}} - \mu\right) / \left(k_B T\right) \right\} \\
&= \sum_{\mathbf{p}} \frac{\mathbf{p}^2}{2m} n_{\mathbf{p}} + \frac{1}{N} \sum_{\mathbf{p},\mathbf{q}} f(\mathbf{p}-\mathbf{q}) n_{\mathbf{p}} n_{\mathbf{q}} \\
&\quad - k_B T \sum_{\mathbf{p}} \log\left(1+n_{\mathbf{p}}\right) - \sum_{\mathbf{p}} \omega_{\mathbf{p}} n_{\mathbf{p}} + \mu N
\end{aligned}
\tag{11.5}
$$

The Gibbs free energy is equal to μN . The chemical potential is equal to ω_0 for the case of $T < T_\lambda$. Accordingly,

$$
G = \mu N = N\omega_0(T) = 2\sum_{\mathbf{q}} f(\mathbf{q}) n_{\mathbf{q}} - \frac{1}{N} \sum_{\mathbf{s},\mathbf{t}} f(\mathbf{s}-\mathbf{t}) n_{\mathbf{s}} n_{\mathbf{t}} \,. \tag{11.6}
$$

Equation (11.5) and (11.6) gives *PV* as follows.

$$
\begin{aligned}
PV &= G - F = \mu N - F \\
&= -\sum_{\mathbf{p}} \frac{\mathbf{p}^2}{2m} n_{\mathbf{p}} - \frac{1}{N} \sum_{\mathbf{p},\mathbf{q}} f(\mathbf{p}-\mathbf{q}) n_{\mathbf{p}} n_{\mathbf{q}} \\
&\quad + k_B T \sum_{\mathbf{p}} \log\left(1+n_{\mathbf{p}}\right) + \sum_{\mathbf{p}} \omega_{\mathbf{p}} n_{\mathbf{p}}
\end{aligned}
\tag{11.7}
$$

Consequently, the pressure *P* is expressed as

$$
\begin{aligned}
P &= -\frac{1}{V} \sum_{\mathbf{p}} \frac{\mathbf{p}^2}{2m} n_{\mathbf{p}} - \frac{1}{NV} \sum_{\mathbf{p},\mathbf{q}} f(\mathbf{p}-\mathbf{q}) n_{\mathbf{p}} n_{\mathbf{q}} \\
&\quad + \frac{k_B T}{V} \sum_{\mathbf{p}} \log\left(1+n_{\mathbf{p}}\right) + \frac{1}{V} \sum_{\mathbf{p}} \omega_{\mathbf{p}} n_{\mathbf{p}} \quad .
\end{aligned}
\tag{11.8}
$$

We can also express the enthalpy *H* using Eqs. (11.2) and (11.7) as the following.

$$
H = E + PV = k_B T \sum_{\mathbf{p}} \log\left(1+n_{\mathbf{p}}\right) + \sum_{\mathbf{p}} \omega_{\mathbf{p}} n_{\mathbf{p}} \tag{11.9}
$$

Therefore, we obtained various kinds of thermodynamic functions *E, F, H, G, S*, and *P*. The functions can also be calculated using a different process. As an example, the entropy and pressure are calculated using the partial derivatives of the free energy *F*. The calculations are executed in Appendix III. Of course, our results through this different process are the same as the previous calculation results in this section. In the calculation

of the partial derivative by *V*, it is noteworthy that the intervals of the momentum-levels vary according to the change of the volume. The details are provided in Appendix III.

If the temperature dependence of the energies does not satisfy the coupled nonlinear equations (8.18a) and (8.18b), then two calculation results of one thermodynamic function via two different processes are not in mutual agreement. The calculation results are incredible when the temperature dependence of elementary excitation energy is artificially chosen (where the energy form does not generally satisfy the coupled equation).

Regarding the quantum dynamics of a many-body system, its eigenenergies do not include temperature variable. The temperature variable appears in statistical physics. The temperature dependence of excitation energy is caused by changing of quasi particle distribution via changing of a temperature value. Therefore the variation of excitation energy does not occur in linear form of eigenenergy like $E = \sum_{\mathbf{p}} \varepsilon_{\mathbf{p}} n_{\mathbf{p}}$ because the excitation energy is independent of quasi particle distribution. Consequently it is doubtful to apply both use of linear form like $E = \sum_{\mathbf{p}} \varepsilon_{\mathbf{p}} n_{\mathbf{p}}$ and use of the temperature dependence of $\varepsilon_{\mathbf{p}}$ simultaneously. If the simultaneous use is employed, two calculation results of one thermodynamic function via two different processes are not in mutual agreement as mentiond above. However, the methods are used widely to explain the temperature dependence of excitation energy. In this article, we have created the more reliable method described above.

XII. Discussion and Conclusions

A nonlinear mechanism has been examined in the previous chapters for a liquid helium system. The total Hamiltonian has a Galilean covariant form. Therefore, the diagonalized form of the total Hamiltonian has a nonlinear form with respect to the number operators of the dressed bosons. This nonlinearity yields the coupled integral equations determining the momentum distribution of dressed bosons. These coupled equations have infinitely numerous solutions at a temperature lower than the λ point. The nonlinearity produces remarkable properties; for example, two-fluid mechanism, logarithmic divergence of specific heat, critical exponent at the λ point, fountain effect, quantum evaporation, and so on.

In this final chapter, we briefly discuss a few phenomena expected from the present theory.

12.1 Width of elementary excitation energy

The dynamic structure factor $S(q,\nu)$ has been measured in experiments of neutron scattering [25] or laser-light scattering [17] of superfluid helium, where q denotes the momentum transfer and ν is the energy transfer. The function form of $S(q,\nu)$ has a peak for changing of energy transfer ν under fixing of q. According to Landau's theory, the peak width becomes larger as the temperature approaches the λ point. On the other hand, the nonlinear theory predicts that the dynamic structure factor has a delta-function peak produced by excitation of a dressed boson inside the Bose condensate to the other momentum state. For the momentum transfer **q**, the dressed boson has the following momentum value.

(Initial momentum)=0, (Final momentum)=**q** (12.1)

(Energy transfer)= $\nu = \omega_{\mathbf{q}} - \omega_0$ (12.2)

The Bose condensate disappears at a temperature higher than the λ- point. Therefore, the delta-function peak also disappears at $T > T_\lambda$.

We can consider another excitation of dressed boson outside the Bose condensate. In the excitation, the initial momentum and final momentum are expressed as follows.

$$\text{(Initial momentum)}=\mathbf{k},\ \text{(Final momentum)}=\mathbf{k}+\mathbf{q}(\ \mathbf{k} \neq 0\ ) \tag{12.3}$$

$$\text{(Energy transfer)}=\nu = \omega_{\mathbf{k}+\mathbf{q}} - \omega_{\mathbf{k}} \tag{12.4}$$

The values of momentum $\mathbf{k}$ ($\mathbf{k} \neq 0$) are distributed in a wide region. Therefore, the energy transfer has various values. This excitation process produces a broad peak in $S(q,\nu)$. Moreover, we can consider the multiple excitations. These excitations also have a broad peak. As an example, we present the schematic behavior of $S(q,\nu)$ at the momentum transfer of roton minimum $q = q_{roton}$ in Fig. 12.1.

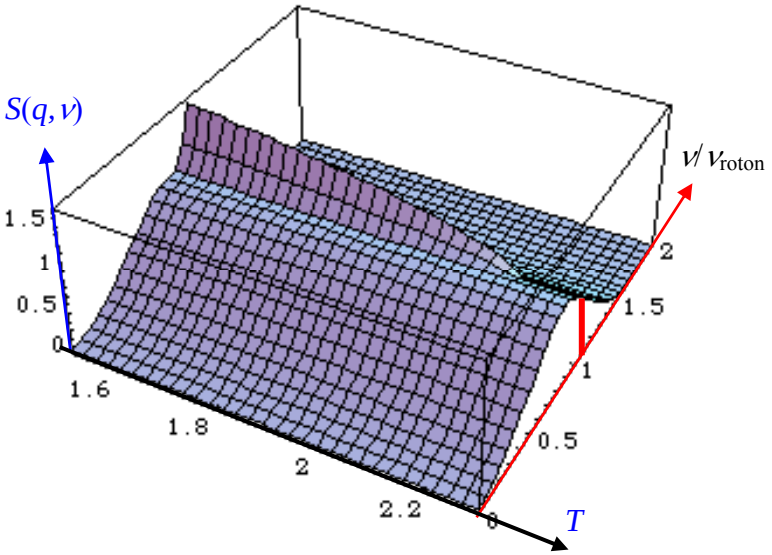

Fig. 12.1 Schematic diagram of dynamic structure factor predicted using the present theory

As presented in Fig. 12.1, in the nonlinear theory, it is predicted that a sharp peak appears at $T < T_\lambda$, but disappears at $T > T_\lambda$. This sharp peak has an instrumental width. The peak energy value of the broad peak differs from that of the sharp peak. The behavior depends on the distribution of the dressed bosons.

We can see precise behaviors of the dynamic structure factor for an extremely small momentum transfer in laser light scatterings. Experimental results were obtained from many experiments [17]. Four peaks are detected. Two correspond to the first sound peak and second sound peak of the Stokes process. The other two peaks belong to the anti-Stokes process. The peak width of the second sound is smaller than that of the first sound near the λ point [17]. The experimental width of the second sound peak is equal to the instrumental linewidth. This fact is a strong impetus to consider the second sound peak near the λ point as the excitation mode from the Bose–Einstein condensate.

This second sound peak had not been detected in any neutron scattering. However, the authors surmise that the peak will also be discovered in neutron scatterings if the instrumental linewidth becomes narrower and if the neutron scattering is carried out in an extremely small momentum transfer near the λ point. (The dynamic structure factor $S(q,\nu)$ observed in neutron scatterings should have the same peaks as in Brillouin scattering of laser-light.) The relevant details are discussed in references [26] and [27].

Brillouin scattering of laser light in superfluid helium has been measured using a Fabry-Perot interferometer, as described in the related literature [17]. The other techniques are investigated to improve accuracy. Eden and Swinny measured Brillouin spectra of xenon gas using an optical beating technique [30]. Sakai and Takagi improved the technique and then achieved a small instrumental linewidth [31]. The second sound peak width will be much smaller than that in Fabry-Perot measurement if this technique is applied to measure the Brillouin spectra of superfluid helium.

12.2 Temperature gap appearing in rotating superfluid helium: (Temperature dependence of critical velocity)

We discuss the temperature dependence of the critical velocity of a superfluid component for the case with zero velocity of normal fluid component. As explained in Sec. 5.4, the energy of the dressed boson near the λ point is expressed as in Eq. (5.17).

$$\omega_{\mathbf{p}} = \frac{n_0}{N} cp + \text{Order}\left(p^2\right) + \omega_0 \tag{12.5}$$

This energy form derives the velocity of the dressed boson for a small momentum near the λ point as

$$\frac{\partial \omega_{\mathbf{p}}}{\partial p} = \frac{n_0}{N} c \propto \left(T_\lambda - T\right)^{1/3}. \tag{12.6}$$

This velocity of the dressed boson becomes smaller than Landau's critical velocity in a vicinity of the λ point. Accordingly, the critical velocity of the present theory is given as

$$V_C \propto \left(T_\lambda - T\right)^{1/3} \qquad \text{(near the } \lambda \text{ point)}. \tag{12.7}$$

We drew a schematic figure of the critical velocity near the λ point in Fig. 12.2.

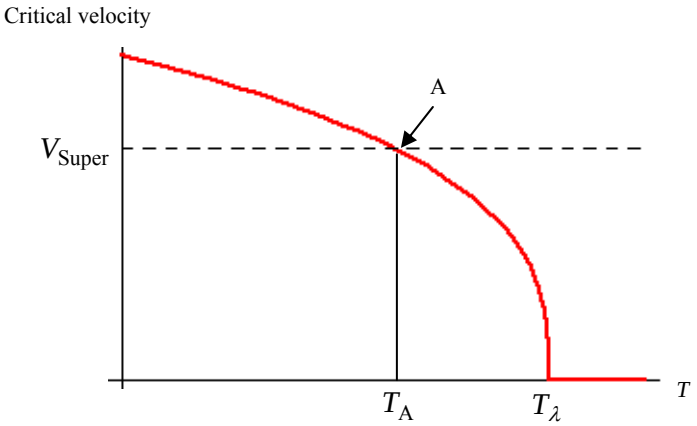

We next consider the following experiment: We prepare a toroidal vessel filled with liquid helium. We rotate the vessel around its axis at a temperature higher than T_λ. The liquid helium rotates with the vessel. The superfluid component of the dressed bosons appears at $T < T_\lambda$ if we lower the temperature while holding the angular velocity constant. These condensed dressed bosons continue to flow along the toroidal channel. The angular velocity of the superfluid component does not change because of the lack of friction, even when we stop the vessel. Subsequently, we heat this state of superfluid helium. What phenomenon will occur?

Our answer is as follows: In this experiment, we express the superfluid velocity by V_{Super} . This value is smaller than the critical velocity V_C at an adequately low temperature as presented in Fig. 12.2. When the temperature value is increased, V_C varies to be a smaller value. Accordingly the value of V_{Super} becomes equal to the critical velocity V_C at temperature T_A, as seen in Fig. 12.2. Thereafter the Bose-condensed dressed bosons transfer to the other momentum states. Then, frictional heat is generated and the temperature becomes high to the value T_B suddenly. The behavior is presented in Fig. 12.3. That is to say, the temperature value jumps from T_A to T_B at time t_0. For that reason, a temperature gap appears in the experiment.

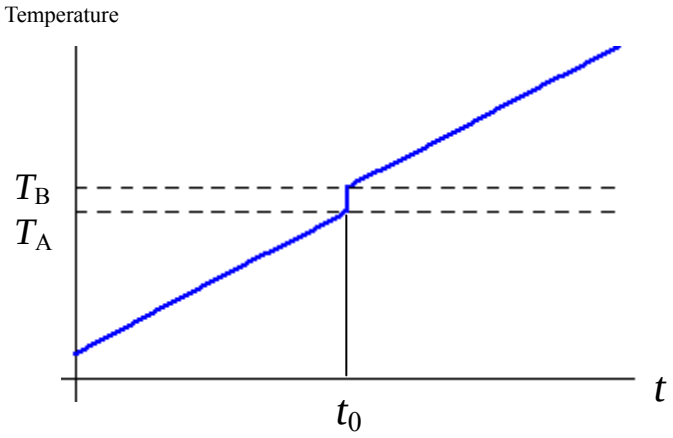

Fig. 12.3 Time dependence of temperature

The horizontal axis represents the time value and the vertical axis represents the temperature.

We can determine the temperature dependence of the critical velocity near the λ point if this phenomenon is discovered. The measurement is repeated for various values of V_{Super} and the value T_A is detected for each value of V_{Super} . We plot the values (T_A,

V_{Super}) and then we obtain the temperature dependence of the critical velocity. Related details are discussed in a previous report [28].

12.3 A. C. Josephson effect in superfluid helium

In superfluid helium, the ac Josephson effect might occur. A few groups attempted to verify this phenomenon [32]. They consider that the phenomena are produced using a phase slip of the vortex. They detected oscillations with very low frequencies. However, it is difficult to confirm the relation between the frequency and the difference of pressures.

We examined this phenomenon in reference [33]. The dressed bosons in the Bose condensate oscillate between two superfluid heliums connected through a pinhole. Then, we can derive the relation as

$$f = mg\ell/(2\pi\hbar), \tag{12.8}$$

where f is the frequency, m is the mass of helium atom, g is the gravitational acceleration, ℓ is the difference of the heights of the two superfluid heliums, and $(2\pi\hbar)$ is Planck's constant. This relation is derived from the fact that the energy of the Bose condensed dressed boson is equal to the chemical potential (see reference [33]). If experiments are executed in a higher pressure difference, high-frequency oscillation might be detected, and the relation might be confirmed (approximately 1 MHz per centimeter difference in height).

(Conclusion)

The concept of the dressed boson and nonlinear mechanism of the energy form are valuable for investigation of liquid helium. The authors earnestly hope that this new viewpoint will be used to improve investigations of superfluid helium and other many-boson systems.

Acknowledgements

This work started about 30 years ago. One of the authors, Sasaki, was encouraged by many people. Heartfelt appreciation is extended to Professor Shigenobu Sunakawa, Professor Fumiaki Iwamoto, Professor Koichi Katsumata, Professor Yasuyuki Kitano, Professor Takeji Kebukawa, Professor Kiyohisa Matsuda, Professor Masahiro Mori, Professor Shuichiro Yamasaki, Professor Masahiko Hirooka, Professor Akitsu Ikeda, Professor Yoshitaka Fujita, Professor Yorihiko Tsunoda, and Professor Takekiyo Matsuo.

Prof. Sunakawa kindly supported investigations. Prof. Iwamoto provided useful advice and encouragement. Prof. Katsumata and Prof. Kitano tirelessly offered encouragement through discussions of various branches of physics. Prof. Kitano collaborated in an experiment related to liquid helium [34]. Prof. Kebukawa has discussed many interesting problems in physics and offered many stimulating ideas [10, 33]. Prof. Matsuda investigated the theory of liquid helium and co-authored a paper announcing those results [7]. Prof. Mori kindly provided important information related to the investigation of physics. Prof. Ikeda of the Shizuoka Institute of Science and Technology has always provided necessary support. Prof. Yamasaki, Prof. Hirooka, Prof. Tsunoda, Prof. Fujita, and Prof. Matsuo all gave valuable encouragement with their kindness and valuable advice.

The present work would not have been completed without their valuable support. Heartfelt gratitude is extended to them all.

Appendix I

We summarize the dynamics of a 1D many-boson system described by the Hamiltonian:

$$H = \sum_p \left(p^2/(2m)\right) a_p^* a_p + \left(g/(2L)\right) \sum_{p,q,k} a_{p+k}^* a_{q-k}^* a_p a_q \ , \tag{A1.1}$$

where a_p and a_p^* respectively signify the annihilation and creation operators of a boson, *m* is the mass of the boson, and *L* is the length of the 1D space. The commutation relations among these operators are

$$\left[a_p, a_q^*\right] = \delta_{p,q}, \quad \left[a_p, a_q\right] = 0, \quad \left[a_p^*, a_q^*\right] = 0. \tag{A1.2}$$

The Hamiltonian is diagonalized completely by the unitary operator *U*, which was obtained by S. Sasaki and T. Kebukawa [10]. The unitary operator is denoted as U_N for the total boson number *N*. Then, the unitary operator U_N is given as

$$U_N = \sum_{q_1 \le q_2 \le q_3 \le \cdots \le q_N} \left[(2/\pi)^{N(N-1)/2} \alpha_{q_1, q_2, q_3 \cdots q_N} \times \left\{ \sum_{\{p_{ij}\}} \left(\prod_{1 \le i < j \le N} \frac{k_{ij}}{k_{ij} - p_{ij}} \right) \left(\prod_{i=1}^{N} a_{q_i}^* + \sum_j p_{ij} \right) \prod_{i=1}^{N} a_{q_i} \right\} \right] \tag{A1.3}$$

in the case of an infinitely large coupling constant *g*.

Therein, $\alpha_{q_1, q_2, q_3 \cdots q_N} = \prod_q \left(1/\sqrt{n_q!}\right)$, (where 0 ! = 1) , (A1.4)

$$k_{ij} = \begin{cases} -\pi\hbar/L \text{ for } i < j \\ 0 \text{ for } i = j \\ \pi\hbar/L \text{ for } i > j \end{cases}, \tag{A1.5}$$

$$\hbar \ = (\text{Planck's constant}) / \left(2\pi\right) \tag{A1.6}$$

$$p_{ij} = -p_{ji} \tag{A1.7}$$

$\alpha_{q_1,q_2,q_3\cdots q_N}$ is the normalization constant of the free state. All the running momenta $q_1, q_2, q_3 \cdots q_N$ and the transfer-momenta p_{ij} take the values $(2\pi\hbar/L)\times$ integer because of the periodic boundary condition as follows:

$$q_i = (2\pi\hbar/L)\times \text{integer},\ p_{ij} = (2\pi\hbar/L)\times \text{integer}\,. \tag{A1.8}$$

We proved in an earlier paper [10] that this operator U satisfies the unitary relations $U^*U = 1$ and $UU^* = 1$. The unitary operator U diagonalizes the total Hamiltonian (A1.1), and the diagonalized form becomes the following form at an infinitely large limit of g (see Ref. [11]):

$$U^*HU = \sum_p \frac{p^2}{2m} a_p^* a_p + \sum_{p,q} \frac{\pi\hbar|p-q|}{2mL} a_p^* a_p a_q^* a_q + \frac{1}{2m}\left(\frac{\pi\hbar}{L}\right)^2 \frac{N(N^2-1)}{3}\,. \tag{A1.9}$$

We define the new creation and annihilation operators as

$$A_p = U a_p U^{-1}, \text{ and } A_p^* = U a_p^* U^{-1}, \tag{A1.10}$$

which represent the operators of the "dressed boson". We can reexpress the total Hamiltonian using only the number operators of dressed bosons $\{A_s^* A_s\}$ as the following.

$$H = \sum_p \frac{p^2}{2m} A_p^* A_p + \sum_{p,q} \frac{\pi\hbar|p-q|}{2mL} A_p^* A_p A_q^* A_q + \frac{1}{2m}\left(\frac{\pi\hbar}{L}\right)^2 \frac{N(N^2-1)}{3} \tag{A1.11}$$

For a finite coupling constant, we can expand the diagonalized form of the

Hamiltonian into the power series of $(1/g)$. The result up to the second order, is the following.

$$H=\sum_p \frac{p^2}{2m}A_p^* A_p+\frac{1}{2m}\left\{-\frac{2\hbar^2}{Lmg}+\left(\frac{2\hbar^2}{Lmg}\right)^2\frac{3N}{2}\right\}\sum_{p,q}(p-q)^2 A_p^* A_p A_q^* A_q$$
$$+\frac{1}{2m}\left\{1-\frac{2\hbar^2}{Lmg}2N+\left(\frac{2\hbar^2}{Lmg}\right)^2 3N^2\right\}\left\{\sum_{p,q}\frac{\pi\hbar|p-q|}{L}A_p^* A_p A_q^* A_q+\left(\frac{\pi\hbar}{L}\right)^2\frac{N\left(N^2-1\right)}{3}\right\}$$
$$+\mathrm{Order}\left(1/g^3\right) \tag{A1.12}$$

Rewriting this expression in a form resembling Eq. (3.18), we obtain

$$\text{(total energy)} = E=\sum_p \frac{p^2}{2m}n_p+\frac{1}{N}\sum_{p,q}f_2(p-q)n_p n_q+\mathrm{Order}\left(1/g^3\right), \tag{A1.13}$$

where the following hold.

$$n_p = A_p^* A_p \tag{A1.14}$$

$$f_2(p-q)=\frac{1}{2m}\left\{-\frac{2\hbar^2 N}{Lmg}+\left(\frac{2\hbar^2 N}{Lmg}\right)^2\frac{3}{2}\right\}(p-q)^2$$
$$+\frac{\pi\hbar N}{2mL}\left\{1-2\frac{2\hbar^2 N}{Lmg}+3\left(\frac{2\hbar^2 N}{Lmg}\right)^2\right\}\left\{|p-q|+\frac{1}{3}\frac{\pi\hbar N}{L}\left(1-\frac{1}{N^2}\right)\right\} \tag{A1.15}$$
$$+\mathrm{Order}\left(1/g^3\right)$$

As might be readily apparent from this expression, all Postulates of Sec. 1 are definitely satisfied in the present 1D system. There is an interesting property of the ground-state, which is

$$(1/N)\langle \text{Ground}-\text{state}|A_0^* A_0|\text{Ground}-\text{state}\rangle = 1, \text{ for any value of } g, \tag{A1.17}$$

$$(1/N)\langle \text{Ground}-\text{state}|a_0^* a_0|\text{Ground}-\text{state}\rangle = 0, \text{ for } g\to\infty \quad N\to\infty. \tag{A1.18}$$

The dressed bosons with momentum zero occupy 100% in the ground-state, but the original free bosons with momentum zero occupy 0% in the ground-state for $g\to\infty$

and $N \to \infty$.

Appendix II

The left-hand-side of (6.15) can be expanded to the series of t as follows: The integral of (6.15) is rewritten as the following.

$$\begin{aligned}&\int_0^{p_s}\frac{1}{p\left(t+ap^3\right)^{1/3}}p^2dp=\int_0^{p_s}\left(\frac{p}{\left(t+ap^3\right)^{1/3}}-\frac{p}{\left(ap^3\right)^{1/3}}\right)dp+\int_0^{p_s}\frac{p}{\left(ap^3\right)^{1/3}}dp\\&=\frac{p_s}{a^{1/3}}+\int_0^{p_s}\left(\frac{\left(ap^3\right)^{1/3}-\left(t+ap^3\right)^{1/3}}{a^{1/3}\left(t+ap^3\right)^{1/3}}\right)dp\end{aligned}\tag{A2.1}$$

$$\int_0^{p_s}\frac{1}{p\left(t+ap^3\right)^{1/3}}p^2dp=\frac{p_s}{a^{1/3}}+\int_0^{p_s}\left(\frac{\left(\frac{ap^3}{t}\right)^{1/3}-\left(1+\frac{ap^3}{t}\right)^{1/3}}{a^{1/3}\left(1+\frac{ap^3}{t}\right)^{1/3}}\right)dp\tag{A2.2}$$

Here, we introduce a new variable y as

$$y=\left(ap^3\right)/t\ .\tag{A2.3}$$

Changing the integral variable p to $\left(ap^3\right)/t$, we obtain the following expressions.

$$\begin{aligned}&\int_0^{p_s}\frac{1}{p\left(t+ap^3\right)^{1/3}}p^2\mathrm{d}p=\frac{p_s}{a^{1/3}}+\int_0^{\left(ap_s{}^3\right)/t}\left(\frac{\left(y\right)^{1/3}-\left(1+y\right)^{1/3}}{a^{1/3}\left(1+y\right)^{1/3}}\right)\frac{\mathrm{d}p}{\mathrm{d}y}\mathrm{d}y\\&=\frac{p_s}{a^{1/3}}+\int_0^{\left(ap_s{}^3\right)/t}\left(\frac{\left(y\right)^{1/3}-\left(1+y\right)^{1/3}}{a^{1/3}\left(1+y\right)^{1/3}}\right)\frac{t}{3ap^2}\mathrm{d}y\\&=\frac{p_s}{a^{1/3}}+\int_0^{\left(ap_s{}^3\right)/t}\left(\frac{\left(y\right)^{1/3}-\left(1+y\right)^{1/3}}{a^{1/3}\left(1+y\right)^{1/3}}\right)\frac{t^{1/3}}{3a^{1/3}y^{2/3}}\mathrm{d}y\end{aligned}\tag{A2.4}$$

We denote the upper limit of y by y_s as

$$y_s=\left(ap_s{}^3\right)/t\ .\tag{A2.5}$$

Equation (A2.4) becomes the following.

$$\int_0^{p_s} \frac{1}{p\left(t+ap^3\right)^{1/3}}\,p^2\mathrm{d}p = \frac{p_s}{a^{1/3}} + \frac{t^{1/3}}{3a^{2/3}}\int_0^{y_s}\left(\frac{(y)^{1/3}-(1+y)^{1/3}}{y^{2/3}(1+y)^{1/3}}\right)\mathrm{d}y \quad \text{(A2.6)}$$

The upper limit y_s becomes very large when the value of t is small. Therefore, the integration (A2.6) is expanded to the expression shown below.

$$\int_0^{p_s} \frac{1}{p\left(t+ap^3\right)^{1/3}}\,p^2\mathrm{d}p = \frac{p_s}{a^{1/3}} - \frac{t^{1/3}}{3a^{2/3}}\left(\int_0^{\infty}\left(\frac{(1+y)^{1/3}-(y)^{1/3}}{y^{2/3}(1+y)^{1/3}}\right)\mathrm{d}y - \int_{y_s}^{\infty}\left(\frac{(1+y)^{1/3}-(y)^{1/3}}{y^{2/3}(1+y)^{1/3}}\right)\mathrm{d}y\right) \quad \text{(A2.7)}$$

The first integral in the right-hand-side of (A2.7) is

$$\frac{1}{3}\int_0^{\infty}\left(\frac{(1+y)^{1/3}-y^{1/3}}{y^{2/3}(1+y)^{1/3}}\right)dy = \frac{\left(\Gamma\left(-\frac{1}{3}\right)\right)^2\Gamma\left(\frac{2}{3}\right)}{6\sqrt{3}\pi} = -\frac{\Gamma\left(-\frac{1}{3}\right)\Gamma\left(\frac{5}{3}\right)}{2\Gamma\left(\frac{1}{3}\right)} \quad . \quad \text{(A2.8)}$$

The second integral in the right-hand-side of (A2.7) is as shown below.

$$\begin{aligned}\int_{y_s}^{\infty}\left(\frac{(1+y)^{1/3}-y^{1/3}}{y^{2/3}(1+y)^{1/3}}\right)\mathrm{d}y &= \int_{y_s}^{\infty} y^{-2/3}\left(\frac{(1+(1/y))^{1/3}-1}{(1+(1/y))^{1/3}}\right)\mathrm{d}y = \int_{y_s}^{\infty} y^{-2/3}\left(\frac{1}{3y}+\mathrm{Order}\left(\frac{1}{y^2}\right)\right)\mathrm{d}y \\ &= \int_{y_s}^{\infty}\left(\left(\frac{1}{3}\right)y^{-5/3}+\mathrm{Order}\left(y^{-8/3}\right)\right)\mathrm{d}y\end{aligned} \quad \text{(A2.9)}$$

The integral value is expanded to the series of y_s as

$$\begin{aligned}\int_{y_s}^{\infty}\left(\frac{(1+y)^{1/3}-y^{1/3}}{y^{2/3}(1+y)^{1/3}}\right)\mathrm{d}y &= \left[-\left(\frac{1}{2}\right)y^{-2/3}+\mathrm{Order}\left(y^{-5/3}\right)\right]_{y_s}^{\infty} \\ &= \left(\frac{1}{2}\right)y_s^{-2/3}-\mathrm{Order}\left(y_s^{-5/3}\right)\end{aligned} \quad . \quad \text{(A2.10)}$$

Substitution of (A2.8) and (A2.10) into (A2.7) yields the following.

$$\int_0^{p_s} \frac{1}{p\left(t+ap^3\right)^{1/3}}\,p^2\,\mathrm{d}p = \frac{p_s}{a^{1/3}} + \frac{t^{1/3}}{a^{2/3}}\frac{\Gamma\left(-\frac{1}{3}\right)\Gamma\left(\frac{5}{3}\right)}{2\Gamma\left(\frac{1}{3}\right)} + \frac{t^{1/3}}{3a^{2/3}}\left(\frac{1}{2}\right){y_s}^{-2/3} - \frac{t^{1/3}}{3a^{2/3}}\mathrm{Order}\left({y_s}^{-5/3}\right)$$

$$= \frac{p_s}{a^{1/3}} + \frac{t^{1/3}}{a^{2/3}}\frac{\Gamma\left(-\frac{1}{3}\right)\Gamma\left(\frac{5}{3}\right)}{2\Gamma\left(\frac{1}{3}\right)} + \frac{t^{1/3}}{3a^{2/3}}\left(\frac{1}{2}\right)\left(\frac{t}{a{p_s}^3}\right)^{2/3} - \frac{t^{1/3}}{3a^{2/3}}\mathrm{Order}\left(\left(\frac{t}{a{p_s}^3}\right)^{5/3}\right)$$

$$= \frac{p_s}{a^{1/3}} + \frac{t^{1/3}}{a^{2/3}}\frac{\Gamma\left(-\frac{1}{3}\right)\Gamma\left(\frac{5}{3}\right)}{2\Gamma\left(\frac{1}{3}\right)} + \frac{t}{6a^{4/3}{p_s}^2} - \mathrm{Order}\left(\frac{t^2}{3a^{7/3}{p_s}^5}\right)$$

(A2.11)

This equation is equivalent to (6.16).

Appendix III

We have expressed the entropy and the pressure using the number distribution of dressed bosons in chapter XI. We will derive the function forms via another process in this Appendix. First, we calculate the partial derivative of free energy F (F is expressed in (11.3)) by T while fixing the values of N and V, as

$$\left[\frac{\partial F}{\partial T}\right]_{N,V} = \sum_{\mathbf{p}} \frac{\mathbf{p}^2}{2m}\left[\frac{\partial n_{\mathbf{p}}}{\partial T}\right]_{N,V} + \frac{2}{N}\sum_{\mathbf{p},\mathbf{q}}\left(f(\mathbf{p}-\mathbf{q})\left[\frac{\partial n_{\mathbf{p}}}{\partial T}\right]_{N,V} n_{\mathbf{q}}\right) \\ -k_B\sum_{\mathbf{p}}\left\{\log\left(1+n_{\mathbf{p}}\right)+n_{\mathbf{p}}\log\left(1+n_{\mathbf{p}}{}^{-1}\right)\right\} - k_B T\sum_{\mathbf{p}}\log\left(1+n_{\mathbf{p}}{}^{-1}\right)\left[\frac{\partial n_{\mathbf{p}}}{\partial T}\right]_{N,V}, \tag{A3.1}$$

where we have used the symmetry property of $f(\mathbf{p}-\mathbf{q}) = f(\mathbf{q}-\mathbf{p})$. The coefficient $\log\left(1+n_{\mathbf{p}}{}^{-1}\right)$ in the last term of (A3.1) is rewritten using of Eqs. (11.4) and (3.2) as

$$\log\left(1+n_{\mathbf{p}}{}^{-1}\right) = \left(\omega_{\mathbf{p}}-\mu\right)/\left(k_{\mathrm{B}}T\right) \\ = \frac{1}{k_{\mathrm{B}}T}\left(\frac{\mathbf{p}^2}{2m}+\frac{2}{N}\sum_{\mathbf{q}} f(\mathbf{p}-\mathbf{q})n_{\mathbf{q}} - \frac{1}{N^2}\sum_{\mathbf{s},\mathbf{t}} f(\mathbf{s}-\mathbf{t})n_{\mathbf{s}}n_{\mathbf{t}} - \mu\right). \tag{A3.2}$$

Substitution of (A3.2) into (A3.1) yields the following expression.

$$\left[\frac{\partial F}{\partial T}\right]_{N,V} = \sum_{\mathbf{p}}\left\{\frac{\mathbf{p}^2}{2m}+\frac{2}{N}\sum_{\mathbf{q}} f(\mathbf{p}-\mathbf{q})n_{\mathbf{q}}\right\}\left[\frac{\partial n_{\mathbf{p}}}{\partial T}\right]_{N,V} \\ -k_B\sum_{\mathbf{p}}\left\{\log\left(1+n_{\mathbf{p}}\right)+n_{\mathbf{p}}\log\left(1+n_{\mathbf{p}}{}^{-1}\right)\right\} \\ -\sum_{\mathbf{p}}\left(\frac{\mathbf{p}^2}{2m}+\frac{2}{N}\sum_{\mathbf{q}} f(\mathbf{p}-\mathbf{q})n_{\mathbf{q}} - \frac{1}{N^2}\sum_{\mathbf{s},\mathbf{t}} f(\mathbf{s}-\mathbf{t})n_{\mathbf{s}}n_{\mathbf{t}} - \mu\right)\left[\frac{\partial n_{\mathbf{p}}}{\partial T}\right]_{N,V}$$

$$\left[\frac{\partial F}{\partial T}\right]_{N,V} = -k_B\sum_{\mathbf{p}}\left\{\log\left(1+n_{\mathbf{p}}\right)+n_{\mathbf{p}}\log\left(1+n_{\mathbf{p}}{}^{-1}\right)\right\} \\ +\sum_{\mathbf{p}}\left(\frac{1}{N^2}\sum_{\mathbf{s},\mathbf{t}} f(\mathbf{s}-\mathbf{t})n_{\mathbf{s}}n_{\mathbf{t}} + \mu\right)\left[\frac{\partial n_{\mathbf{p}}}{\partial T}\right]_{N,V} \tag{A3.3}$$

The second term of the right-hand side of Eq. (A3.3) is rewritten as

$$\sum_{\mathbf{p}}\left(\frac{1}{N^2}\sum_{\mathbf{s},\mathbf{t}} f(\mathbf{s}-\mathbf{t})n_{\mathbf{s}}n_{\mathbf{t}}+\mu\right)\left[\frac{\partial n_{\mathbf{p}}}{\partial T}\right]_{N,V}=\left(\frac{1}{N^2}\sum_{\mathbf{s},\mathbf{t}} f(\mathbf{s}-\mathbf{t})n_{\mathbf{s}}n_{\mathbf{t}}+\mu\right)\sum_{\mathbf{p}}\left[\frac{\partial n_{\mathbf{p}}}{\partial T}\right]_{N,V}$$
$$=\left(\frac{1}{N^2}\sum_{\mathbf{s},\mathbf{t}} f(\mathbf{s}-\mathbf{t})n_{\mathbf{s}}n_{\mathbf{t}}+\mu\right)\left[\frac{\partial N}{\partial T}\right]_{N,V}=0. \tag{A3.4}$$

Therein the total number N is fixed in the partial derivative; therefore this term becomes zero. Substitution of (A3.4) into (A3.3) yields

$$S=-\left[\frac{\partial F}{\partial T}\right]_{N,V}=k_B\sum_{\mathbf{p}}\left\{\log\left(1+n_{\mathbf{p}}\right)+n_{\mathbf{p}}\log\left(1+n_{\mathbf{p}}^{-1}\right)\right\}. \tag{A3.5}$$

Consequently, Eq. (A3.5) reproduces Eq. (11.1).

Next, we take the partial derivative of F by volume V in fixing the values of T and N. It is important in this differentiation by V that the level interval of the momenta varies along with the change of the volume. At the thermodynamic limit, the summation can be replaced with integration. Consequently, we obtain the partial derivative by V for the example shown below.

$$\frac{\partial}{\partial V}\left[\frac{1}{N}\sum_{\mathbf{p},\mathbf{q}} f(\mathbf{p}-\mathbf{q})n_{\mathbf{p}}n_{\mathbf{q}}\right]_{N,T}=\frac{\partial}{\partial V}\left[\frac{V^2}{(2\pi\hbar)^6 N}\iint f(\mathbf{p}-\mathbf{q})n_{\mathbf{p}}n_{\mathbf{q}}\mathrm{d}^3\mathbf{p}\mathrm{d}^3\mathbf{q}\right]_{N,T}$$
$$=\frac{2V}{(2\pi\hbar)^6 N}\iint f(\mathbf{p}-\mathbf{q})n_{\mathbf{p}}n_{\mathbf{q}}\mathrm{d}^3\mathbf{p}\mathrm{d}^3\mathbf{q}+\frac{2V^2}{(2\pi\hbar)^6 N}\iint\left(f(\mathbf{p}-\mathbf{q})\left[\frac{\partial n_{\mathbf{p}}}{\partial V}\right]_{N,T}n_{\mathbf{q}}\right)\mathrm{d}^3\mathbf{p}\mathrm{d}^3\mathbf{q}$$
$$=\frac{2}{NV}\sum_{\mathbf{p},\mathbf{q}} f(\mathbf{p}-\mathbf{q})n_{\mathbf{p}}n_{\mathbf{q}}+\frac{2}{N}\sum_{\mathbf{p}}\left(\sum_{\mathbf{q}} f(\mathbf{p}-\mathbf{q})n_{\mathbf{q}}\right)\left[\frac{\partial n_{\mathbf{p}}}{\partial V}\right]_{N,T}$$

Applying the same procedure to the partial derivative of F, we obtain

$$\left(\frac{\partial F}{\partial V}\right)_{N,T}=\frac{1}{V}\sum_{\mathbf{p}}\frac{\mathbf{p}^2}{2m}n_{\mathbf{p}}+\frac{2}{NV}\sum_{\mathbf{p},\mathbf{q}} f(\mathbf{p}-\mathbf{q})n_{\mathbf{p}}n_{\mathbf{q}}+\sum_{\mathbf{p}}\left(\frac{\mathbf{p}^2}{2m}+\frac{2}{N}\sum_{\mathbf{q}} f(\mathbf{p}-\mathbf{q})n_{\mathbf{q}}\right)\left[\frac{\partial n_{\mathbf{p}}}{\partial V}\right]_{N,T}$$
$$-\frac{k_BT}{V}\sum_{\mathbf{p}}\left\{\log\left(1+n_{\mathbf{p}}\right)+n_{\mathbf{p}}\log\left(1+n_{\mathbf{p}}^{-1}\right)\right\}-k_BT\sum_{\mathbf{p}}\left(\log\left(1+n_{\mathbf{p}}^{-1}\right)\right)\left[\frac{\partial n_{\mathbf{p}}}{\partial V}\right]_{N,T}. \tag{A3.6}$$

Substitution of (A3.2) into (A3.6) yields

$$\left(\frac{\partial F}{\partial V}\right)_{N,T} = \frac{1}{V}\sum_{\mathbf{p}}\frac{\mathbf{p}^2}{2m}n_{\mathbf{p}} + \frac{2}{NV}\sum_{\mathbf{p},\mathbf{q}} f(\mathbf{p}-\mathbf{q})n_{\mathbf{p}}n_{\mathbf{q}} \qquad \text{(A3.7)}$$
$$-\frac{k_B T}{V}\sum_{\mathbf{p}}\left\{\log\left(1+n_{\mathbf{p}}\right)+n_{\mathbf{p}}\log\left(1+n_{\mathbf{p}}^{-1}\right)\right\}+\sum_{\mathbf{p}}\left(\frac{1}{N^2}\sum_{\mathbf{s},\mathbf{t}} f(\mathbf{s}-\mathbf{t})n_{\mathbf{s}}n_{\mathbf{t}}+\mu\right)\left[\frac{\partial n_{\mathbf{p}}}{\partial V}\right]_{N,T}$$

Therein the last partial derivative must be treated carefully because of the following relation:

$$\left(\frac{\partial N}{\partial V}\right)_{N,T} = \left(\frac{\partial\sum_{\mathbf{p}} n_{\mathbf{p}}}{\partial V}\right)_{N,T} = \frac{\sum_{\mathbf{p}} n_{\mathbf{p}}}{V} + \sum_{\mathbf{p}}\left[\frac{\partial n_{\mathbf{p}}}{\partial V}\right]_{N,T}. \qquad \text{(A3.8)}$$

The left-hand side of Eq. (A3.8) is zero because of the fixed value of N. Thus, we obtain

$$\sum_{\mathbf{p}}\left[\frac{\partial n_{\mathbf{p}}}{\partial V}\right]_{N,T} = -\frac{N}{V}. \qquad \text{(A3.9)}$$

Substitution of (A3.9) into (A3.7) yields the following expression.

$$\begin{aligned}\left(\frac{\partial F}{\partial V}\right)_{N,T} &= \frac{1}{V}\sum_{\mathbf{p}}\frac{\mathbf{p}^2}{2m}n_{\mathbf{p}} + \frac{2}{NV}\sum_{\mathbf{p},\mathbf{q}} f(\mathbf{p}-\mathbf{q})n_{\mathbf{p}}n_{\mathbf{q}} \\ &\quad -\frac{k_B T}{V}\sum_{\mathbf{p}}\left\{\log\left(1+n_{\mathbf{p}}\right)+n_{\mathbf{p}}\log\left(1+n_{\mathbf{p}}^{-1}\right)\right\}-\frac{N}{V}\left(\frac{1}{N^2}\sum_{\mathbf{s},\mathbf{t}} f(\mathbf{s}-\mathbf{t})n_{\mathbf{s}}n_{\mathbf{t}}+\mu\right) \\ &= \frac{1}{V}\sum_{\mathbf{p}}\frac{\mathbf{p}^2}{2m}n_{\mathbf{p}} + \frac{1}{NV}\sum_{\mathbf{p},\mathbf{q}} f(\mathbf{p}-\mathbf{q})n_{\mathbf{p}}n_{\mathbf{q}} \\ &\quad -\frac{k_B T}{V}\sum_{\mathbf{p}}\left\{\log\left(1+n_{\mathbf{p}}\right)+n_{\mathbf{p}}\log\left(1+n_{\mathbf{p}}^{-1}\right)\right\}-\frac{N}{V}\mu\end{aligned} \qquad \text{(A3.10)}$$

We substitute equation (A3.2), i.e.

$$\log\left(1+n_{\mathbf{p}}^{-1}\right) = \left(\omega_{\mathbf{p}}-\mu\right)/\left(k_{\mathrm{B}}T\right),$$

into (A3.10); then we obtain the following.

$$\left(\frac{\partial F}{\partial V}\right)_{N,T} = \frac{1}{V}\sum_{\mathbf{p}}\frac{\mathbf{p}^2}{2m}n_{\mathbf{p}} + \frac{1}{NV}\sum_{\mathbf{p},\mathbf{q}} f(\mathbf{p}-\mathbf{q})n_{\mathbf{p}}n_{\mathbf{q}}$$
$$-\frac{k_B T}{V}\sum_{\mathbf{p}}\log(1+n_{\mathbf{p}}) - \frac{1}{V}\sum_{\mathbf{p}}(\omega_{\mathbf{p}}-\mu)n_{\mathbf{p}} - \frac{N}{V}\mu \quad \text{(A3.11)}$$
$$= \frac{1}{V}\sum_{\mathbf{p}}\frac{\mathbf{p}^2}{2m}n_{\mathbf{p}} + \frac{1}{NV}\sum_{\mathbf{p},\mathbf{q}} f(\mathbf{p}-\mathbf{q})n_{\mathbf{p}}n_{\mathbf{q}}$$
$$-\frac{k_B T}{V}\sum_{\mathbf{p}}\log(1+n_{\mathbf{p}}) - \frac{1}{V}\sum_{\mathbf{p}}\omega_{\mathbf{p}}n_{\mathbf{p}}$$

Consequently, we obtain the function form of pressure as shown below.

$$P = -\left(\frac{\partial F}{\partial V}\right)_{N,T} = -\frac{1}{V}\sum_{\mathbf{p}}\frac{\mathbf{p}^2}{2m}n_{\mathbf{p}} - \frac{1}{NV}\sum_{\mathbf{p},\mathbf{q}} f(\mathbf{p}-\mathbf{q})n_{\mathbf{p}}n_{\mathbf{q}} \quad \text{(A3.12)}$$
$$+\frac{k_B T}{V}\sum_{\mathbf{p}}\log(1+n_{\mathbf{p}}) + \frac{1}{V}\sum_{\mathbf{p}}\omega_{\mathbf{p}}n_{\mathbf{p}}$$

This result has the same form as that in (11.8). Therefore, the pressure calculation has reproduced the same result via a process that differs from the one presented in chapter XI.

References

[1] W. H. Keesom, Helium (Elsevier, 1942).

J. Wilks, The Property of Liquid and Solid Helium (Clarendon Press Oxford, 1967).

K. R. Atkins, Liquid Helium (Cambridge University Press, 1959).

[2] F. London, Superfluids, Vol. **2** (Wiley, 1954).

[3] L. Tisza, C.r. hebd. Seanc. Acad. Sci., Paris **207**, (1938) 1035, 1186.

L. D. Landau, Zh. Eksp. Teor. Fiz. **11** (1941) 592; J. Phys. Moscow **5** (1941) 71; ibid. **11** (1947) 91.

I. M. Khalatnikov, An Introduction to the theory of Superfluidity, (W. A. Benjamin Inc. New York, Amsterdam 1965).

[4] N. N. Bogoliubov, J. Phys. **11** (1947) 23.

R. Balian and C. de Dominicis, Physica **30** (1964) 1933.

P. Nozieres and D. Pines, The Theory of Quantum Liquids, Vol. II Superfluid Bose Liquids, (Addison-Wesley Pub. Comp, Inc. 1991).

[5] M. Girardeau, J. Math. Phys. **1** (1960) 516.

E. H. Lieb and W. Liniger, Phys. Rev. **130** (1963) 1605.

E. H. Lieb, Phys. Rev. **130** (1963) 1616.

[6] R. P. Feynman, Phys. Rev. **94** (1954) 265.

R. P. Feynman and M. Cohen, Phys. Rev. **102** (1956) 1183.

M. Cohen and R. P. Feynman, Phys. Rev.**107** (1957) 13.

A. Miller, D. Pines, and P. Nozieres, Phys. Rev. **127** (1962) 1452.

E. Feenberg, Theory of Quantum Fluids (Academic Press, New York and London, 1969).

T. Nishiyama, Prog. Theor. Phys. **7** (1952) 417; ibid. **8** (1952) 655; ibid. **38** (1967) 1062; ibid. **45** (1971) 730; ibid. **54** (1975) 384.

S. Sunakawa, S. Yamasaki, and T. Kebukawa, Prog. Theor. Phys. **41** (1969) 919.

T. Kebukawa, S. Yamasaki, and S. Sunakawa, Prog. Theor. Phys. **44** (1970) 565.

F. Iwamoto, Prog. Theor. Phys. **44**, (1970) 1121, 1135.

S. Yamasaki, T. Kebukawa, and S. Sunakawa, Prog. Theor. Phys. **53** (1975) 1243; ibid. **54** (1975) 348; ibid. **61** (1979) 996, 1012.

S. Yamasaki, Prog. Theor. Phys. **72** (1984) 441; ibid. **73** (1985) 598.

[7] S. Sasaki and K. Matsuda, Prog. Theor. Phys. **56** (1976) 375.
S. Sasaki, Jpn. J. Appl. Phys. **26** (1987) 23.
[8] R. A. Cowley and A. D. B. Woods, Canadian Journal of Phys. **49** (1971) 177.
D. G. Henshaw and A. D. B. Woods, Phys. Rev. **121** (1961) 1266.
A. D. B. Woods, Phys. Rev. Lett. **14** (1965) 355.
A. D. B. Woods and R. A. Cowley, Phys. Rev. Lett. **24** (1970) 646.
[9] H. Kojima, W. Veith, E. Guyon and I. Rudnick, Proc. LT13 (Boulder), Vol.**1**, (1972) 279.
H. Kojima, W. Veith, S. Putterman, E. Guyon, and I. Rudnick, Phys. Rev. Lett. **27** (1971) 714.
I. Rudnick, H. Kojima, W. Veith, and R. S. Kagiwada, Phys. Rev. Lett. **23** (1969) 1220.
G. Kukich, R. P.Henkel, and J. R. Reppy, Phys. Rev. Lett. **21** (1968) 197.
[10] S. Sasaki and T. Kebukawa, Prog. Theor. Phys. **65** (1981) 1198, 1217, 1798; ibid. **66**, (1981) 831.
[11] S. Sasaki, Prog. Theor. Phys. **81** (1989) 1158.
S. Sasaki, Physica B **169** (1991) 591.
S. Sasaki and T. Kunimasa, J. Phys. Soc. Jpn. **59** (1990) 1593.
[12] S. Sasaki, Proc. Int. Conf. on Low Temp. Phys., J. J. A. P. **26** (1987) 23.
S. Sasaki, Physica B **165** (1990) 507.
S. Sasaki, Sci. Rep. Col. Gen. Educ. Osaka Univ. **35** (1986) 1.
[13] P. J. Bendt, R. D. Cowan, and J. L. Yarnell, Phys. Rev. **113** (1959) 1386.
[14] J. S. Brooks and R. J. Donnelly, J. Phys. Chem. Ref. Data **6** (1977) 51.
R. J. Donnelly, Phys. Lett. A **39** (1972) 221.
J. S. Brooks and R. J. Donnelly, LT-**13** Vol.**1** (1974), Phys. Lett. **46A** (1973) 111.
[15] G. Ahlers, Phys. Rev. A **3**, (1971) 696.
M. J. Buckingham, W. F. Fairbank, in Progress in Low Temperature Physics, vol. **3**, ed. By C. J. Gorter (Amsterdam, North-Holland, 1961), p. 80.
[16] J. A. Lipa, J. A. Nissen, D. A. Stricker, D. R. Swanson, and T. C. P. Chui, Phys. Rev. B **68** 174518 (2003).
[17] W. F.Vinen, C. J.Palin and J. M.Vaughan, Proc. of 13th Conf. on Low Temperature Physics, Boulder, Colorado, (1972) 524.

J. M. Vaughan, W. F. Vinen, and C. J. Paulin, Proc. of 13th Conf. on Low Temperature Physics, Boulder, Colorado, (1972) 532.

T. J. Greytak, in Proc. of 13th Conf. on Low Temperature Physics, Boulder, Colorado, (1972) 9.

E. R. Pike J. de Phys. **33 C1** (1972) 25.

G. Winterling, F. S.Holmes, and T. J.Greytak, Phys. Rev. Lett. **30** (1973) 427.

G. Winterling, J. Miller, and T. J. Greytak, Phys. Lett. **48A** (1974) 343.

[18] D. S. Greyawll, G. Ahlers, Phys. Rev. **A7** (1973) 2145.

[19] S. Sasaki, Journal of Low Temperature Physics **148** (2007) 97.

[20] S. Sasaki, Journal of Low Temperature Physics **148** (2007) 103.

[21] L. D. Landau, E. M. Lifshitz, Statistical Physics, 2nd Edition, Pergamon Press, Oxford, 1968, p.195.

F. London, Superfluid, Vol. **2**. Dover Publications, Paris, 1964, p. 44.

[22] S. Sasaki, Physica B **329** (2003) 232.

[23] H. London, Proc. R. Soc. A **171** (1939) 484.

[24] A. F. G. Wyatt: Physica B **126** (1984) 392.

F. R. Hope, M. J. Baird, and A. F. G. Wyatt, Phys. Rev. Lett. **52** (1984) 1528.

[25] H. Palevsky, K. Otnes, and K. E. Larsson, Phys. Rev. **112** (1958) 11.

A. D. B.Woods and R. A. Cowley, Phys. Rev. Lett. **24** (1970) 646.

R. A. Cowley and A. D. B.Woods, Can. J. Phys. **49** (1971) 177.

A. D. B.Woods and E. C. Svensson, Phys. Rev. Lett. **41** (1978) 974.

E. C. Svensson, V. F. Sears, A. D. B.Woods, and P. Martel, Phys. Rev. B **21** (1980) 3638.

E. C. Svensson, W. G. Stirling, E. Talbot, H. R. Glyde, in Proc. of 18th Conf. on Low Temperature Physics, Kyoto, Jpn. J. Appl. Phys. **26** (1987) 33.

[26] S. Sasaki, Physica B **194** (1994) 503.

[27] S. Sasaki, Springer Series in Solid-State Sciences, **79**, (1989) 160.

[28] S. Sasaki, Physica B **194** (1994) 497.

[29] S. Sasaki and T. Kunimasa, J. Phys. Soc. Jpn. **58** (1989) 3651.

[30] D. Eden and H. L. Swinny, Opt. Commun. **10** (1974) 191.

H. L. Swinny, in Photon Correlation and Light Beating Spectroscopy, edited by H. Z. Cummins and E. R. Pike (Plenum, New York 1974), p331.

[31] T. Matsuoka, K. Sakai, and K. Takagi, Rev. Sci. Instrum. **64** (1993) 2136.
K. Sakai, P. K. Choi, H. Tanaka, and K. Takagi, Rev. Sci. Instrum. **62** (1991) 1192.
[32] O. Avenel and E. Varoquaux, Jpn. J. Appl. Phys., Supplement **26-3** (1987) 1798.
W. Zimmermann, Jr., O. Avenel, and E. Varoquaux, Physica B **165&166** (1990) 749; ibid. (1990) 751.
A. Amar, J. C. Davis, R. E. Packard and R. L. Lozes, Physica B **165&166** (1990) 753.
R. Y. Chiao, Phys. Rev. B **25** (1982) 1665. D. L. Musinski and D. H. Douglass, Phys. Rev. Lett. **29** (1972) 1541.
J. P. Hulin, C. Laroche, A. Libchaber, and B. Perrin, Phys. Rev. **A 5** (1972) 1830.
P. L. Richards, Phys. Rev. A **2** (1970) 1532.
B. M. Khorana and B. S. Chandrasekhar, Phys. Rev. Lett. **18** (1967) 230.
P. L. Richards and P. W. Anderson, Phys. Rev. Lett. **14** (1965) 540.
[33] T. Kebukawa and S. Sasaki, J. Phys. Soc. Jpn. **59** (1990) 601.
T. Kebukawa and S. Sasaki, Physica B **165&166** (1990) 763.
T. Kebukawa and S. Sasaki, Sci. Rep. Col. Gen. Educ. Osaka Univ. **38** (1989) 5.
[34] Y. Kitano and S. Sasaki, Jpn. J. Appl. Phys. **26** (1987) 81.

Mathematica Program 1 (Determination of nonlinear term)

This program determines the function forms (2.68a-e) and the perameter values of (2.47)-(2.66).

```
(*  This program determines the non-linear functional form of dressed bosons *)
(*  ========= constant values =========  *)
(*  NA:Avogadro number   *)
NA=6.0221367*10^23
(*  hbar:Planck's constant/(2 Pi)   *)
hbar=6.6260755*10^-34/(2*Pi)
(*  kB:Boltzmann constant   *)
kB=1.380658*10^-23
(* m=mass of He atom, unit: kg  *)
m=(4.002602/(6.0221367*10^23))*10^-3
(* roh= mass density of liquid helium,
      at saturated vapor pressure and 1.1Kelvin unit: kg/m^3  *)
roh=145.5
(* numberDensity: number density of liquid helium unit: 1/m^3   *)
numberDensity=roh/m
(* energyData is the excitation energy data by neutron scatterings.  \
{(momentum/hbar)*10^-10, data=energy/Boltzmann constant}  namely,
  unit {angstrom^-1,Kelvin} *)
energyData={{0.0894,1.6131},{0.0946,1.7175},{0.1150,2.1005},{0.1210,
    2.2514},{0.1390,2.6111},{0.1430,2.6343},{0.1594,2.9709},{0.1767,
    3.2958},{0.1818,3.3887},{0.1938,3.6324},{0.1990,3.7368},{0.2000,
    3.7000},{0.2110,3.9689},{0.2162,4.0850},{0.2278,4.2822},{0.2329,
    4.3867},{0.2445,4.6072},{0.2495,4.7116},{0.2611,4.9205},{0.2776,
    5.2339},{0.2825,5.3267},{0.2938,5.5240},{0.2988,5.6284},{0.3000,
    5.5700},{0.3000,5.6500},{0.4000,7.4000},{0.4036,7.6361},{0.4082,
    7.7173},{0.4187,7.9146},{0.4232,7.9958},{0.4355,8.1815},{0.4498,
    8.3788},{0.4643,8.6457},{0.4785,8.8662},{0.4926,9.1099},{0.5000,
    9.1500},{0.5605,10.1544},{0.6000,10.7500},{0.6243,11.0015},{0.6965,
    11.8023},{0.7000,11.7500},{0.7649,12.4173},{0.8000,12.7200},{0.8000,
    12.6500},{0.8300,12.8815},{0.8925,13.2297},{0.9000,13.1500},{1.0000,
    13.5500},{1.1000,13.8000},{1.1300,13.8200},{1.2000,13.7500},{1.3000,
    13.5000},{1.4000,12.9500},{1.5000,12.2000},{1.6000,11.2000},{1.7000,
    10.2500},{1.8000,9.2500},{1.8800,8.6940},{1.8900,8.6570},{1.9000,
    8.7000},{1.9000,8.6540},{1.9000,8.6340},{1.9100,8.6350},{1.9100,
```

```
    8.6160},{1.9150,8.6110},{1.9200,8.6260},{1.9200,8.6100},{1.9250,
    8.6060},{1.9300,8.6260},{1.9300,8.6060},{1.9350,8.6300},{1.9350,
    8.6120},{1.9400,8.6300},{1.9400,8.6090},{1.9500,8.6500},{1.9500,
    8.6330},{1.9600,8.6830},{1.9600,8.6720},{1.9700,8.6950},{2.0000,
    8.9500},{2.1000,10.0000},{2.2000,11.6500},{2.3000,13.5500},{2.4000,
    15.5000},{2.5000,16.4500},{2.6000,17.0000},{2.7000,17.3000},{2.8000,
    17.5000},{2.9000,17.7000},{3.0000,17.8500},{3.1000,18.0000},{3.2000,
    18.1500},{3.3000,18.3000},{3.4000,18.3500},{3.5000,18.4000},{3.6000,
    18.4500}}
(* We use phonon velocity value 238 which is the experimental value at \
0.2-1.0K. *)
(* We use roton minimum energy =
   8.61*kB  at p/(10^10*hbar) = 1.92 from experimental data   *)
(* eData is the data for high momentum (momentum/(hbar*10^10))>2.4   *)
eData={}; Do[
 If[energyData[[n,1]]>2.4,eData=Join[eData,{energyData[[n]]}]],{n,1,
   Length[energyData]}]
eData
(* best fit curve of the excitation energy
    for momentum p=>2.55*10^10*hbar        *)
func=Fit[eData,{1,kkk,kkk^2},kkk]
ggg=ListPlot[eData,PlotStyle\[Rule]{PointSize[0.015],RGBColor[1,0,0]}]
gg=Plot[func,{kkk,2.5,3.6}]
Show[ggg,gg]
g=ListPlot[energyData,PlotStyle\[Rule]{PointSize[0.015],RGBColor[1,0,0]}]
(* ==== elementary excitation energy near zero Kelvin  *)
(*  velocity of first sound =c1=238 :unit:[m/s] *)
(*  e0phonon is the phonon energy at zero Kelvin :unit:J,
 where p is momentum.
    This function is equal to (2.42) in chaper II of my book  *)
e0phonon[p_]:=c1*p
c1=238.
(*  dPhonon is the derivative of phonon energy by momentum   *)
dPhonon[p_]:=c1
(*  maxon energy at zero Kelvin :unit:J.
        This function is equal to (2.43) in chaper II of my book  *)
e0maxon[p_]:=
 maxon1*kB+(maxon2+maxon3*(p-pMax)+maxon4*(p-pMax)^2+
```

```
        maxon5*(p-pMax)^3)(p-pMax)^2
maxon1=13.82;pMax=1.13*10^10*hbar
(* Maximum energy data in maxon region is 13.82 at pMax=
   1.13. Therefore we use the data in this program. *)
dMaxon[p_]:=(2*maxon2+3*maxon3*(p-pMax)+4*maxon4*(p-pMax)^2+5*
        maxon5*(p-pMax)^3)(p-pMax)
(*  roton energy at zero Kelvin :unit:J.
         This function is equal to (2.44) in chaper II of my book  *)
e0roton[p_]:=fDelta0*kB+1/(2*fM0*m)*(p-fQ0*10^10*hbar)^2
fDelta0=8.61;fQ0=1.92;fM0=0.153
dRoton[p_]:=1/(fM0*m)*(p-fQ0*10^10*hbar)
(* e0high1 is the excitation energy for higher region 1
     p3<=p<p4.
      This function is equal to (2.45) in chaper II of my book *)
e0high1[p_]:=hh+c1*(p-p3)+aaa*(p-p3)^2+bbb*(p-p3)^3
dHigh1[p_]:=c1+2*aaa*(p-p3)+3*bbb*(p-p3)^2
(* hh is the energy at p=p3 *)
(* higher energy region 2
   This function is equal to (2.46) in chaper II of my book *)
e0high2[p_]:=kB*func/.{kkk\[Rule]p/(10^10*hbar)}
(* p1 is the momentum of upper bound for phonon : its momentum unit:kg m/sec *)
(* p2 is the momentum of lower bound for roton : its momentum unit:kg m/sec *)
(* p3 is the momentum of upper bound for roton : its momentum unit:kg m/sec,
  p3 is determined by equality of derivative coefficient at the boundary \
between roton and higher region *)
(* p4 is the momentum of upper bound for higher region 1 :
   its momentum unit:kg m/sec  *)
p1=0.5*10^10*hbar;p2=1.78*10^10*hbar;p4=2.55*10^10*hbar;
(* Solve the parameters in order to connect the excitation energy functions \
in three regions. *)
sol=Solve[{e0maxon[p1]==e0phonon[p1],dMaxon[p1]\[Equal]dPhonon[p1],
     e0maxon[p2]==e0roton[p2],dMaxon[p2]\[Equal]dRoton[p2]},{maxon2,maxon3,
     maxon4,maxon5}]
maxon2=maxon2/.sol[[1,1]]
maxon3=maxon3/.sol[[1,2]]
maxon4=maxon4/.sol[[1,3]]
maxon5=maxon5/.sol[[1,4]]
(* Solve the parameter p3 in order to connect the excitation energy at the \
```

```
boundary between roton and higer region. *)
sol=Solve[dRoton[p3]\[Equal]c1,p3]
p3=p3/.sol[[1,1]]
(* Solve the parameter hh in order to connect the excitation energy \
continuously *)
sol=Solve[e0roton[p3]\[Equal]hh,hh]
hh=hh/.sol[[1,1]]
D[e0high2[p],p]/.p\[Rule]p4
(* Solve the parameters aaa and bbb in order to connect the excitation energy \
at p=p4 continuously *)
sol=Solve[{e0high1[p4]\[Equal]e0high2[p4],
    dHigh1[p4]\[Equal]D[e0high2[p],p]/.p\[Rule]p4},{aaa,bbb}]
aaa=aaa/.sol[[1,1]];bbb=bbb/.sol[[1,2]]
(* We define new function e0[p].
      This function is equal to the function defined by (2.42)-(2.46) in \
chapter II of my book *)
e0[p_]:=e0phonon[p]/;0<=p<p1
e0[p_]:=e0maxon[p]/;p1<=p<p2
e0[p_]:=e0roton[p]/;p2<=p<p3
e0[p_]:=e0high1[p]/;p3<=p<p4
e0[p_]:=e0high2[p]/;p4<=p
(* We will confirm that the function of func is identical to High2  *)
func
(*  The function High2[k] is equal to (2.46) in chaper II of my book,
 but the variable k is different from p  *)
High2[k_]:=dd0+dd1*(k-p4/(10^10*hbar))+dd2*(k-p4/(10^10*hbar))^2
dd0=func/.kkk->p4/(10^10*hbar)
dd1=D[func,kkk]/.kkk->p4/(10^10*hbar)
dd2=D[func,{kkk,2}]/2
(* test of  (HIgh2=func)     *)
{High2[2.6],func/.kkk\[Rule]2.6}
{High2[2.9],func/.kkk\[Rule]2.9}
(* We write parameter values (2.47)-(2.66) in chapter II of Sasaki's book.
      The parameters in Sasaki's book are related by the following equation \
*)
(* c1=c1, Delta=fDelta0*kB; p0=fQ0*10^10*hbar; r=fM0 *)
c1
fDelta0
```

```
fQ0
fM0
(* g0=maxon1 ; pM=pMax  *)
maxon1
pMax/(10^10*hbar)
(* d0=dd0*kB ; d1=dd1*kB/(10^10*hbar) ; d2=dd2*kB/(10^10*hbar)^2  *)
dd0
dd1
dd2
(* p1=p1 ; p2=p2 ; p3=p3 ; p4=p4   *)
p1/(10^10*hbar)
p2/(10^10*hbar)
p3/(10^10*hbar)
p4/(10^10*hbar)
(* b0=hh, g2=magnon2/kB , g3=magnon3/kB , g4=magnon4/kB, g5=magnon5/kB,
  b2=aaa, b3=bbb  *)
hh/kB
maxon2*(10^10*hbar)^2/kB
maxon3*(10^10*hbar)^3/kB
maxon4*(10^10*hbar)^4/kB
maxon5*(10^10*hbar)^5/kB
aaa*(10^10*hbar)^2/kB
bbb*(10^10*hbar)^3/kB
(* We show that the experimental data of elementary excitation energy are \
agreement with the function e0  *)
ge0=Plot[e0[k*10^10*hbar]/kB,{k,0,3.6}]
Show[g,ge0]
(* We show the behavior of elementary excitation energy in the region of -3.6<
   k<3.6  *)
ge0=Plot[e0[Abs[k]*10^10*hbar]/kB,{k,-3.6,3.6}]
```

Mathematica Program 2 (Approxmation in second order)

This program determines the kernel function and the temperature dependence of the dressed boson excitation energy from Bose-Einstein condensate. The kernel values and the energy values are saved in the files "kernelListNonLinearTheory", "e1ListNonLinearTheory" and "e2ListNonLinearTheory". Therefore further calculations

can start from reading these three files.

```
(*  This program is used the parameters which are determined by experimental \
data at 1.1K. The values are shown in (2.47)-(2.66) of this book.  *)
(* These parameters are almost equal to ones of Bendt et al.
     If we change the fuctional forms in phonon region and high \
momentumregion 2,
  we can obtain more sutable parameters fitting to experimental data of \
elementary excitation energy *)
(* Running time of this program is about 3 hours at first running.
      This program makes the three files "kernelListNonLinearTheory", \
"e1ListNonLinearTheory", "e2ListNonLinearTheory". *)
(*  ======== constant values ========  *)
(*  NA:Avogadro number   *)
NA=6.0221367*10^23
(*  hbar:Planck's constant/(2 Pi)   *)
hbar=6.6260755*10^-34/(2*Pi)
(*  kB:Boltzmann constant   *)
kB=1.380658*10^-23
(* m=mass of He atom, unit: kg  *)
m=(4.002602/(6.0221367*10^23))*10^-3
(* roh= mass density of liquid helium,
       at saturated vapor pressure and 1.1Kelvin unit: kg/m^3  *)
roh=145.5
(* numberDensity: number density of liquid helium unit: 1/m^3   *)
numberDensity=roh/m
(* We set the function of excitation energy *)
(* Parameter values of (2.47)-(2.66)  *)
c1=238.
delta=8.61*kB
p0=1.92*10^10*hbar
r=0.153
g0=13.82
pM=1.13*10^10*hbar
d0=16.7526*kB
d1=3.22877*kB/(10^10*hbar)
d2=-1.56968*kB/(10^10*hbar)^2
p1=0.5*10^10*hbar
```

```
p2=1.78*10^10*hbar
p3=2.1495*10^10*hbar
p4=2.55*10^10*hbar
b0=10.696*kB
b2=14.4344*kB/(10^10*hbar)^2
b3=-55.0958*kB/(10^10*hbar)^3
g2=-10.8805/(10^10*hbar)^2
g3=-1.81497/(10^10*hbar)^3
g4=-0.966809/(10^10*hbar)^4
g5=7.19044/(10^10*hbar)^5
(* We define new function e0 *)
e0[p_]:=c1*p/;0<=p<p1
e0[p_]:=kB*(g0+g2*(p-pM)^2+g3*(p-pM)^3+g4*(p-pM)^4+g5*(p-pM)^5) /;p1<=p<p2
e0[p_]:=delta+(1/(2*m*r))*(p-p0)^2 /;p2<=p<p3
e0[p_]:=b0+c1*(p-p3)+b2*(p-p3)^2+b3*(p-p3)^3 /;p3<=p<p4
e0[p_]:=d0+d1*(p-p4)+d2*(p-p4)^2 /;p4<=p
ge0=Plot[e0[k*10^10*hbar]/kB,{k,0,3.6}]
energyData={{0.0894,1.6131},{0.0946,1.7175},{0.1150,2.1005},{0.1210,
    2.2514},{0.1390,2.6111},{0.1430,2.6343},{0.1594,2.9709},{0.1767,
    3.2958},{0.1818,3.3887},{0.1938,3.6324},{0.1990,3.7368},{0.2000,
    3.7000},{0.2110,3.9689},{0.2162,4.0850},{0.2278,4.2822},{0.2329,
    4.3867},{0.2445,4.6072},{0.2495,4.7116},{0.2611,4.9205},{0.2776,
    5.2339},{0.2825,5.3267},{0.2938,5.5240},{0.2988,5.6284},{0.3000,
    5.5700},{0.3000,5.6500},{0.4000,7.4000},{0.4036,7.6361},{0.4082,
    7.7173},{0.4187,7.9146},{0.4232,7.9958},{0.4355,8.1815},{0.4498,
    8.3788},{0.4643,8.6457},{0.4785,8.8662},{0.4926,9.1099},{0.5000,
    9.1500},{0.5605,10.1544},{0.6000,10.7500},{0.6243,11.0015},{0.6965,
    11.8023},{0.7000,11.7500},{0.7649,12.4173},{0.8000,12.7200},{0.8000,
    12.6500},{0.8300,12.8815},{0.8925,13.2297},{0.9000,13.1500},{1.0000,
    13.5500},{1.1000,13.8000},{1.1300,13.8200},{1.2000,13.7500},{1.3000,
    13.5000},{1.4000,12.9500},{1.5000,12.2000},{1.6000,11.2000},{1.7000,
    10.2500},{1.8000,9.2500},{1.8800,8.6940},{1.8900,8.6570},{1.9000,
    8.7000},{1.9000,8.6540},{1.9000,8.6340},{1.9100,8.6350},{1.9100,
    8.6160},{1.9150,8.6110},{1.9200,8.6260},{1.9200,8.6100},{1.9250,
    8.6060},{1.9300,8.6260},{1.9300,8.6060},{1.9350,8.6300},{1.9350,
    8.6120},{1.9400,8.6300},{1.9400,8.6090},{1.9500,8.6500},{1.9500,
    8.6330},{1.9600,8.6830},{1.9600,8.6720},{1.9700,8.6950},{2.0000,
    8.9500},{2.1000,10.0000},{2.2000,11.6500},{2.3000,13.5500},{2.4000,
```

```
    15.5000},{2.5000,16.4500},{2.6000,17.0000},{2.7000,17.3000},{2.8000,
    17.5000},{2.9000,17.7000},{3.0000,17.8500},{3.1000,18.0000},{3.2000,
    18.1500},{3.3000,18.3000},{3.4000,18.3500},{3.5000,18.4000},{3.6000,
    18.4500}}
g=ListPlot[energyData,PlotStyle\[Rule]{PointSize[0.015],RGBColor[1,0,0]}]
Show[g,ge0]
(*   function kernel is defined as below    *)
kernel[p_,q_]:=
  NIntegrate[e0[Sqrt[Abs[p^2-2*p*q*t+q^2]]],{t,-1,1}]-2*e0[p]-2*e0[q]/;
    p≠0||q≠0
kernel[p_,q_]:=0/;p==0 && q==0
(*   Approximation of function kernel is defined as below    *)
(* Next command should be done at the first execution of program in order to \
make the file "kernelListNonLinearTheory".
     Making of the file needs a long time. Therefore,
  we should read the file in the second execution.   *)
kList=Table[{x,y,kernel[x*10^10*hbar,y*10^10*hbar]},{x,0,3.62,0.01},{y,0,3.62,
      0.01}]>>"kernelListNonLinearTheory"
OpenRead["kernelListNonLinearTheory"];kList=
  Get["kernelListNonLinearTheory"];Close["kernelListNonLinearTheory"]
kApp1[p_,q_]:=
  z/.{x=p/(10^10*hbar);y=q/(10^10*hbar);nx=IntegerPart[x*100]+1;
     ny=IntegerPart[y*100]+1;a00=kList[[nx,ny,3]];a10=kList[[nx+1,ny,3]];
     a01=kList[[nx,ny+1,3]];a11=kList[[nx+1,ny+1,3]];
     z->a11*(100*x-nx+1)*(100*y-ny+1)+a10*(100*x-nx+1)*(1-100*y+ny-1)+
        a01*(1-100*x+nx-1)*(100*y-ny+1)+a00*(1-100*x+nx-1)*(1-100*y+ny-1)}
kApp3[p_,q_]:=
  z/.{x=p/(10^10*hbar);y=q/(10^10*hbar);nx=IntegerPart[x*100];
     ny=IntegerPart[y*100];tx=100*x-nx-0.5;ty=100*y-ny-0.5;
     zz1=kList[[nx,ny,3]];zz2=kList[[nx+1,ny,3]];zz3=kList[[nx+2,ny,3]];
     zz4=kList[[nx+3,ny,3]];
     z1=((zz2+zz3)/2-(zz1-zz2-zz3+zz4)/
           16)+((zz3-zz2)-(zz4-zz1-3*zz3+3*zz2)/24)*
        tx+(zz1-zz2-zz3+zz4)/4*tx^2+(zz4-zz1-3*zz3+3*zz2)/6*tx^3;
     zz1=kList[[nx,ny+1,3]];zz2=kList[[nx+1,ny+1,3]];
     zz3=kList[[nx+2,ny+1,3]];zz4=kList[[nx+3,ny+1,3]];
     z2=((zz2+zz3)/2-(zz1-zz2-zz3+zz4)/
           16)+((zz3-zz2)-(zz4-zz1-3*zz3+3*zz2)/24)*
```

```
        tx+(zz1-zz2-zz3+zz4)/4*tx^2+(zz4-zz1-3*zz3+3*zz2)/6*tx^3;
    zz1=kList[[nx,ny+2,3]];zz2=kList[[nx+1,ny+2,3]];
    zz3=kList[[nx+2,ny+2,3]];zz4=kList[[nx+3,ny+2,3]];
    z3=((zz2+zz3)/2-(zz1-zz2-zz3+zz4)/
          16)+((zz3-zz2)-(zz4-zz1-3*zz3+3*zz2)/24)*
        tx+(zz1-zz2-zz3+zz4)/4*tx^2+(zz4-zz1-3*zz3+3*zz2)/6*tx^3;
    zz1=kList[[nx,ny+3,3]];zz2=kList[[nx+1,ny+3,3]];
    zz3=kList[[nx+2,ny+3,3]];zz4=kList[[nx+3,ny+3,3]];
    z4=((zz2+zz3)/2-(zz1-zz2-zz3+zz4)/
          16)+((zz3-zz2)-(zz4-zz1-3*zz3+3*zz2)/24)*
        tx+(zz1-zz2-zz3+zz4)/4*tx^2+(zz4-zz1-3*zz3+3*zz2)/6*tx^3;
    z->((z2+z3)/2-(z1-z2-z3+z4)/16)+((z3-z2)-(z4-z1-3*z3+3*z2)/24)*
        ty+(z1-z2-z3+z4)/4*ty^2+(z4-z1-3*z3+3*z2)/6*ty^3}
kApprox[p_,q_]:=kApp1[p,q]/;p<=0.01*10^10*hbar || q<=0.01*10^10*hbar
kApprox[p_,q_]:=
 kApp3[p,q]/;
  0.01*10^10*hbar<p<=3.6*10^10*hbar && 0.01*10^10*hbar<q<=3.6*10^10*hbar
(* ======= test of approximation ========  *)
pp=1.135*10^10*hbar;qq=1.875*10^10*hbar;{kernel[pp,qq],
 kApprox[pp,qq],(kApprox[pp,qq]-kernel[pp,qq])/kernel[pp,qq]}
pp=0.005*10^10*hbar;qq=1.875*10^10*hbar;{kernel[pp,qq],
 kApprox[pp,qq],(kApprox[pp,qq]-kernel[pp,qq])/kernel[pp,qq]}
(* result
   kApp1 is worse function than kApp3,
 and therefore kApprox has larger error for p<=0.01*10^10*hbar ||
   q<=0.01*10^10*hbar than in the other region   *)
pp=1.555*10^10*hbar;qq=1.555*10^10*hbar;t1=TimeUsed[];Do[
 kernel[pp,qq],{pp,1.556*10^10*hbar,1.566*10^10*hbar,0.0001*10^10*hbar}];t2=
 TimeUsed[];Do[
 kApprox[pp,qq],{pp,1.556*10^10*hbar,1.566*10^10*hbar,0.0001*10^10*hbar}];t3=
 TimeUsed[];{t2-t1,t3-t2}
(* This result shows that the approximation is precise for almost all region,
 and is more speedy program *)
(* ======= end of approximation test ========  *)
(* nnn[q_,T_] is the dreesed boson number in zeroth order aproximation *)
nnn[q_,T_]:=1/(Exp[e0[q]/(kB*T)]-0.9999999)
(* Divergence occurs because of numerical evaluation error,
 when denominator is extremely small. Therefore,
```

```
  we change the value 1 to 0.9999999 ;
  Deviation caused by this change is negligibly small  *)
(* excitation energy of first order *)
e1[p_,T_]:=e0[p]+r1[p,T]/;p≠0 && T≠0
e1[p_,T_]:=e0[p]/; p≠0 && T==0
e1[p_,T_]:=0/;p==0
(* recidual part of energy: r1 *)
r1[p_,T_]:=(2Pi/(numberDensity(2Pi*hbar)^3))*
    NIntegrate[kApprox[p,q]*nnn[q,T]*q^2,{q,0,3.6*10^10*hbar},
      PrecisionGoal\[Rule]4]
(* The integral region is 0\[LessEqual]q\[LessEqual]3.6*10^10*hbar,
  and the contribution from q>
    3.6*10^10*
      hbar is negligibly small.
        Therefore we have neglected the higher momentum region. *)
(* ======== approximation of e1[p,T] ========= *)
(* Next command should be done at the first execution of program in order to \
make the file "e1ListNonLinearTheory". Making of the file needs a long time.
      Therefore, we should read the file in the second execution.   *)
e1List=Table[{k,T,e1[k*10^10*hbar,T]},{k,0,3.6,0.01},{T,0,2.4,
       0.1}]>>"e1ListNonLinearTheory"
OpenRead["e1ListNonLinearTheory"];e1List=
  Get["e1ListNonLinearTheory"];Close["e1ListNonLinearTheory"]
e1App1[p_,T_]:=
  z/.{x=p/(10^10*hbar);y=T;nx=IntegerPart[x*100];ny=IntegerPart[y*10];
      tx=x*100-nx;ty=y*10-ny;zz1=e1List[[nx+1,ny+1,3]];
      zz2=e1List[[nx+2,ny+1,3]];
      z1=tx*zz2+(1-tx)*zz1;
      zz1=e1List[[nx+1,ny+2,3]];zz2=e1List[[nx+2,ny+2,3]];
      z2=tx*zz2+(1-tx)*zz1;z\[Rule]ty*z2+(1-ty)*z1}
e1App3[p_,T_]:=z/.{x=p/(10^10*hbar);y=T;nx=IntegerPart[x*100];
      ny=IntegerPart[y*10];tx=100*x-nx-0.5;ty=10*y-ny-0.5;
      zz1=e1List[[nx,ny,3]];zz2=e1List[[nx+1,ny,3]];zz3=e1List[[nx+2,ny,3]];
      zz4=e1List[[nx+3,ny,3]];
      z1=((zz2+zz3)/2-(zz1-zz2-zz3+zz4)/
             16)+((zz3-zz2)-(zz4-zz1-3*zz3+3*zz2)/24)*
          tx+(zz1-zz2-zz3+zz4)/4*tx^2+(zz4-zz1-3*zz3+3*zz2)/6*tx^3;
      zz1=e1List[[nx,ny+1,3]];zz2=e1List[[nx+1,ny+1,3]];
```

```
    zz3=e1List[[nx+2,ny+1,3]];
    zz4=e1List[[nx+3,ny+1,3]];
    z2=((zz2+zz3)/2-(zz1-zz2-zz3+zz4)/
          16)+((zz3-zz2)-(zz4-zz1-3*zz3+3*zz2)/24)*
        tx+(zz1-zz2-zz3+zz4)/4*tx^2+(zz4-zz1-3*zz3+3*zz2)/6*tx^3;
    zz1=e1List[[nx,ny+2,3]];zz2=e1List[[nx+1,ny+2,3]];
    zz3=e1List[[nx+2,ny+2,3]];zz4=e1List[[nx+3,ny+2,3]];
    z3=((zz2+zz3)/2-(zz1-zz2-zz3+zz4)/
          16)+((zz3-zz2)-(zz4-zz1-3*zz3+3*zz2)/24)*
        tx+(zz1-zz2-zz3+zz4)/4*tx^2+(zz4-zz1-3*zz3+3*zz2)/6*tx^3;
    zz1=e1List[[nx,ny+3,3]];zz2=e1List[[nx+1,ny+3,3]];
    zz3=e1List[[nx+2,ny+3,3]];zz4=e1List[[nx+3,ny+3,3]];
    z4=((zz2+zz3)/2-(zz1-zz2-zz3+zz4)/
          16)+((zz3-zz2)-(zz4-zz1-3*zz3+3*zz2)/24)*
        tx+(zz1-zz2-zz3+zz4)/4*tx^2+(zz4-zz1-3*zz3+3*zz2)/6*tx^3;
    z\[Rule](z2+z3)/2-(z1-z2-z3+z4)/16)+((z3-z2)-(z4-z1-3*z3+3*z2)/24)*
        ty+(z1-z2-z3+z4)/4*ty^2+(z4-z1-3*z3+3*z2)/6*ty^3}
e1Approx[p_,T_]:=e1[p,T]/;p==3.6*10^10*hbar
e1Approx[p_,T_]:=
 e1App1[p,T]/;
  0\[LessEqual]p\[LessEqual]0.01*10^10*hbar ||
   3.59*10^10*hbar\[LessEqual]p<3.6*10^10*hbar || T\[LessEqual]0.1
e1Approx[p_,T_]:=
 e1App3[p,T]/;0.01*10^10*hbar<p<3.59*10^10*hbar && 0.1<T\[LessEqual]2.2
(* ======= test of approximation for e1 =======  *)
T=1.85;pp=1.155*10^10*hbar;{e1[pp,T],
 e1Approx[pp,T],(e1Approx[pp,T]-e1[pp,T])/e1[pp,T]}
T=1.85;pp=0.005*10^10*hbar;{e1[pp,T],
 e1Approx[pp,T],(e1Approx[pp,T]-e1[pp,T])/e1[pp,T]}
T=1.85;pp=1.155*10^10*hbar;t1=TimeUsed[];Do[
 e1[pp,T],{pp,1.556*10^10*hbar,1.566*10^10*hbar,0.0001*10^10*hbar}];t2=
 TimeUsed[];Do[
 e1Approx[pp,T],{pp,1.556*10^10*hbar,1.566*10^10*hbar,0.0001*10^10*hbar}];t3=
 TimeUsed[];{t2-t1,t3-t2}
(* This result shows that the approximation is precise for all region,
 and is more speedy program *)
(* ===\[Equal] end of test ============  *)
(* ------------------------------ *)
```

```
(* excitation energy of second order *)
(* n1[q_,T_] is the dreesed boson number in first order aproximation *)
n1[q_,T_]:=1/(Exp[e1Approx[q,T]/(kB*T)]-0.9999999)
e2[p_,T_]:=e0[p]+r2[p,T]/;p≠0 && T≠0
e2[p_,T_]:=e0[p]/; p≠0 && T==0
e2[p_,T_]:=0/;p==0
(* recidual part of energy: r2 *)
r2[p_,T_]:=(2Pi/(numberDensity(2Pi*hbar)^3))*
   NIntegrate[kApprox[p,q]*n1[q,T]*q^2,{q,0,3.6*10^10*hbar},
    PrecisionGoal\[Rule]4]
(* The integral region is 0\[LessEqual]q\[LessEqual]3.6*10^10*hbar,
 and the contribution from q>
  3.6*10^10*
    hbar is negligibly small.
     Therefore we have neglected the higher momentum region. *)
(* ======== approximation of e2[p,T] ========= *)
(* Next command should be done at the first execution of program in order to \
make the file "e2ListNonLinearTheory". Making of the file needs a long time.
    Therefore, we should read the file in the second execution.   *)
e2List=Table[{k,T,e2[k*10^10*hbar,T]},{k,0,3.6,0.01},{T,0,2.2,
     0.1}]>>"e2ListNonLinearTheory"
OpenRead["e2ListNonLinearTheory"];e2List=
 Get["e2ListNonLinearTheory"];Close["e2ListNonLinearTheory"]
e2App1[p_,T_]:=
 z/.{x=p/(10^10*hbar);y=T;nx=IntegerPart[x*100];ny=IntegerPart[y*10];
    tx=x*100-nx;ty=y*10-ny;zz1=e2List[[nx+1,ny+1,3]];
    zz2=e2List[[nx+2,ny+1,3]];
    z1=tx*zz2+(1-tx)*zz1;
    zz1=e2List[[nx+1,ny+2,3]];zz2=e2List[[nx+2,ny+2,3]];
    z2=tx*zz2+(1-tx)*zz1;z\[Rule]ty*z2+(1-ty)*z1}
e2App3[p_,T_]:=z/.{x=p/(10^10*hbar);y=T;nx=IntegerPart[x*100];
    ny=IntegerPart[y*10];tx=100*x-nx-0.5;ty=10*y-ny-0.5;
    zz1=e2List[[nx,ny,3]];zz2=e2List[[nx+1,ny,3]];zz3=e2List[[nx+2,ny,3]];
    zz4=e2List[[nx+3,ny,3]];
    z1=((zz2+zz3)/2-(zz1-zz2-zz3+zz4)/
          16)+((zz3-zz2)-(zz4-zz1-3*zz3+3*zz2)/24)*
       tx+(zz1-zz2-zz3+zz4)/4*tx^2+(zz4-zz1-3*zz3+3*zz2)/6*tx^3;
    zz1=e2List[[nx,ny+1,3]];zz2=e2List[[nx+1,ny+1,3]];
```

```
    zz3=e2List[[nx+2,ny+1,3]];
    zz4=e2List[[nx+3,ny+1,3]];
    z2=((zz2+zz3)/2-(zz1-zz2-zz3+zz4)/
          16)+((zz3-zz2)-(zz4-zz1-3*zz3+3*zz2)/24)*
        tx+(zz1-zz2-zz3+zz4)/4*tx^2+(zz4-zz1-3*zz3+3*zz2)/6*tx^3;
    zz1=e2List[[nx,ny+2,3]];zz2=e2List[[nx+1,ny+2,3]];
    zz3=e2List[[nx+2,ny+2,3]];zz4=e2List[[nx+3,ny+2,3]];
    z3=((zz2+zz3)/2-(zz1-zz2-zz3+zz4)/
          16)+((zz3-zz2)-(zz4-zz1-3*zz3+3*zz2)/24)*
        tx+(zz1-zz2-zz3+zz4)/4*tx^2+(zz4-zz1-3*zz3+3*zz2)/6*tx^3;
    zz1=e2List[[nx,ny+3,3]];zz2=e2List[[nx+1,ny+3,3]];
    zz3=e2List[[nx+2,ny+3,3]];zz4=e2List[[nx+3,ny+3,3]];
    z4=((zz2+zz3)/2-(zz1-zz2-zz3+zz4)/
          16)+((zz3-zz2)-(zz4-zz1-3*zz3+3*zz2)/24)*
        tx+(zz1-zz2-zz3+zz4)/4*tx^2+(zz4-zz1-3*zz3+3*zz2)/6*tx^3;
    z\[Rule]((z2+z3)/2-(z1-z2-z3+z4)/16)+((z3-z2)-(z4-z1-3*z3+3*z2)/24)*
        ty+(z1-z2-z3+z4)/4*ty^2+(z4-z1-3*z3+3*z2)/6*ty^3}
e2Approx[p_,T_]:=e0[p]/; T\[Equal]0.0
e2Approx[p_,T_]:=e2[p,T]/;p==3.6*10^10*hbar || T\[Equal]2.2
e2Approx[p_,T_]:=
  e2App1[p,T]/;
    0\[LessEqual]p\[LessEqual]0.01*10^10*hbar ||
     3.59*10^10*hbar\[LessEqual]p<3.6*10^10*hbar ||0< T\[LessEqual]0.1||
     2.1\[LessEqual]T<2.2
e2Approx[p_,T_]:=e2App3[p,T]/;0.01*10^10*hbar<p<3.59*10^10*hbar && 0.1<T<2.1
(* ======= test of approximation for e2 =======  *)
T=1.85;pp=1.155*10^10*hbar;{e2[pp,T],
  e2Approx[pp,T],(e2Approx[pp,T]-e2[pp,T])/e2[pp,T]}
(* ===\[Equal] end of test ===========  *)
```

Mathematica Program 3 (Calculation of entropy)

This program determines the temperature dependence of entropy.

```
(*  This program calculates entropy  *)
(* The excitation energy values of the second order are already saved in the \
files "e2ListNonLinearTheory"  *)
```

```
(*  ======== constant values ========  *)
(*  NA:Avogadro number   *)
NA=6.0221367*10^23
(*  hbar:Planck's constant/(2 Pi)   *)
hbar=6.6260755*10^-34/(2*Pi)
(*  kB:Boltzmann constant   *)
kB=1.380658*10^-23
(* m=mass of He atom, unit: kg  *)
m=(4.002602/(6.0221367*10^23))*10^-3
(* roh= mass density of liquid helium,
      at saturated vapor pressure and 1.1Kelvin unit: kg/m^3  *)
roh=145.5
(* numberDensity: number density of liquid helium unit: 1/m^3   *)
numberDensity=roh/m
(* We set the function of excitation energy *)
(* Parameter values of (2.47)-(2.66)  *)
c1=238.
delta=8.61*kB
p0=1.92*10^10*hbar
r=0.153
g0=13.82
pM=1.13*10^10*hbar
d0=16.7526*kB
d1=3.22877*kB/(10^10*hbar)
d2=-1.56968*kB/(10^10*hbar)^2
p1=0.5*10^10*hbar
p2=1.78*10^10*hbar
p3=2.1495*10^10*hbar
p4=2.55*10^10*hbar
b0=10.696*kB
b2=14.4344*kB/(10^10*hbar)^2
b3=-55.0958*kB/(10^10*hbar)^3
g2=-10.8805/(10^10*hbar)^2
g3=-1.81497/(10^10*hbar)^3
g4=-0.966809/(10^10*hbar)^4
g5=7.19044/(10^10*hbar)^5
(* We define new function e0 *)
e0[p_]:=c1*p/;0<=p<p1
```

```
e0[p_]:=kB*(g0+g2*(p-pM)^2+g3*(p-pM)^3+g4*(p-pM)^4+g5*(p-pM)^5) /;p1<=p<p2
e0[p_]:=delta+(1/(2*m*r))*(p-p0)^2 /;p2<=p<p3
e0[p_]:=b0+c1*(p-p3)+b2*(p-p3)^2+b3*(p-p3)^3 /;p3<=p<p4
e0[p_]:=d0+d1*(p-p4)+d2*(p-p4)^2 /;p4<=p
(* nnn[q_,T_] is the dreesed boson number in zeroth order aproximation *)
nnn[q_,T_]:=1/(Exp[e0[q]/(kB*T)]-0.9999999)
(* ======== approximation of e1[p,T] ========= *)
(* We read the file "e1ListNonLinearTheory". Then,
  we calculate the approximate value of e1[p,T].   *)
OpenRead["e1ListNonLinearTheory"];e1List=
  Get["e1ListNonLinearTheory"];Close["e1ListNonLinearTheory"]
e1App1[p_,T_]:=
  z/.{x=p/(10^10*hbar);y=T;nx=IntegerPart[x*100];ny=IntegerPart[y*10];
      tx=x*100-nx;ty=y*10-ny;zz1=e1List[[nx+1,ny+1,3]];
      zz2=e1List[[nx+2,ny+1,3]];
      z1=tx*zz2+(1-tx)*zz1;
      zz1=e1List[[nx+1,ny+2,3]];zz2=e1List[[nx+2,ny+2,3]];
      z2=tx*zz2+(1-tx)*zz1;z\[Rule]ty*z2+(1-ty)*z1}
e1App3[p_,T_]:=z/.{x=p/(10^10*hbar);y=T;nx=IntegerPart[x*100];
      ny=IntegerPart[y*10];tx=100*x-nx-0.5;ty=10*y-ny-0.5;
      zz1=e1List[[nx,ny,3]];zz2=e1List[[nx+1,ny,3]];zz3=e1List[[nx+2,ny,3]];
      zz4=e1List[[nx+3,ny,3]];
      z1=((zz2+zz3)/2-(zz1-zz2-zz3+zz4)/
            16)+((zz3-zz2)-(zz4-zz1-3*zz3+3*zz2)/24)*
          tx+(zz1-zz2-zz3+zz4)/4*tx^2+(zz4-zz1-3*zz3+3*zz2)/6*tx^3;
      zz1=e1List[[nx,ny+1,3]];zz2=e1List[[nx+1,ny+1,3]];
      zz3=e1List[[nx+2,ny+1,3]];
      zz4=e1List[[nx+3,ny+1,3]];
      z2=((zz2+zz3)/2-(zz1-zz2-zz3+zz4)/
            16)+((zz3-zz2)-(zz4-zz1-3*zz3+3*zz2)/24)*
          tx+(zz1-zz2-zz3+zz4)/4*tx^2+(zz4-zz1-3*zz3+3*zz2)/6*tx^3;
      zz1=e1List[[nx,ny+2,3]];zz2=e1List[[nx+1,ny+2,3]];
      zz3=e1List[[nx+2,ny+2,3]];zz4=e1List[[nx+3,ny+2,3]];
      z3=((zz2+zz3)/2-(zz1-zz2-zz3+zz4)/
            16)+((zz3-zz2)-(zz4-zz1-3*zz3+3*zz2)/24)*
          tx+(zz1-zz2-zz3+zz4)/4*tx^2+(zz4-zz1-3*zz3+3*zz2)/6*tx^3;
      zz1=e1List[[nx,ny+3,3]];zz2=e1List[[nx+1,ny+3,3]];
      zz3=e1List[[nx+2,ny+3,3]];zz4=e1List[[nx+3,ny+3,3]];
```

```
    z4=((zz2+zz3)/2-(zz1-zz2-zz3+zz4)/
          16)+((zz3-zz2)-(zz4-zz1-3*zz3+3*zz2)/24)*
        tx+(zz1-zz2-zz3+zz4)/4*tx^2+(zz4-zz1-3*zz3+3*zz2)/6*tx^3;
    z\[Rule]((z2+z3)/2-(z1-z2-z3+z4)/16)+((z3-z2)-(z4-z1-3*z3+3*z2)/24)*
        ty+(z1-z2-z3+z4)/4*ty^2+(z4-z1-3*z3+3*z2)/6*ty^3}
e1Approx[p_,T_]:=e1[p,T]/;p==3.6*10^10*hbar
e1Approx[p_,T_]:=
 e1App1[p,T]/;
   0\[LessEqual]p\[LessEqual]0.01*10^10*hbar ||
    3.59*10^10*hbar\[LessEqual]p<3.6*10^10*hbar || T\[LessEqual]0.1
e1Approx[p_,T_]:=
 e1App3[p,T]/;0.01*10^10*hbar<p<3.59*10^10*hbar && 0.1<T\[LessEqual]2.2
(* n1[q_,T_] is the dreesed boson number in first order aproximation *)
n1[q_,T_]:=1/(Exp[e1Approx[q,T]/(kB*T)]-0.9999999)
(* ======== approximation of e2[p,T] ========= *)
(* We read the file "e2ListNonLinearTheory". Then,
 we calculate the approximate value of e2[p,T].   *)
OpenRead["e2ListNonLinearTheory"];e2List=
 Get["e2ListNonLinearTheory"];Close["e2ListNonLinearTheory"]
e2App1[p_,T_]:=
 z/.{x=p/(10^10*hbar);y=T;nx=IntegerPart[x*100];ny=IntegerPart[y*10];
    tx=x*100-nx;ty=y*10-ny;zz1=e2List[[nx+1,ny+1,3]];
    zz2=e2List[[nx+2,ny+1,3]];
    z1=tx*zz2+(1-tx)*zz1;
    zz1=e2List[[nx+1,ny+2,3]];zz2=e2List[[nx+2,ny+2,3]];
    z2=tx*zz2+(1-tx)*zz1;z\[Rule]ty*z2+(1-ty)*z1}
e2App3[p_,T_]:=z/.{x=p/(10^10*hbar);y=T;nx=IntegerPart[x*100];
    ny=IntegerPart[y*10];tx=100*x-nx-0.5;ty=10*y-ny-0.5;
    zz1=e2List[[nx,ny,3]];zz2=e2List[[nx+1,ny,3]];zz3=e2List[[nx+2,ny,3]];
    zz4=e2List[[nx+3,ny,3]];
    z1=((zz2+zz3)/2-(zz1-zz2-zz3+zz4)/
          16)+((zz3-zz2)-(zz4-zz1-3*zz3+3*zz2)/24)*
        tx+(zz1-zz2-zz3+zz4)/4*tx^2+(zz4-zz1-3*zz3+3*zz2)/6*tx^3;
    zz1=e2List[[nx,ny+1,3]];zz2=e2List[[nx+1,ny+1,3]];
    zz3=e2List[[nx+2,ny+1,3]];
    zz4=e2List[[nx+3,ny+1,3]];
    z2=((zz2+zz3)/2-(zz1-zz2-zz3+zz4)/
          16)+((zz3-zz2)-(zz4-zz1-3*zz3+3*zz2)/24)*
```

```
        tx+(zz1-zz2-zz3+zz4)/4*tx^2+(zz4-zz1-3*zz3+3*zz2)/6*tx^3;
    zz1=e2List[[nx,ny+2,3]];zz2=e2List[[nx+1,ny+2,3]];
    zz3=e2List[[nx+2,ny+2,3]];zz4=e2List[[nx+3,ny+2,3]];
    z3=((zz2+zz3)/2-(zz1-zz2-zz3+zz4)/
          16)+((zz3-zz2)-(zz4-zz1-3*zz3+3*zz2)/24)*
        tx+(zz1-zz2-zz3+zz4)/4*tx^2+(zz4-zz1-3*zz3+3*zz2)/6*tx^3;
    zz1=e2List[[nx,ny+3,3]];zz2=e2List[[nx+1,ny+3,3]];
    zz3=e2List[[nx+2,ny+3,3]];zz4=e2List[[nx+3,ny+3,3]];
    z4=((zz2+zz3)/2-(zz1-zz2-zz3+zz4)/
          16)+((zz3-zz2)-(zz4-zz1-3*zz3+3*zz2)/24)*
        tx+(zz1-zz2-zz3+zz4)/4*tx^2+(zz4-zz1-3*zz3+3*zz2)/6*tx^3;
    z\[Rule](z2+z3)/2-(z1-z2-z3+z4)/16)+((z3-z2)-(z4-z1-3*z3+3*z2)/24)*
        ty+(z1-z2-z3+z4)/4*ty^2+(z4-z1-3*z3+3*z2)/6*ty^3}
e2Approx[p_,T_]:=e0[p]/; T\[Equal]0.0
e2Approx[p_,T_]:=e2[p,T]/;p==3.6*10^10*hbar || T\[Equal]2.2
e2Approx[p_,T_]:=
 e2App1[p,T]/;
   0\[LessEqual]p\[LessEqual]0.01*10^10*hbar ||
    3.59*10^10*hbar\[LessEqual]p<3.6*10^10*hbar ||0< T\[LessEqual]0.1||
    2.1\[LessEqual]T<2.2
e2Approx[p_,T_]:=e2App3[p,T]/;0.01*10^10*hbar<p<3.59*10^10*hbar && 0.1<T<2.1
(* n2[q_,T_] is the dreesed boson number in the second order aproximation *)
n2[q_,T_]:=1/(Exp[e2Approx[q,T]/(kB*T)]-0.9999999)
(* ================================ *)
(* calculation of entropy per atom    *)
(* zeroth order entropy s0[T] (per atom)    *)
s0[T_]:=(kB*4*Pi/(numberDensity*(2*Pi*hbar)^3))*
   NIntegrate[(Log[1+nnn[p,T]]+(e0[p]/(kB*T))nnn[p,T])*p^2,{p,0,
      3.6*10^10*hbar}]
(* first order entropy s1[T] (per atom)    *)
s1[T_]:=(kB*4*Pi/(numberDensity*(2*Pi*hbar)^3))*
   NIntegrate[(Log[1+n1[p,T]]+(e1Approx[p,T]/(kB*T))n1[p,T])*p^2,{p,0,
      3.6*10^10*hbar},PrecisionGoal\[Rule]4]
(* second order entropy s2[T] (per atom)    *)
s2[T_]:=(kB*4*Pi/(numberDensity*(2*Pi*hbar)^3))*
   NIntegrate[(Log[1+n2[p,T]]+(e2Approx[p,T]/(kB*T))n2[p,T])*p^2,{p,0,
      3.6*10^10*hbar},PrecisionGoal\[Rule]4]
(* Calculation result of entropy:
```

```
    s2[T]/m indicates entropy per kg, (s2[T]/m)/
    1000 indicates entropy per g *)
Table[{T,(s0[T]/m)/1000,(s1[T]/m)/1000,(s2[T]/m)/1000},{T,0.5,2.15,0.05}]
(* The List obtained above indicates{temperature, entropy of zeroth order,
    first order, second order}
   where the entropy unit is J/(K*g)   *)
(* entropyExp is the entropies of experiment *)
entropyExp={{0.2,0.00005},{0.3,0.00018},{0.4,0.00044},{0.5,0.00085},{0.6,
    0.00147},{0.7,0.00276},{0.8,0.00475},{0.9,0.00885},{1.0,0.0168},{1.1,
    0.0304},{1.2,0.0523},{1.3,0.0853},{1.4,0.132},{1.5,0.197},{1.6,
    0.284},{1.7,0.395},{1.8,0.535},{1.9,0.715},{2.0,0.940},{2.1,1.24}}
gExp=ListPlot[entropyExp,PlotStyle\[Rule]{RGBColor[1,0,0],PointSize[0.02]}]
entropyCal=Table[{T,(s2[T]/m)/1000},{T,0.2,2.15,0.005}];
gCal=ListPlot[entropyCal,PlotStyle\[Rule]{RGBColor[0,0,0],PointSize[0.007]}]
Show[gExp,gCal]
entropyExpLog10=
   Table[{entropyExp[[n,1]],Log[10,entropyExp[[n,2]]]},{n,1,
     Length[entropyExp]}];
entropyCalLog10=
   Table[{entropyCal[[n,1]],Log[10,entropyCal[[n,2]]]},{n,1,
     Length[entropyCal]}];
gExpLog10=
 ListPlot[entropyExpLog10,PlotStyle\[Rule]{RGBColor[1,0,0],PointSize[0.02]}]
gCalLog10=
 ListPlot[entropyCalLog10,PlotStyle\[Rule]{RGBColor[0,0,0],PointSize[0.005]}]
Show[gExpLog10,gCalLog10]
```

Mathematica Program 4 (Calculation of specific heat for 0.2-2.15K)

This program calculates the temperature dependence of specific heat in the temperature region 0.2 - 2.15 K.

```
(*  This program "AppendixSpecificHeat0.2-2.15.nb" uses the excitation energy \
form at 1.1 K calculated by program "AppendixEnergyForm" *)
(* This program also uses the two files "e1ListNonLinearTheory",
  "e2ListNonLinearTheory" which are obtained by the program \
"AppendixKernelEnergy". *)
```

```
(*  ======== constant values ========  *)
(*  NA:Avogadro number   *)
NA=6.0221367*10^23
(*  hbar:Planck's constant/(2 Pi)   *)
hbar=6.6260755*10^-34/(2*Pi)
(*  kB:Boltzmann constant   *)
kB=1.380658*10^-23
(* m=mass of He atom, unit: kg  *)
m=(4.002602/(6.0221367*10^23))*10^-3
(* roh= mass density of liquid helium,
      at saturated vapor pressure and 1.1Kelvin unit: kg/m^3  *)
roh=145.5
(* numberDensity: number density of liquid helium unit: 1/m^3   *)
numberDensity=roh/m
(* We set the function of excitation energy *)
(* Parameter values of (2.47)-(2.66)  *)
c1=238.
delta=8.61*kB
p0=1.92*10^10*hbar
r=0.153
g0=13.82
pM=1.13*10^10*hbar
d0=16.7526*kB
d1=3.22877*kB/(10^10*hbar)
d2=-1.56968*kB/(10^10*hbar)^2
p1=0.5*10^10*hbar
p2=1.78*10^10*hbar
p3=2.1495*10^10*hbar
p4=2.55*10^10*hbar
b0=10.696*kB
b2=14.4344*kB/(10^10*hbar)^2
b3=-55.0958*kB/(10^10*hbar)^3
g2=-10.8805/(10^10*hbar)^2
g3=-1.81497/(10^10*hbar)^3
g4=-0.966809/(10^10*hbar)^4
g5=7.19044/(10^10*hbar)^5
(* We define new function e0 *)
e0[p_]:=c1*p/;0<=p<p1
```

```
e0[p_]:=kB*(g0+g2*(p-pM)^2+g3*(p-pM)^3+g4*(p-pM)^4+g5*(p-pM)^5) /;p1<=p<p2
e0[p_]:=delta+(1/(2*m*r))*(p-p0)^2 /;p2<=p<p3
e0[p_]:=b0+c1*(p-p3)+b2*(p-p3)^2+b3*(p-p3)^3 /;p3<=p<p4
e0[p_]:=d0+d1*(p-p4)+d2*(p-p4)^2 /;p4<=p
(* nnn[q_,T_] is the dreesed boson number in zeroth order aproximation *)
nnn[q_,T_]:=1/(Exp[e0[q]/(kB*T)]-0.9999999)
(* ======== approximation of e1[p,T] ========= *)
(* We read the file "e1ListNonLinearTheory". Then,
  we calculate the approximate value of e1[p,T].   *)
OpenRead["e1ListNonLinearTheory"];e1List=
  Get["e1ListNonLinearTheory"];Close["e1ListNonLinearTheory"]
e1App1[p_,T_]:=
  z/.{x=p/(10^10*hbar);y=T;nx=IntegerPart[x*100];ny=IntegerPart[y*10];
      tx=x*100-nx;ty=y*10-ny;zz1=e1List[[nx+1,ny+1,3]];
      zz2=e1List[[nx+2,ny+1,3]];
      z1=tx*zz2+(1-tx)*zz1;
      zz1=e1List[[nx+1,ny+2,3]];zz2=e1List[[nx+2,ny+2,3]];
      z2=tx*zz2+(1-tx)*zz1;z\[Rule]ty*z2+(1-ty)*z1}
e1App3[p_,T_]:=z/.{x=p/(10^10*hbar);y=T;nx=IntegerPart[x*100];
      ny=IntegerPart[y*10];tx=100*x-nx-0.5;ty=10*y-ny-0.5;
      zz1=e1List[[nx,ny,3]];zz2=e1List[[nx+1,ny,3]];zz3=e1List[[nx+2,ny,3]];
      zz4=e1List[[nx+3,ny,3]];
      z1=((zz2+zz3)/2-(zz1-zz2-zz3+zz4)/
            16)+((zz3-zz2)-(zz4-zz1-3*zz3+3*zz2)/24)*
          tx+(zz1-zz2-zz3+zz4)/4*tx^2+(zz4-zz1-3*zz3+3*zz2)/6*tx^3;
      zz1=e1List[[nx,ny+1,3]];zz2=e1List[[nx+1,ny+1,3]];
      zz3=e1List[[nx+2,ny+1,3]];
      zz4=e1List[[nx+3,ny+1,3]];
      z2=((zz2+zz3)/2-(zz1-zz2-zz3+zz4)/
            16)+((zz3-zz2)-(zz4-zz1-3*zz3+3*zz2)/24)*
          tx+(zz1-zz2-zz3+zz4)/4*tx^2+(zz4-zz1-3*zz3+3*zz2)/6*tx^3;
      zz1=e1List[[nx,ny+2,3]];zz2=e1List[[nx+1,ny+2,3]];
      zz3=e1List[[nx+2,ny+2,3]];zz4=e1List[[nx+3,ny+2,3]];
      z3=((zz2+zz3)/2-(zz1-zz2-zz3+zz4)/
            16)+((zz3-zz2)-(zz4-zz1-3*zz3+3*zz2)/24)*
          tx+(zz1-zz2-zz3+zz4)/4*tx^2+(zz4-zz1-3*zz3+3*zz2)/6*tx^3;
      zz1=e1List[[nx,ny+3,3]];zz2=e1List[[nx+1,ny+3,3]];
      zz3=e1List[[nx+2,ny+3,3]];zz4=e1List[[nx+3,ny+3,3]];
```

```
    z4=((zz2+zz3)/2-(zz1-zz2-zz3+zz4)/
          16)+((zz3-zz2)-(zz4-zz1-3*zz3+3*zz2)/24)*
        tx+(zz1-zz2-zz3+zz4)/4*tx^2+(zz4-zz1-3*zz3+3*zz2)/6*tx^3;
    z\[Rule]((z2+z3)/2-(z1-z2-z3+z4)/16)+((z3-z2)-(z4-z1-3*z3+3*z2)/24)*
        ty+(z1-z2-z3+z4)/4*ty^2+(z4-z1-3*z3+3*z2)/6*ty^3}
e1Approx[p_,T_]:=e1[p,T]/;p==3.6*10^10*hbar
e1Approx[p_,T_]:=
 e1App1[p,T]/;
   0\[LessEqual]p\[LessEqual]0.01*10^10*hbar ||
    3.59*10^10*hbar\[LessEqual]p<3.6*10^10*hbar || T\[LessEqual]0.1
e1Approx[p_,T_]:=
 e1App3[p,T]/;0.01*10^10*hbar<p<3.59*10^10*hbar && 0.1<T\[LessEqual]2.2
(* n1[q_,T_] is the dreesed boson number in first order aproximation *)
n1[q_,T_]:=1/(Exp[e1Approx[q,T]/(kB*T)]-0.9999999)
(* ======== approximation of e2[p,T] ========= *)
(* We read the file "e2ListNonLinearTheory". Then,
 we calculate the approximate value of e2[p,T].   *)
OpenRead["e2ListNonLinearTheory"];e2List=
 Get["e2ListNonLinearTheory"];Close["e2ListNonLinearTheory"]
e2App1[p_,T_]:=
 z/.{x=p/(10^10*hbar);y=T;nx=IntegerPart[x*100];ny=IntegerPart[y*10];
    tx=x*100-nx;ty=y*10-ny;zz1=e2List[[nx+1,ny+1,3]];
    zz2=e2List[[nx+2,ny+1,3]];
    z1=tx*zz2+(1-tx)*zz1;
    zz1=e2List[[nx+1,ny+2,3]];zz2=e2List[[nx+2,ny+2,3]];
    z2=tx*zz2+(1-tx)*zz1;z\[Rule]ty*z2+(1-ty)*z1}
e2App3[p_,T_]:=z/.{x=p/(10^10*hbar);y=T;nx=IntegerPart[x*100];
    ny=IntegerPart[y*10];tx=100*x-nx-0.5;ty=10*y-ny-0.5;
    zz1=e2List[[nx,ny,3]];zz2=e2List[[nx+1,ny,3]];zz3=e2List[[nx+2,ny,3]];
    zz4=e2List[[nx+3,ny,3]];
    z1=((zz2+zz3)/2-(zz1-zz2-zz3+zz4)/
          16)+((zz3-zz2)-(zz4-zz1-3*zz3+3*zz2)/24)*
        tx+(zz1-zz2-zz3+zz4)/4*tx^2+(zz4-zz1-3*zz3+3*zz2)/6*tx^3;
    zz1=e2List[[nx,ny+1,3]];zz2=e2List[[nx+1,ny+1,3]];
    zz3=e2List[[nx+2,ny+1,3]];
    zz4=e2List[[nx+3,ny+1,3]];
    z2=((zz2+zz3)/2-(zz1-zz2-zz3+zz4)/
          16)+((zz3-zz2)-(zz4-zz1-3*zz3+3*zz2)/24)*
```

```
        tx+(zz1-zz2-zz3+zz4)/4*tx^2+(zz4-zz1-3*zz3+3*zz2)/6*tx^3;
    zz1=e2List[[nx,ny+2,3]];zz2=e2List[[nx+1,ny+2,3]];
    zz3=e2List[[nx+2,ny+2,3]];zz4=e2List[[nx+3,ny+2,3]];
    z3=((zz2+zz3)/2-(zz1-zz2-zz3+zz4)/
          16)+((zz3-zz2)-(zz4-zz1-3*zz3+3*zz2)/24)*
        tx+(zz1-zz2-zz3+zz4)/4*tx^2+(zz4-zz1-3*zz3+3*zz2)/6*tx^3;
    zz1=e2List[[nx,ny+3,3]];zz2=e2List[[nx+1,ny+3,3]];
    zz3=e2List[[nx+2,ny+3,3]];zz4=e2List[[nx+3,ny+3,3]];
    z4=((zz2+zz3)/2-(zz1-zz2-zz3+zz4)/
          16)+((zz3-zz2)-(zz4-zz1-3*zz3+3*zz2)/24)*
        tx+(zz1-zz2-zz3+zz4)/4*tx^2+(zz4-zz1-3*zz3+3*zz2)/6*tx^3;
    z\[Rule](z2+z3)/2-(z1-z2-z3+z4)/16)+((z3-z2)-(z4-z1-3*z3+3*z2)/24)*
        ty+(z1-z2-z3+z4)/4*ty^2+(z4-z1-3*z3+3*z2)/6*ty^3}
e2Approx[p_,T_]:=e0[p]/; T\[Equal]0.0
e2Approx[p_,T_]:=e2[p,T]/;p==3.6*10^10*hbar || T\[Equal]2.2
e2Approx[p_,T_]:=
 e2App1[p,T]/;
   0\[LessEqual]p\[LessEqual]0.01*10^10*hbar ||
    3.59*10^10*hbar\[LessEqual]p<3.6*10^10*hbar ||0< T\[LessEqual]0.1||
    2.1\[LessEqual]T<2.2
e2Approx[p_,T_]:=e2App3[p,T]/;0.01*10^10*hbar<p<3.59*10^10*hbar && 0.1<T<2.1
(* ======== approximation for the derivative of e2[p,T]
      We should note that dTe2Approx[p,T]  is not defined at p=
   3.6*10^10*hbar. Also it is not defined at T=2.2. ========== *)
dTe2App1[p_,T_]:=
 z/.{x=p/(10^10*hbar);y=T;nx=IntegerPart[x*100];ny=IntegerPart[y*10];
    tx=x*100-nx;ty=y*10-ny;zz1=e2List[[nx+1,ny+1,3]];
    zz2=e2List[[nx+2,ny+1,3]];
    z1=tx*zz2+(1-tx)*zz1;
    zz1=e2List[[nx+1,ny+2,3]];zz2=e2List[[nx+2,ny+2,3]];
    z2=tx*zz2+(1-tx)*zz1;z\[Rule]10*z2-10*z1}
dTe2App3[p_,T_]:=z/.{x=p/(10^10*hbar);y=T;nx=IntegerPart[x*100];
    ny=IntegerPart[y*10];tx=100*x-nx-0.5;ty=10*y-ny-0.5;
    zz1=e2List[[nx,ny,3]];zz2=e2List[[nx+1,ny,3]];zz3=e2List[[nx+2,ny,3]];
    zz4=e2List[[nx+3,ny,3]];
    z1=((zz2+zz3)/2-(zz1-zz2-zz3+zz4)/
          16)+((zz3-zz2)-(zz4-zz1-3*zz3+3*zz2)/24)*
        tx+(zz1-zz2-zz3+zz4)/4*tx^2+(zz4-zz1-3*zz3+3*zz2)/6*tx^3;
```

```
    zz1=e2List[[nx,ny+1,3]];zz2=e2List[[nx+1,ny+1,3]];
    zz3=e2List[[nx+2,ny+1,3]];
    zz4=e2List[[nx+3,ny+1,3]];
    z2=((zz2+zz3)/2-(zz1-zz2-zz3+zz4)/
          16)+((zz3-zz2)-(zz4-zz1-3*zz3+3*zz2)/24)*
       tx+(zz1-zz2-zz3+zz4)/4*tx^2+(zz4-zz1-3*zz3+3*zz2)/6*tx^3;
    zz1=e2List[[nx,ny+2,3]];zz2=e2List[[nx+1,ny+2,3]];
    zz3=e2List[[nx+2,ny+2,3]];zz4=e2List[[nx+3,ny+2,3]];
    z3=((zz2+zz3)/2-(zz1-zz2-zz3+zz4)/
          16)+((zz3-zz2)-(zz4-zz1-3*zz3+3*zz2)/24)*
       tx+(zz1-zz2-zz3+zz4)/4*tx^2+(zz4-zz1-3*zz3+3*zz2)/6*tx^3;
    zz1=e2List[[nx,ny+3,3]];zz2=e2List[[nx+1,ny+3,3]];
    zz3=e2List[[nx+2,ny+3,3]];zz4=e2List[[nx+3,ny+3,3]];
    z4=((zz2+zz3)/2-(zz1-zz2-zz3+zz4)/
          16)+((zz3-zz2)-(zz4-zz1-3*zz3+3*zz2)/24)*
       tx+(zz1-zz2-zz3+zz4)/4*tx^2+(zz4-zz1-3*zz3+3*zz2)/6*tx^3;
    z\[Rule]10(((z3-z2)-(z4-z1-3*z3+3*z2)/24)+(z1-z2-z3+z4)/2*
          ty+(z4-z1-3*z3+3*z2)/2*ty^2)}
dTe2Approx[p_,T_]:=0/; T\[Equal]0.0
dTe2Approx[p_,T_]:=
  dTe2App1[p,T]/;
   0\[LessEqual]p\[LessEqual]0.01*10^10*hbar ||
    3.59*10^10*hbar\[LessEqual]p<3.6*10^10*hbar ||0< T\[LessEqual]0.1||
    2.1\[LessEqual]T<2.2
dTe2Approx[p_,T_]:=
  dTe2App3[p,T]/;0.01*10^10*hbar<p<3.59*10^10*hbar && 0.1<T<2.1
(* ======= test of approximation for derivative of e2 by T =======  *)
T=1.65;pp=1.155*10^10*hbar;{dTe2App1[pp,T],
  dTe2App3[pp,T],(dTe2App1[pp,T]-dTe2App3[pp,T])/dTe2App3[pp,T]}
{-1.19005 × 10\^-23,-1.18632 × 10\^-23,0.00313924}
T=2.199999;pp=3.599999*10^10*hbar;dTe2Approx[pp,T]
-6.14294 × 10\^-23
(* ===\[Equal] end of test ===========  *)
(* ================================ *)
(* calculation of specific heat per atom    *)
(* zeroth order specific heat C0[T] (per atom)    *)
C0[T_]:=(4*Pi/(numberDensity*(2*Pi*hbar)^3))*
   NIntegrate[((nnn[p,T])^2*Exp[e0[p]/(kB*T)](e0[p]/(kB*T))^2)*kB*p^2,{p,0,
```

```
      3.6*10^10*hbar}]
(* second order specific heat C2[T] (per atom)    *)
(* n2[q_,T_] is the dreesed boson number in second order aproximation *)
n2[q_,T_]:=1/(Exp[e2Approx[q,T]/(kB*T)]-0.9999999)
C2[T_]:=(4*Pi/(numberDensity*(2*Pi*hbar)^3))*
   NIntegrate[(n2[p,T])^2*
      Exp[e2Approx[p,T]/(kB*T)]*((e2Approx[p,T]/(kB*T))^2*
         kB-(e2Approx[p,T]/(kB*T))*dTe2Approx[p,T])*p^2,{p,0,
      3.599999*10^10*hbar}]
T=1.9;C2[T]/m/1000
(* The next Table is the calculated List as{temperature,
    specific heat of zeroth order, second order}  *)
Table[{T,(C0[T]/m)/1000,(C2[T]/m)/1000},{T,0.2,2.15,0.05}]
(* We make the list of specific heat{temperature,
      specific heat (unit:J/(K*g)} *)
t1=TimeUsed[];specificHeatCal=Table[{T,C2[T]/m/1000},{T,0.2,2.15,0.005}];t2=
 TimeUsed[];t2-t1
(* specificHeatExp is the specific heat of experiment *)
specificHeatExp={{0.2,0.0002},{0.3,0.0005},{0.4,0.0013},{0.5,0.0025},{0.6,
    0.0044},{0.7,0.0098},{0.8,0.0222},{0.9,0.0510},{1.0,0.1042},{1.1,
    0.191},{1.2,0.322},{1.3,0.516},{1.4,0.780},{1.5,1.127},{1.6,1.572},{1.7,
    2.11},{1.8,2.81},{1.9,3.79},{2.0,5.18},{2.1,7.51}}
gExp=ListPlot[specificHeatExp,
   PlotStyle\[Rule]{RGBColor[1,0,0],PointSize[0.02]}]
specificExpLog10=
   Table[{specificHeatExp[[n,1]],Log[10,specificHeatExp[[n,2]]]},{n,1,
      Length[specificHeatExp]}];
specificCalLog10=
   Table[{specificHeatCal[[n,1]],Log[10,specificHeatCal[[n,2]]]},{n,1,
      Length[specificHeatCal]}];
gExpLog10=
 ListPlot[specificExpLog10,PlotStyle\[Rule]{RGBColor[1,0,0],PointSize[0.02]}]
gCalLog10=
 ListPlot[specificCalLog10,
   PlotStyle\[Rule]{RGBColor[0,0,0],PointSize[0.005]}]
Show[gExpLog10,gCalLog10]
```

Mathematica program 5 (Calculation of specific heat near the λ point)

This program calculates specific heat near the λ point. We use the temperature dependence of experimental data for second sound verocity.

```
(* Calculation of Specific Heat near the lambda transition  *)
(*  alpha:
   expansion coefficient of liquid helium near lambda transition :
      unit:K^-1
      where T and P indicate the temperature and pressure respectively.*)
\!\(alpha[P_, T_] =
   0.20821014177938688`\[InvisibleSpace] - 0.19315882351879696`\ P +
    0.001665065420298923`\ P\^2 + 5.000779466327585`*^-6\ P\^3 -
    3.3575696795459315`*^-7\ P\^4 - 0.1817968215507505`\ T +
    0.1935429711624159`\ P\ T - 0.00042826241460284105`\ P\^2\ T +
    0.035644114587116915`\ T\^2 - 0.04892332663996617`\ P\ T\^2 -
    0.00024311096857724168`\ P\^2\ T\^2\)
(*    energy of phonon part (second sound) :unit:J   *)
\!\( (*\ \ velocity\ of\ second\ sound\  = \(21.547\ tt\^\(1/3\) -
       0.35276\ P\ tt\^\(1/3\) + 32.226\ \@tt - 0.27876\ P\ \@tt +
       0.0051713\ P\^2\ \@tt\ \ \ \ where\ tt = 1 - T/Tlambda\)\ \ *) \)
energyPhonon[tt_,p_]:=
  p(c1+c2*P)(tt+(a*p/(2*m))^3)^(1/3)+p(d1+d2*P+d3*P^2)(tt+(b*p/(2*m))^2)^(1/2)
(* dedTPhonon = the derivative coefficient, namely D[energyPhonon,T]   *)
dedTPhonon[tt_,
   p_]:=-(1/(3*Tlambda))*
    p*(c1+c2*P)(tt+(a*p/(2*m))^3)^(-2/3)-(1/(2*Tlambda))*
    p(d1+d2*P+d3*P^2)(tt+(b*p/(2*m))^2)^(-1/2)
derivPhonon[tt_,
   p_]:=(c1+c2*P)(tt+(a*p/(2*m))^3)^(1/3)+(d1+d2*P+
       d3*P^2)(tt+(b*p/(2*m))^2)^(1/2)+(a*p/(2*m))^3*(c1+
       c2*P)(tt+(a*p/(2*m))^3)^(-2/3)+(b*p/(2*m))^2*(d1+d2*P+
       d3*P^2)(tt+(b*p/(2*m))^2)^(-1/2)
c1=21.547;c2=-0.35276;d1=32.226;d2=-0.27876;d3=0.0051713;bb=0.565;b=
  bb*(1-(c1+c2*P)a)/(d1+d2*P+d3*P^2)
(*   functions   *)
```

```
exPhonon[tt_,q_]:=Exp[energyPhonon[tt,q*hbar]/(kB*Tlambda*(1-tt))]
nPhonon[tt_,q_]:=1/(exPhonon[tt,q]-1)
fPhonon[tt_,q_]:=
 alpha[P,Tlambda*(1-tt)]*(kB*Tlambda*(1-tt)*Log[1+nPhonon[tt,q]]+
       energyPhonon[tt,q*hbar]*nPhonon[tt,q])+
   exPhonon[tt,
      q]*(energyPhonon[tt,
         q*hbar]/(kB*Tlambda*(1-tt)))(energyPhonon[tt,
           q*hbar]/(Tlambda*(1-tt))-dedTPhonon[tt,q*hbar])*nPhonon[tt,q]^2
(*  specific heat for phonon region:   unit is J/(mole K)    *)
q1=0.47*10^10
cPhonon[tt_]:=
 NIntegrate[fPhonon[tt,q]*q^2/((1000/4.0026)*roh*2*Pi^2),{q,1,q1}]
(* ================ *)
(*  energy form of thermal roton   *)
(*  These function forms are derived from BD theory.
      fDelta=roton minimum energy, unit K
     fQ=roton minimum wave vector,unit A^-1
     fMeff=effective mass of roton,ratio to the mass of He atom    *)
\!\(fDelta[P_, T_] =
   11.817996949160221`\[InvisibleSpace] + 0.005462313498632458`\ P +
     0.00007060004218597404`\ P\^2 - 1.994136758893095`\ T -
     0.03904567848829687`\ P\ T - 0.0004472451972962349`\ P\^2\ T\)
(* cD is the derivative coefficient D[fDelta,T]   *)
\!\(cD = \(-1.994136758893095`\)\  -
     0.03904567848829687`\ P\  - \(\(0.0004472451972962349`\)\(\ \
\)\(P\^2\)\(\ \)\)\)
\!\(fQ[P_, T_] =
   1.9117207681118162`\[InvisibleSpace] - 0.0025819515490051043`\ P +
     0.0002580457099968077`\ P\^2 + 0.0019883653842202686`\ T +
     0.005281830335301087`\ P\ T - 0.00018934972954181802`\ P\^2\ T\)
(* cQ is the derivative coefficient D[fQ,T]   *)
\!\(cQ = \(+0.0019883653842202686`\)\  +
     0.005281830335301087`\ P\  - \(\(0.00018934972954181802`\)\(\ \
\)\(P\^2\)\(\ \)\)\)
\!\(fMeff[P_, T_] =
   0.21803261551944467`\[InvisibleSpace] + 0.00003466145724840003`\ P +
     5.577735788725462`*^-7\ P\^2 - 0.03676347248658116`\ T -
```

```
     0.0007115671371523195`\ P\ T - 7.100620816409547`*^-6\ P\^2\ T\)
(* cM is the derivative coefficient D[fMeff,T]   *)
\!\(cM = \(-0.03676347248658116`\)\  -
     0.0007115671371523195`\ P\  - \(\(7.100620816409547`*^-6\)\(\ \
\)\(P\^2\)\(\ \)\)\)\)
(* energyRoton=roton energy, unit J   *)
energyRoton[tt_,p_]:=
  1/(2*fMeff[P,Tlambda*(1-tt)]*m)*(p-fQ[P,Tlambda*(1-tt)]*10^10*hbar)^2+
    fDelta[P,Tlambda*(1-tt)]*kB
(* derivRoton is the derivative coefficient D[energyRoton,p]   *)
derivRoton[tt_,p_]:=
  1/(fMeff[P,Tlambda*(1-tt)]*m)*(p-fQ[P,Tlambda*(1-tt)]*10^10*hbar)
d2Roton[tt_,p_]:=1/(fMeff[P,Tlambda*(1-tt)]*m)
(* dedTRoton is the derivative coefficient D[energyRoton,T]   *)
dedTRoton[tt_,
    p_]:=-cM/(2*fMeff[P,Tlambda*(1-tt)]^2*m)*(p-
          fQ[P,Tlambda*(1-tt)]*10^10*hbar)^2-2(cQ*10^10*
         hbar/(2*fMeff[P,Tlambda*(1-tt)]*m))*(p-
         fQ[P,Tlambda*(1-tt)]*10^10*hbar)+cD*kB
(* calculation of heat capacity for roton region  *)
exRoton[tt_,q_]:=Exp[energyRoton[tt,q*hbar]/(kB*Tlambda*(1-tt))]
nRoton[tt_,q_]:=1/(exRoton[tt,q]-1)
fRoton[tt_,q_]:=
  alpha[P,Tlambda*(1-tt)]*(kB*Tlambda*(1-tt)*Log[1+nRoton[tt,q]]+
        energyRoton[tt,q*hbar]*nRoton[tt,q])+
    exRoton[tt,
       q]*(energyRoton[tt,
          q*hbar]/(kB*Tlambda*(1-tt)))(energyRoton[tt,
            q*hbar]/(Tlambda*(1-tt))-dedTRoton[tt,q*hbar])*nRoton[tt,q]^2
(*  specific heat for roton region:   unit is J/(mole K)    *)
q2=1.75*10^10
(*  We will set q3 after *)
cRoton[tt_]:=NIntegrate[fRoton[tt,q]*q^2/((1000/4.0026)*roh*2*Pi^2),{q,q2,q3}]
(* ====================== constant values   *)
(* NA:Avogadro constant   *)
NA=6.0221367*10^23
hbar=6.626*10^-34/(2*Pi)
h=6.626*10^-34
```

```
kB=1.381*10^-23
(* m=mass of He atom, unit: kg  *)
m=(4.0026/(6.0221367*10^23))*10^-3
\!\( (*\ \ \((0.02210\[InvisibleSpace] + 0.0002426\ P -
        2.621*10^\(-6\)\ P\^2)\)\  = \
    number\ of\ atoms\ per\ unit\ volume\ 1  Å \^\(-3\)\ \ *) \)
(*  roh is the mass density which depends on P and T. unit:kg/m^3  ========== *)
\!\(roh =
   m*10^30*\((0.02210\[InvisibleSpace] + 0.0002426\ P -
        2.621*10^\(-6\)\ P\^2)\)\)
roh=146.89+1.6125 P-0.01742 P^2
(* These two expressions of roh are equivalent. *)
\!\(Tlambda = 2.1725 - 0.00977\ P - 0.000127\ P\^2\)
T=Tlambda*(1-tt)
(* energy function for maxon *)
(* maxon1 is a peak energy of maxon which is derived from BD (Brooks & \
Donnelly) theory  unit: K *)
\!\(maxon1 =
   3.206405433445097`\[InvisibleSpace] + 0.27134388495988193`\ P -
     0.011766735067301868`\ P\^2 + 0.00397264308273967 15`\ P\^3 -
     5.301226864013549`*^-6\ P\^4 + 12.668467578023716`\ T -
     0.09966957241809207`\ P\ T - 3.8815941717254123`\ T\^2 +
     0.023402114681846813`\ P\ T\^2\)
(* maxon curve *)
pMax=1.4*10^10*hbar
energyMaxon[tt_,p_]:=
  maxon1*kB+(maxon2+maxon3*(p-pMax)+maxon4*(p-pMax)^2+
       maxon5*(p-pMax)^3)(p-pMax)^2
derivMaxon[p_]:=
  2*maxon2*(p-pMax)+3*maxon3*(p-pMax)^2+4*maxon4*(p-pMax)^3+5*
    maxon5*(p-pMax)^4
energyMaxon[tt,q1*hbar]
energyPhonon[tt,q1*hbar]
energyRoton[tt,q2*hbar]
sol=Solve[{energyMaxon[tt,q1*hbar]==energyPhonon[tt,q1*hbar],
      derivMaxon[q1*hbar]\[Equal]derivPhonon[tt,q1*hbar],
      energyMaxon[tt,q2*hbar]==energyRoton[tt,q2*hbar],
      derivMaxon[q2*hbar]\[Equal]derivRoton[tt,q2*hbar]},{maxon2,maxon3,
```

```
      maxon4,maxon5}];
maxon2=maxon2/.sol[[1,1]]
maxon3=maxon3/.sol[[1,2]]
maxon4=maxon4/.sol[[1,3]]
maxon5=maxon5/.sol[[1,4]]
(*   define functions  This definition is important. We donot use ":=".
     This delayed definition ":="  derives the incorrect result. *)
dedTMaxon[tt_,p_]=-D[energyMaxon[tt,p],tt]/Tlambda
(* calculation of heat capacity for maxon region  *)
exMaxon[tt_,q_]:=Exp[energyMaxon[tt,q*hbar]/(kB*Tlambda*(1-tt))]
nMaxon[tt_,q_]:=1/(exMaxon[tt,q]-1)
fMaxon[tt_,q_]:=
 alpha[P,Tlambda*(1-tt)]*(kB*Tlambda*(1-tt)*Log[1+nMaxon[tt,q]]+
       energyMaxon[tt,q*hbar]*nMaxon[tt,q])+
   exMaxon[tt,
      q]*(energyMaxon[tt,
         q*hbar]/(kB*Tlambda*(1-tt)))(energyMaxon[tt,
          q*hbar]/(Tlambda*(1-tt))-dedTMaxon[tt,q*hbar])*nMaxon[tt,q]^2
(*  specific heat for maxon region:   unit is J/(mole K)    *)
cMaxon[tt_]:=
 NIntegrate[fMaxon[tt,q]*q^2/((1000/4.0026)*roh*2*Pi^2),{q,10^10,q2}]
cPhMaxon[tt_]:=
 NIntegrate[fMaxon[tt,q]*q^2/((1000/4.0026)*roh*2*Pi^2),{q,q1,10^10}]
(* high momentum curve  *)
firstVelocity={{0.05,237},{2.533125`,257},{5.06625`,273},{10.1325`,
    300},{15.19875`,326},{20.265`,346},{25.33125`,365}}
h1=Fit[firstVelocity,{1,P,P^2},P]
p3List=Table[
    Join[{P,tt},p/.Solve[derivRoton[tt,p]\[Equal]h1,p]],{tt,0,0.01,
     0.002},{P,0,29}];
p3List=Join[p3List[[1]],p3List[[2]],p3List[[3]],p3List[[4]],p3List[[5]],
    p3List[[6]]];
p3=Fit[p3List,{1,P,tt,P*tt},{P,tt}]
q3=p3/hbar
h2=energyRoton[tt,p3]
energyHigh[tt_,p_]:=h1*(p-p3)+h2
Clear[tt];dedTHigh[tt_,p_]=-D[energyHigh[tt,p],tt]/Tlambda
(* calculation of heat capacity for High momentum region  q3 < q < 5*10^10 *)
```

```
exHigh[tt_,q_]:=Exp[energyHigh[tt,q*hbar]/(kB*Tlambda*(1-tt))]
nHigh[tt_,q_]:=1/(exHigh[tt,q]-1)
fHigh[tt_,q_]:=
 alpha[P,Tlambda*(1-tt)]*(kB*Tlambda*(1-tt)*Log[1+nHigh[tt,q]]+
       energyHigh[tt,q*hbar]*nHigh[tt,q])+
   exHigh[tt,
      q]*(energyHigh[tt,
         q*hbar]/(kB*Tlambda*(1-tt)))(energyHigh[tt,
           q*hbar]/(Tlambda*(1-tt))-dedTHigh[tt,q*hbar])*nHigh[tt,q]^2
(*  specific heat for High momentum region :   unit is J/(mole K)    *)
cHigh[tt_]:=
 NIntegrate[fHigh[tt,q]*q^2/((1000/4.0026)*roh*2*Pi^2),{q,q3,5*10^10}]
(* Figure of function form of excitation energy *)
P=0.05;ttt=0.01;a=0.005426;g1=Plot[energyPhonon[ttt,p]/kB,{p,0,q1*hbar}]
q2
q3
P=0.05;tt=0.01;g2=Plot[energyMaxon[tt,p]/kB,{p,q1*hbar,q2*hbar}]
P=0.05;tt=0.01;g3=Plot[energyRoton[tt,p]/kB,{p,q2*hbar,q3*hbar}]
P=0.05;tt=0.01;g4=Plot[energyHigh[tt,p]/kB,{p,q3*hbar,2.6*10^10*hbar}]
pMax/hbar
Show[g1,g2,g3,g4]
Show[g1,g2,PlotRange\[Rule]{0,5}]
(*  next functions indicate the fractions of the dressed boson numbers inside \
various momentum regions for the total number of helium atoms  *)
(*  fraction1 = phonon region / total   *)
ratioPhonon[tt_]:=NIntegrate[nPhonon[tt,q]*q^2/((roh/m)*2*Pi^2),{q,1,q1}]
(*  fraction2 = Maxon region / total   *)
ratioMaxon[tt_]:=NIntegrate[nMaxon[tt,q]*q^2/((roh/m)*2*Pi^2),{q,10^10,q2}]
(*  fraction3 = the region between phonon and maxon / total   *)
ratioPhMaxon[tt_]:=NIntegrate[nMaxon[tt,q]*q^2/((roh/m)*2*Pi^2),{q,q1,10^10}]
(*  fraction4 = roton region / total   *)
ratioRoton[tt_]:=NIntegrate[nRoton[tt,q]*q^2/((roh/m)*2*Pi^2),{q,q2,q3}]
(*  fraction5 = High momentum region / total   *)
ratioHigh[tt_]:=NIntegrate[nHigh[tt,q]*q^2/((roh/m)*2*Pi^2),{q,q3,5*10^10}]
ratioHR[tt_]:=ratioHigh[tt]+ratioRoton[tt];
ratioHRM[tt_]:=ratioHR[tt]+ratioMaxon[tt];
ratioTotal[tt_]:=ratioPhonon[tt]+ratioPhMaxon[tt]+ratioHRM[tt]
(* Next, we clarify that the transition temperature is certainly equal to the \
```

```
T=Tlambda=2.172 K  *)
P=0.05;tt=0;ratioPhonon[tt]+ratioPhMaxon[tt]
P=0.05;tt=0;ratioMaxon[tt]
P=0.05;tt=0;ratioRoton[tt]
P=0.05;tt=0;ratioHigh[tt]
P=0.05;tt=0;ratioTotal[tt]
Tlambda
(* This result indicates that the total number of dressed bosons with non-
     zero momentum is equal to the total number of helium atoms at T=
   Tlambda. Accordingly,
  Bose condensation disappears at T=Tlambda. That is to say,
  the transition temperature is certainly equal to Tlambda *)
(* calculation of heat capacity,
  make the list area  *)
r=Table[{0.1,n},{n,1,15}]
(* calculation of heat capacity of roton;
  momentum region from q2*hbar to q3*hbar *)
P=0.05;tt=0.01;cRoton[tt]
P=0.05;Do[{tt=2^-n/128;r[[n,1]]=tt;r[[n,2]]=cRoton[tt]},{n,1,15}]
(*  heat capacity (unit:J/(K\[Bullet]mole)) of roton region
       horizontal axis is t=1-T/Tlambda *)
g1=ListPlot[r,PlotStyle->PointSize[0.02]]
Clear[tt];cRotonFit[tt_]=Fit[r,{1,tt},tt]
(* calculation of maxon momentum region from 1 to 1.75 A^-1  *)
(*  heat capacity (unit:J/(K\[Bullet]mole)) for maxon region
      from 1 to 1.75 A^-1 *)
tt=0.01;cMaxon[tt]
P=0.05;Do[{tt=2^-n/128;r[[n,1]]=tt;r[[n,2]]=cMaxon[tt]},{n,1,15}]
g1=ListPlot[r,PlotStyle->PointSize[0.02]]
Clear[tt];cMaxonFit[tt_]=Fit[r,{1,tt},tt]
(* calculation of phonon-maxon momentum region from q1 to 1 A^-1  *)
(*  heat capacity (unit:J/(K\[Bullet]mole)) for phonon-
   maxon region from q1 to 1 A^-1 *)
P=0.05;Do[{tt=2^-n/128;r[[n,1]]=tt;r[[n,2]]=cPhMaxon[tt]},{n,1,15}]
g1=ListPlot[r,PlotStyle->PointSize[0.02]]
Clear[tt];cPhMaxonFit[tt_]=Fit[r,{1,tt},tt]
(* calculation of another momentum region from q3 to 5 A^-1  *)
Do[{P=0.05;tt=2^-n/128;r[[n,1]]=tt;r[[n,2]]=cHigh[tt]},{n,1,15}];ListPlot[r,
```

```
  PlotStyle->PointSize[0.02]]
Clear[tt];cHighFit[tt_]=Fit[r,{1,tt},tt]
Clear[tt];cRotonFit[tt]
cMaxonFit[tt]
cHighFit[tt]
(* experimental data of heat capacity for svp   *)
(*   CsDataLow={{t=(1-T/Tlambda),Cs},\[Bullet]\[Bullet]\[Bullet]\[Bullet]}
     Cs:unit is J/(mole K)    *)
CsDataLow={{6.6758747697974216`*^-6,76},{4.511970534069982`*^-6,
     78},{2.5782688766114177`*^-6,83.5`},{6.583793738489871`*^-6,
     77.1`},{3.7292817679558014`*^-6,80.5`},{4.604051565377532`*^-6,
     77.7`},{8.47145488029466`*^-6,75.9`},{2.302025782688766`*^-6,
     82.8`},{8.747697974217312`*^-6,74},{3.2228360957642724`*^-6,
     81.9`},{2.9926335174953956`*^-6,82.2`},{1.1049723756906076`*^-6,
     86.8`},{0.00008291896869244934`,63.7`},{0.000015750460405156538`,
     71.8`},{0.003007366482504604`,44.67`},{0.002845051565375324`,
     44.92`},{0.002698895027624309 3`,45.25`},{0.00254143646408 8398`,
     45.54`},{0.002379834254143646`,45.93`},{0.00222237569060 7735`,
     46.27`},{0.001912983425414 3646`,47.07`},{0.00175736648250 4604`,
     47.6`},{0.0016012891344383059`,48.06`},{0.001443830570902394`,
     48.61`},{0.001285451197053407`,49.23`},{0.00113259668508 28728`,
     49.88`},{0.000979281767955801`,50.65`},{0.000808471454880 2946`,
     51.71`},{0.0006523941068139964`,52.85`},{0.000496187845303868`,
     54.28`},{0.0003450736648250461`,56.2`},{0.00022895948434622468`,
     58.32`},{0.0001328268876611 4178`,61.05`},{0.0000590239410 6813996`,
     65.28`},{0.000792357274401 4733`,51.84`},{0.000716390423 5727441`,
     52.28`},{0.000639502762430 9393`,52.93`},{0.000562615101 2891344`,
     53.58`},{0.000485727440147 3297`,54.44`},{0.000408885819 5211787`,
     55.22`},{0.000331353591160221`,56.36`},{0.000464088397790055 2`,
     54.6`},{0.0003863720073664 8243`,55.56`},{0.000308839779 0055249`,
     56.72`},{0.0002315837937384 8986`,58.3`},{0.000154143646 4088398`,
     60.31`},{0.0000775782688766 1141`,63.88`},{0.0002239871 0865561693`,
     58.34`},{0.0001463167587476 9796`,60.5`},{0.000055939226 51933702`,
     65.37`},{0.0002382596685 0828727`,57.97`},{0.000162661 1418047882`,
     60.04`},{0.0000851749539 5948435`,63.29`},{0.007739410681399631`,
     39.17`},{0.004604051565377532`,42.3`},{0.003066298342541436`,
     44.6`},{0.0006823204419889503`,52.6`},{0.000530847145488 0295`,
     54.02`},{0.0003670349907 918969`,55.92`},{0.000206353591 16022098`,
```

58.98`},{0.002012891344383057`,46.86`},{0.0016984346224677715`,
47.79`},{0.0013964088397790053`,48.86`},{0.0007941988950276243`,
51.79`},{0.0004930939226519337`,54.28`},{0.0002181860036832412 3`,
58.46`},{0.000056169429097605894`,65.51`},{0.007315837937384899`,
39.48`},{0.006533149171270718`,39.76`},{0.004990791896869245`,
41.76`},{0.004216850828729282`,42.76`},{0.0034507366482504605`,
43.89`},{0.00268232044198895`,45.3`},{0.0021404235727440148`,
46.52`},{0.0012094843462246777`,49.61`},{0.000901012891344383`,
51.12`},{0.0005920810313075507`,53.32`},{0.00028747697974217313`,
57.03`},{0.0000998158379373849`,62.4`},{0.016445672191528544`,
34.04`},{0.014742173112338858`,34.94`},{0.012767034990791896`,
35.89`},{0.011063535911602211`,36.97`}}
CsDataLipa={{0.0091136`,38.294`},{0.0075245`,39.44`},{0.0063279`,
40.449`},{0.0048267`,41.991`},{0.0037505`,43.384`},{0.0033287`,
44.034`},{0.0026579000000000004`,45.247`},{0.002016`,
46.744`},{0.0016499`,47.778`},{0.0011681999999999999`,
49.584`},{0.0010217`,50.278`},{0.00077205`,51.734`},{0.00065997`,
52.535`},{0.00048398`,54.11`},{0.00036973`,
55.491`},{0.00024743000000000003`,57.548`},{0.0001862`,
58.987`},{0.00014084`,60.394999999999996`},{0.00010746`,
61.775000000000006`},{0.000081065`,63.166`},{0.000060605`,
64.615`},{0.00004564`,66.03099999999999`},{0.000039284000000000005`,
66.774`},{0.000029536`,68.215`},{0.000025569`,
68.905`},{0.000018917999999999997`,70.389`},{0.000013931`,
71.894`},{0.000011789`,72.69099999999999`},{0.000010101`,
73.465`},{7.1855999999999994`*^-6,75.127`},{5.2386999999999995`*^-6,
76.6`},{3.7254999999999997`*^-6,78.282`},{3.0057`*^-6,
79.27199999999999`},{2.501`*^-6,80.22`},{1.9984`*^-6,
81.214`},{1.6451`*^-6,82.228`},{9.015`*^-7,85.095`},{5.8475`*^-7,
87.091`},{4.0001`*^-7,88.965`},{2.8675`*^-7,90.447`},{2.382`*^-7,
91.46600000000001`},{1.9685`*^-7,92.212`},{1.4472`*^-7,
93.734`},{1.3269`*^-7,93.811`},{9.4706`*^-8,
95.544`},{7.165899999999999`*^-8,96.836`},{5.8321`*^-8,
97.98400000000001`},{5.004`*^-8,98.051`},{4.0329`*^-8,
99.24300000000001`},{2.9670999999999998`*^-8,101.04`},{2.4924`*^-8,
102.72`},{2.0000999999999998`*^-8,103.53`},{1.572`*^-8,
104.28999999999999`},{1.2073`*^-8,106.22`},{9.794199999999999`*^-9,
108.13000000000001`},{7.8027`*^-9,105.77`},{6.2719`*^-9,

```
    108.75999999999999`},{4.8799`*^-9,108.38000000000001`},{4.01`*^-9,
    110.92`},{3.1344`*^-9,108.71000000000001`},{2.4785`*^-9,
    111.91`},{1.9753`*^-9,116.07000000000001`},{1.5505`*^-9,
    118.`},{1.2454999999999999`*^-9,116.91`},{1.0115`*^-9,
    111.97`},{7.9398`*^-10,122.09`}}
data1=ListPlot[CsDataLow,PlotStyle\[Rule]{RGBColor[1,0,0],PointSize[0.01]}]
data2=ListPlot[CsDataLipa,PlotStyle\[Rule]{RGBColor[0,0,1],PointSize[0.01]}]
P=0.05;th=
 Plot[{cHighFit[ttt],cRotonFit[ttt]+cHighFit[ttt],
    cMaxonFit[ttt]+cRotonFit[ttt]+cHighFit[ttt],
    cPhonon[ttt]+cMaxonFit[ttt]+cPhMaxonFit[ttt]+cRotonFit[ttt]+
     cHighFit[ttt]},{ttt,0.0000000001,0.017},
   PlotStyle\[Rule]{RGBColor[1,0,1],RGBColor[0,1,0],RGBColor[0,0,1],
     RGBColor[1,0,0]}]
Show[data1,data2,th,PlotRange\[Rule]{{0,0.017},{0,125}}]
CsDataLowLog=
   Table[{Log[10,CsDataLow[[n,1]]],CsDataLow[[n,2]]},{n,1,
     Length[CsDataLow]}];
dataLowLog=
 ListPlot[CsDataLowLog,PlotStyle\[Rule]{RGBColor[0,0,1],PointSize[0.02]}]
CsDataLipaLog=
   Table[{Log[10,CsDataLipa[[n,1]]],CsDataLipa[[n,2]]},{n,1,
     Length[CsDataLipa]}];
dataLipaLog=
 ListPlot[CsDataLipaLog,PlotStyle\[Rule]{RGBColor[1,0,0],PointSize[0.012]}]
theoryLog=
 ParametricPlot[{xx,
    cPhonon[10^xx]+cRotonFit[10^xx]+cMaxonFit[10^xx]+cPhMaxonFit[10^xx]+
     cHighFit[10^xx]},{xx,-9.2,-1.6},
   PlotRange\[Rule]{{-9.2,-1.6},{20,125}},
   PlotStyle\[Rule]{Thickness[0.0045]}]
Show[dataLowLog,dataLipaLog,theoryLog,PlotRange\[Rule]{{-9.2,-1.6},{0,125}}]
```